SAPIENZA
UNIVERSITÀ DI ROMA

A TRANSMISSION SYSTEM OPERATOR APPROACH TO REACTIVE POWER PLANNING

PhD. in Engineering and Applied Science for Energy and Industry XXXVI cycle

Student: Jacopo Dell'Olmo

Advisor: Prof. Fabio Massimo Gatta

Acknowledgments

This PhD path has been a unique and life-changing experience that would not have been possible to pursue without the support and guidance I received from many people.

I would like to first express my deepest gratitude to my supervisor, Prof. Fabio Massimo Gatta, who wisely and patiently guided me throughout this hard and amazing journey. I would like to thank Prof. Ferdinando Salata for his trust and support.

I would like to thank Professors Stefano Lauria and Marco Maccioni for their constant advice and the opportunity to participate in important projects that have enriched this thesis A thank you goes to Prof. Geri, for his continuous professional spur.

A big thank you goes to Marco Graziani, Ludovico Nati and Tommaso Bragatto for frequent exchanges and collaborations.

Special thanks go to Prof. Luigi Martirano and Maria Carmen Falvo for the opportunity to extend the duration of the course to give full development to the subject matter.

The anonymous reviewers are thanked for their input that helped to greatly improve the final work.

A unique thank you goes to my parents and my friend, for the biggest support and trust, these years. A particular thanks to Marta for his help in recovering during this challenging period.

An unmeasurable thanks to Alba for her love and support in every moment.

Contents

Glossary Of Acronyms

Acronym	**Full Name**
AC	Alternate Current
AC-OPF	Alternate Current Optimal Power Flow
ACSR	Aluminium Conductor Steel Reinforced
ARERA	Autorità di Regolazione per Energia Reti e Ambiente
ASM	Ancillary Service Market
CIGRE	Conseil International des Grands Réseaux Électriques
DC	Direct Current
DC-OPF	Direct Current Optimal Power Flow
DFIG	Doubly-Fed Induction Generator
DOE	Department Of Energy
DSO	Distribution System Operator
ENTSO-E	European Network of Transmission System Operators for Electricity
EP	Evolutive Programming
EU	European Union
FACTS	Flexible Alternating Current Transmission Systems
GA	Genetic Algorithm
GDP	Gross Domestic Product
HVDC	High Voltage Direct Current
IEC	International Electrotechnical Commission
IEEE	Institute of Electrical and Electronics Engineers
IPCC	Intergovernmental Panel on Climate Change
LCC	Line Commutated Converter
LP	Linear Programming
MINLP	Mixed Integer Non-Linear Programming
MIQP	Mixed-Integer Quadratic Programming
NLP	Non-Linear Programming
NSGA-II	Non-dominated Sorting Genetic Algorithm
OHL	OverHead Line
OPF	Optimal Power Flow

PSO	Particle Swarm Optimization
PV	PhotoVoltaic
RES	Renewable Energy Sources
ROCOF	Rate Of Change Of Frequency
ROPF	Reactive Constraint Optimal Power Flow
RPP	Reactive Power Planning
SC	Synchronous Condenser
SCOPF	Security Constraint Optimal Power Flow
SPEA2	Strength Pareto Evolutionary Algorithm
STATCOM	STATic synchronous COMpensator
SVC	Static Var Compensator
TCSC	Tyristor Controlled Series Capacitors
TEP	Transmission Expansion Planning
TSO	Transmission System Operator
UPFC	Unified Power Flow Controller
UPSEB	Uttar Pradesh State Electricity Board
VS-SCOPF	Voltage Stability Security Constraint Optimal Power Flow
VSC	Voltage Source Coverter

Introduction

The electricity system has always been a system in transformation. The drivers of these transformations have been multiple, depending on the historical era and the development phase of the electricity system.

The main transformations we are witnessing now is due to the desire to decarbonize the electricity system by switching to low-carbon primary sources. This is pushing many states to incentivize the construction of electricity generation plants from renewable sources which, due to their subsidized construction costs, are very competitive in the electricity market. This change in primary source involves a corresponding technological adaptation in electricity generation devices and network managers, in order to deal with this technological change must make significant investments to keep the electricity system safe and reliable.

This doctoral thesis mainly addressed the issue of how to keep the electricity system adequate in a context of strong energy production from renewable sources with a deregulated electricity sector. The issue was addressed by focusing on the needs that arise when conventional generation based on rotating machines is replaced by "inverter based" generation. Particular attention has been paid to the satisfaction of the reactive power requirement and to the maintenance of an adequate level of short circuit of the electrical system. This topic has been treated starting from the de-regulated context of the electrical sector typical of the European realities and in particular of the Italian one. Furthermore, a new optimization methodology has been developed to verify and guarantee the adequacy of the electrical system by minimizing the intervention costs in a free market context. This methodology has been subsequently applied and positively tested to several case studies and using different optimization algorithms.

This thesis is structured as follows. In Chapter 1 presents the context of this research. Chapter 2 describes the structure of the European Electrical sector. Chapter 3 Discusses the electrical computation models used in this thesis. Chapter 4 presents a comprehensive review about reactive power planning techniques and approaches. Chapter 5 shows the most common measures and installation for voltage regulation. Chapter 6 discussed the proposed method and the used instruments. Chapter 7 shows the implemented optimization algorithms. In chapter 8 is presented the first case study on a IEEE standard network. Chapter 9 presents a vast study on part of the Italian national grid. Chapter 10 presents the other works in which I contributed during this PhD. Finally, Chapter 11 contains the conclusion.

Chapter 1 – The Context

Energy plays a crucial role in our society for human well-being. According to DOE data [1] there is a strong correlation between GDP and energy consumption, showing how as the wealth and advancement of nations increase, energy consumption increases. As for electricity, since it is not available in nature, it has always been obtained from other energy sources. The sources used have been different over time and in the various regions of the world. In the early stages of electrification, nations generally drew on hydroelectric resources. This form of energy was the first to be exploited and only when, due to the exhaustion of economically profitable sites, it was no longer suitable to support the growth of electricity consumption, the various nations invested in other primary energy sources for the production of electricity. In this scenario, the major protagonists became fossil fuels, accompanied in a smaller and very uneven percentage in the various regions of the world by nuclear energy. Coal was the first to be used, since there was a greater industry linked to it for its exploitation for means of transport (trains and ships) and industrial processes. Subsequently, with the maturing of technologies, petroleum derivatives and natural gas were added. The widespread use of fossil fuels has led and still leads to a large release of climate-altering gases into the atmosphere. These emissions have already contributed to the increase in the average temperature of the Earth from pre-industrial levels. To avoid excessive changes in the climate, it is necessary to contain this increase in temperature.

The IPCC Sixth Warning Global Warming Report [2] urges halving carbon emissions by 2030 in order to avoid major changes to World Climate. According to this report, this emission reduction trajectory is necessary to limit the global average temperature increase under 1.5 C°.

Reducing carbon dioxide emissions necessarily involves changing the means of producing electricity. This is possible by replacing fossil fuels with other less polluting energy sources. Discarding hydroelectric energy, which is more tied to environmental availability, authorization issues and long payback times, the other primary energy sources that are currently available on the "off-the-shelf" market, and with low carbon intensity, are nuclear, wind and solar [3,4]. In the European context, to which we will mainly refer, this technological change is encouraged by various national and international policies.

In 2014 the "Climate & Energy Framework" set final objective of reaching carbon neutrality by 2050 and an intermediate of halving the CO_2 emissions respect the ones in 1990[5].

Furthermore, in 2019 the "EU Green Deal" stressed the community aim of achieving carbon neutrality by 2050 (setting a higher target for 2030 in terms of GHG emissions reduction, with respect to the previous "2030 Climate & Energy Framework", and equal to 55% by 2030) [6]. Then the "REPowerEU" program was approved, to set new and more specific objectives in terms of energy efficiency and production from renewable energy sources [7]. All these European directives led to the creation of specific national plans [8].

As emerges from the content of the programs, all the attention is placed on the growth of production from wind and solar sources. The general shelving of nuclear energy is due to several factors. Concerns about safety and waste management are combined with those related to the costs of construction and dismantling of plants at the end of their life. These concerns have pushed public opinion to oppose the construction of new plants in several European countries, unlike other parts of the world. The objective of decarbonizing the electricity sector combined with the abandonment of nuclear energy has led almost all investments towards the construction of new production plants from wind and solar sources.

This direction has already shown its effects leading the production of energy from wind and solar sources to grow considerably in recent years and since 2010.

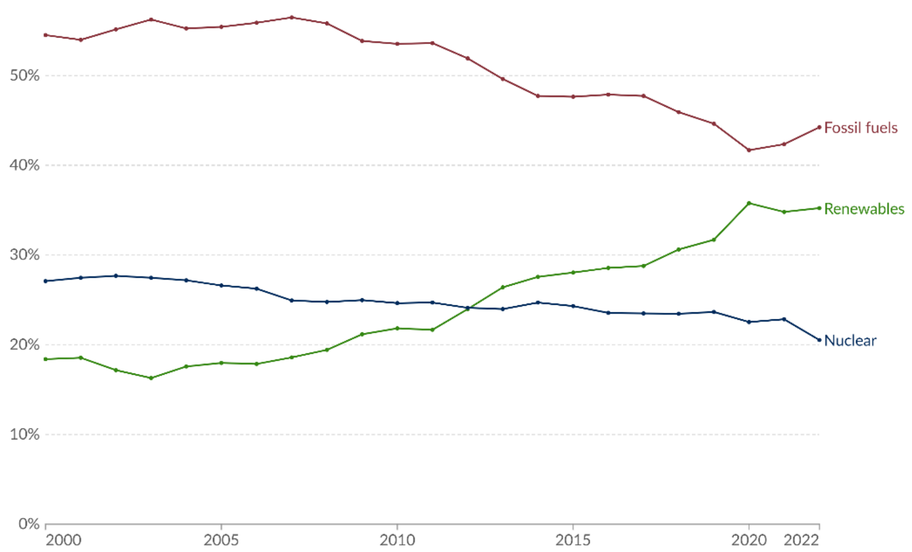

Figure 1.1 - Share of electricity generation in Europe [9]

Since the early 2000s can be seen a slow reduction of electricity production by nuclear and fossil fuel and from 2010 a faster increase in renewable energy generation. Analysing more in detail the energy mix composition reveals and confirm the above-mentioned trends.

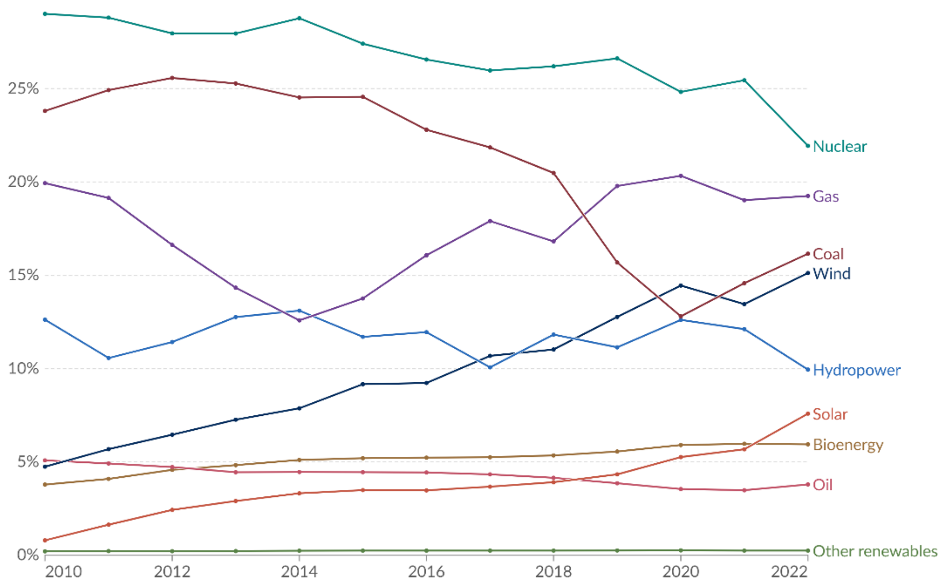

Figure 1.2 Share of electricity generation by source, Europe[10]

Analysing this chart from the most used source, nuclear energy is experiencing the above-mentioned slow decrease in utilisation. Among the power plants that use fossil fuels, the coal-powered ones have been the first to experience a significant decline. This is because coal-fired power plants have been the ones that have received the most attention in terms of the volume of energy produced and the related emissions. Their average carbon intensity is considered, depending on the technology, between 753 and 1095 gCO_2/kWh according to the "United Nation Economic Commission for Europe" while gas-fired plants are between 403 and 513 gCO_2/kWh [11].

CO_2 taxation mechanisms, such as green certificates and incentives for renewables, have put this technology out of the market.

Similarly, fuel oil-fired plants are following, albeit more slowly, the trajectory of coal.

As already mentioned, sites suitable for hosting plants for the production of energy from hydroelectric sources have already been widely used. The only substantial changes that these plants are experiencing are renovation and efficiency actions that could lead to a maximum increase in energy produced of 9.4% [12]. Despite the increase in energy is only a few percentage points, it is still an intervention that has a much shorter payback period than the construction of new plants. Although recent studies have reassessed the economic sustainability of new sites for hydroelectric plants, identifying a possible growth in hydroelectric energy that can be produced in Europe, the difficulties in obtaining authorization for the works and the long payback periods of the plants lead producers to invest in other technologies such as wind and photovoltaic. The variation in energy produced by hydroelectric plants is due to natural variations in rainfall over the years and this justifies the fluctuations in the graph.

Turning to renewable sources, the percentage of energy produced by wind power has tripled between 2010 and 2022, going from 5% to 15%. The percentage of energy produced by solar power, on the other hand, has gone from just over 1% to almost 8% in the same years [10,12].

During this technological change, emissions from the European electricity system have decreased by 27%, going from 369gCO_2/kWh in 2010 to 269 gCO_2/kWh in 2022.

The measures implemented to encourage the transition of the electricity system towards less carbon-intensive production sources are therefore producing the desired results, even if the speed is not that desired by the scientific community [13] even in advanced countries [14].

Returning to a larger scale, the decarbonization of the electrical system is one of the strategies implemented by the European Union to reduce CO_2 emissions and combat climate change. Other strategies that indirectly concern the electrical system are energy efficiency and the electrification of consumption.

The first strategy is self-explanatory and aims to reduce energy needs without having to give up the service that that energy provided. Therefore, trying to obtain the same results with less energy. Examples of measures that have pushed in that direction are, for example, interventions to reduce the consumption of buildings, such as re-insulation and the renewal of air conditioning systems. We can also mention initiatives that encourage mass public transport and the reduction of the use of private cars.

The second strategy involves the replacement of fuels with the use of electricity. Since the latter can be produced with a low carbon intensity, replacing users who use fuels with users powered by electricity can reduce CO_2 emissions overall. This strategy is, according to many, fundamental because many of the cheapest and low carbon energy sources produce electricity (solar wind) and many governments are incentivizing this strategy [15]. In addition to this, many end-uses can reduce their emissions by switching to low-carbon electricity, and city utilities are a prime example of this [16].

Recalling that decarbonization does not want to sacrifice economic and social development, a useful tool for this assessment is the Kaya Identity [17].

In 1989 and during a seminar organized by IPCC, a Japanese professor named Yoichi Kaya introduced a simple but extensively applicable model to conduct quantitative analysis on CO_2 emissions. This model entitled "Kaya Identity" established a simple mathematical equation which relates economic, demographic and environmental factors to estimate CO_2 emission of human activities as Eq. 1.1.

$$E_{carbon} = Pop * GDP_{capita} * EnergyIntesity * CarbonIntensity \quad (1.1)$$

Where Pop is the national population E_{carbon} is carbon emission rate ($GtCO_2$/yr); GDP_{capita} is per capita of gross domestic product (€/person-yr); $EnergyIntesity$ is primary energy per unit of GDP (EJ/€) and finally $CarbonIntensity$ is carbon emissions per unit of primary energy ($GtCO_2$/EJ).

The trend over the years of the various terms of the kaya allows us to see the effect of the above-mentioned policies. The reduction of the energy and GDP carbon intensity due to the policies for energy efficiency end low carbon energy sources allowed the total emission to decrease despite the growth of the population and the GDP per capita.

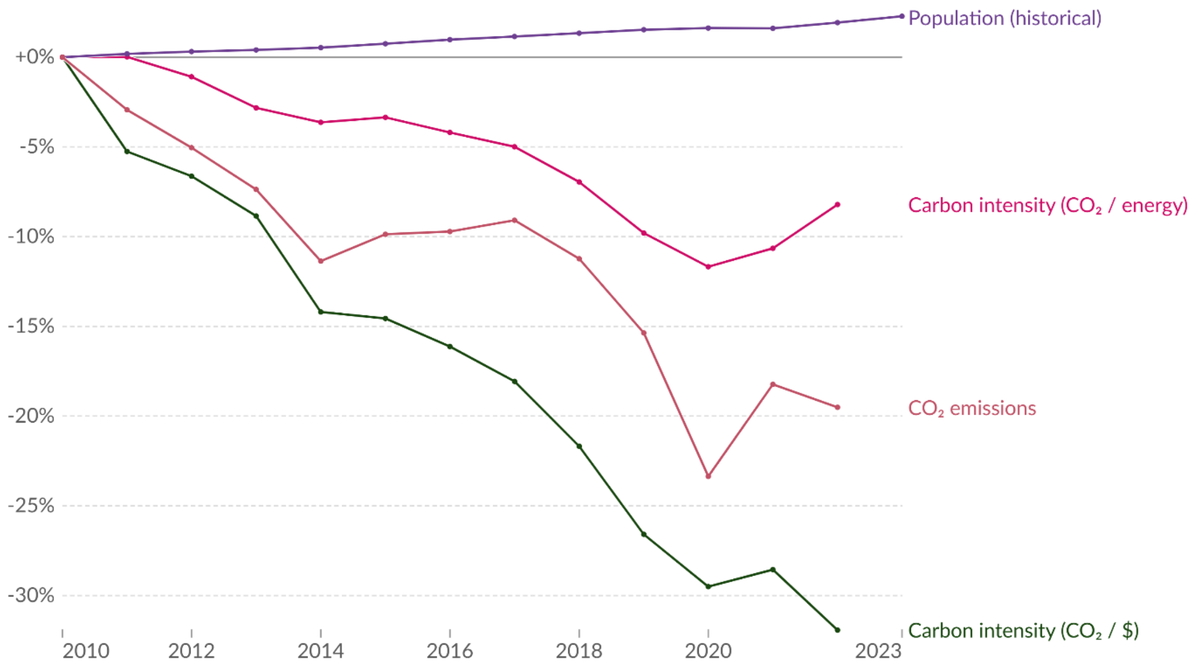

Figure 1.3 – Terms of the kaya identity in the European Union [18]

In the same years, the European GPD passed from 24 930 € to 29 030 € according to EU data[19].

This means that climate change policies are effectively reducing greenhouse gas emissions without compromising economic and social development. This will probably lead European and national institutions to continue, at least in the short term, with current energy policies.

From the data presented so far, we can deduce that climate change adaptation strategies are bringing beneficial effects without compromising economic development. If the institutions continue with current policies, there will be two dynamics that will affect the electricity system. The first is the choice to invest heavily in wind and photovoltaic as low-carbon sources since hydroelectric cannot grow and nuclear is strongly debated. The second is the electrification of many consumptions that will therefore increase the electrical load on the grid.

Let us therefore briefly introduce the problems that the electricity sector will have to face.

Renewable sources based on wind and solar energy are almost completely inverter-based. This is an important technological difference compared to synchronous generators with which energy is fed into the grid by “conventional” power plants. The use of a set of inverters instead of a synchronous compensator involves several technical problems including: a lower voltage regulation capacity, a lower contribution to the short circuit power and a very different behavior regarding frequency stability. In addition to this, it is necessary to mention the non-programmability of the sources and their uneven availability on the territory. These two factors involve several operational problems. In particular, several studies demonstrate how, to favor the integration of non-programmable renewable sources, the increase in the transport capacity of the electricity grids plays an important role [20–22] also reducing the necessary investments in storage technologies [23]. Several European operators are planning major plans to upgrade their electricity grids, both by upgrading existing AC power lines and by building new DC power lines [24]. In some long-term scenarios there are also projects for a direct current mesh network superimposed on the current alternating current infrastructure [25]. The desire to build new direct current connections will also be considered in this thesis.

As regards the increase, in electrification and efficiency of consumption, two trends are expected. The first is the simple increase in electrical loads. The second is that the loads will also be more dependent on inverters. This will be due to two effects: the first is that some rotating loads historically connected directly to the electricity grid will instead be connected via inverters. This is due to a significant reduction in consumption when rotation speeds lower than the nominal speeds are requested. The second effect is dependent on the fact that the new loads that we will see connected to the grid will be mainly inverter-based. Just think of heat pumps for heating and charging stations for electric vehicles. This change in the nature of the loads will lead to a change in the power factor of the loads themselves and therefore it will be necessary to implement strategies to adapt to the reactive needs of the loads.

Therefore, current policies will lead to changes for the electricity grid. In this thesis we wanted to focus on the management of reactive power (and therefore on voltage regulation) and on short circuit power. These are two aspects of primary competence of network operators who are facing important changes following the current decarbonization policies. These changes are part of a trend that several bodies predict will be confirmed and accelerated in the coming years. As regards energy production, the IEA report estimates that the installed power of renewable sources will grow from 750 GW in 2022 to 1300 GW by 2028 in Europe alone [26]. If we want to focus on the European context, it must be said that these changes are part of a particularly fragmented context, especially compared to the years in which national electricity systems were unified and administered by a single manager for each state. As we will see in Chapter 2, there are many more players in play with different roles and interests.

Chapter 2 – The Structure of the Electric Power Sector

An electricity system needs three main systems. The generation system, the transmission system and the distribution system. These three systems make up the electricity infrastructure. The generation system is made up of all the power plants that produce electricity. Here we include both the conventional power plants of large power connected to the transmission network and those of lower power connected to the distribution network. The transmission system is made up of the high and very high voltage power transmission network. This network has a meshed structure and is operated meshed to increase the reliability of the system. The distribution system is made up of the various power distribution networks, usually medium voltage. These networks have local extension and are not connected to each other. In the past, these three systems were all controlled by the same state body. In Europe since 1996 [27,28] a process of liberalization of the electricity sector has begun, giving rise to a multiplicity of entities, each responsible for a specific activity. Since the years of liberalization, there has been a gradual dismantling of the state-controlled companies that managed the various European national networks, entrusting parts of their responsibilities to other entities. At present, each sector of the electricity system has undergone a different change, in particular:

- In the production sector, the various production plants were auctioned off to private companies. The individual plants of the various companies participate in the production of electricity through a free market system;
- As for the power transmission sector, it did not undergo a division like the generation system. Since the transmission system infrastructure is structurally a natural monopoly, it was ill-suited to being managed by a multiplicity of different entities. Therefore, one or more state entities were established for each nation with the mandate to maintain, operate and expand the transmission system. These entities are known as Transmission System Operators (TSOs).
- As regards the distribution sector, this has been entrusted through a system of multi-year concessions to a multiplicity of entities that operate on a mostly regional basis. These entities are known as Distribution System Operators (DSO).

In addition to the TSOs, DSOs and energy producers, it was necessary to establish other regulatory bodies necessary for understanding the functioning and needs of the current European electricity systems: the electricity market manager and the regulatory body that arbitrates the relationships between the various actors seen so far. A final fundamental actor is the ENTSO-E (European Network of Transmission System Operators for Electricity) [29] which brings together and coordinates the various European electricity network Operators. The various national TSOs must comply with the ENTSO-E (European) rules, which regulate the interactions between TSOs and the standards they must meet. This is since the various national networks have been interconnected over the years to form the European electricity system, which is currently the largest interconnected electricity system in the world. In total, ENTSO-E brings together 40 network operators from 36 different nations [30].

How the Electricity Market Works

The electricity market is divided into various sections where different services are exchanged. Each market has its own different type of service and different time sessions. There are two markets of greatest interest regarding the topic discussed: the energy market and the dispatching services market. In the energy market, through an auction mechanism, producers offer their availability to produce electricity and wholesalers declare their purchasing needs. This market has different divisions that operate at a different distance from real time with an increasingly higher resolution. The purpose of this market is to determine which sales and purchase offers are accepted in compliance with the operating limits of the network. This is determined by ordering the supply and demand curves by price and identifying their intersection point.

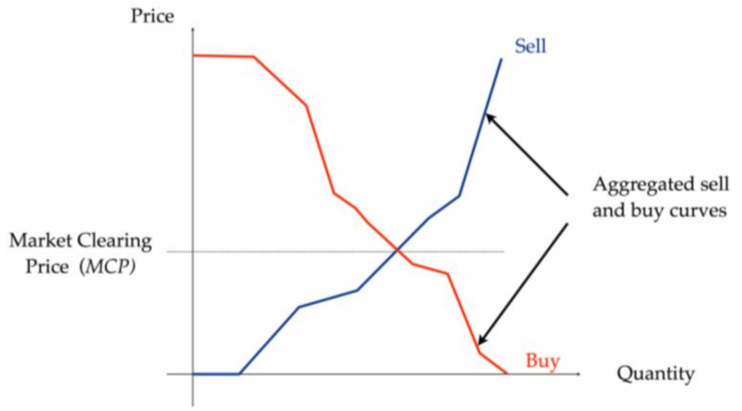

Fig 2.1 Electric market clearing price determination

- In fact, the outcome of the energy market is the dispatching of energy, or the position and amount of electricity injected and withdrawn from the grid.

It is necessary to make a special mention of the procedure that is followed when the outcome of the market does not respect certain grid constraints. In the first phase of market resolution and therefore of identification of the dispatching, the system is considered to be a single bar with unlimited transit capacity between participants. At a later stage, the identified dispatching is verified by the TSO. If certain transit limits, predetermined in advance by the TSO, are exceeded, the market is divided into two smaller sessions. This can happen if there is a large price differential between neighboring areas.

These two parallel sessions represent the two grid zones and in the resolution of the two markets, the energy that these can exchange based on the limits identified by the TSO is considered. This procedure, called market splitting, divides the market into two zones that exchange a finite amount of energy. Based on the operation just described, the two market sessions will settle on two different energy prices and the market has been divided. The new dispatching must be verified again and congestion in other areas and further divisions may occur. It is important to add that depending on the market remuneration mechanisms, the market splitting procedure produces an economic deficit between the total purchase volume and the total sales volume that is collected by the TSO.

This money resulting from the price differential and the separation of the market areas must be allocated by law by the TSO for network enhancement interventions to increase the transit limits between the areas. This procedure and the reinvestment of the deficit due to congestion serves to increase the transmittable power and the "competitiveness" of the market by trying to reduce the territorial advantages of one area compared to the other.

The second market is the ancillary services market where, through a call mechanism, the TSO buys some services from other entities authorized to this market for the correct functioning of the network. Entities authorized to participate in this market can be either energy producers, consumers or prosumers, therefore entities that can have an active or negative power balance. To be authorized to participate in this market, the requested performance must be guaranteed within established timeframes.

Depending on the entity participating in the market, this can offer different services such as:

- For Producers:
  - The possibility of varying the production of a given plant both upwards and downwards with respect to the outcome of the energy market.
  - The willingness to turn on or off a system that would have been on or off depending on the market outcome.
- For the Consumers:
  - The ability to increase or decrease their power consumption.
  - The ability to be disconnected from the grid.

Prosumers can provide all services.

Both services, being paid on an on-call basis, are generally very expensive and TSOs try to use them as little as possible within the limits of the security of the electricity system.

Needs for a TSO and need to resort to the Ancillary Service Market

The obligations that a TSO must satisfy are multiple and can be summarized in maintaining a stable and continuous power supply to all loads. To keep the electrical system safe and stable, the following must be guaranteed:

- Stability of frequency
- Voltage stability
- High continuity and quality of service

As regards frequency stability, there must be enough synchronous generators connected to the grid, to guarantee rotating inertia, and there must be sufficient additional generation capacity divided into various reserves depending on the time in which they can guarantee the additional power they have available.

The availability of a certain plant to act as a rotating reserve is guaranteed through the Capacity Market and its commissioning purchased through the auxiliary services market. Already in this way we can see how the TSO needs to resort to the ancillary services market to guarantee the safety of the grid. Again, regarding active power, in the event of a deviation from the scheduled dispatching or in the event of a fault, it may be necessary to force generators and loads to change their power balance. Both services are purchased on the ancillary services market. Similarly, to ensure voltage stability and protection selectivity, it may be necessary to use the ancillary services market to increase the capacity to regulate reactive power or short-circuit power at a given node in the network.

As anticipated, using this market involves an expense for TSOs and many of them are actively investing to connect components and machinery to the network that replace some of the services that can be purchased on the ancillary services market to become autonomous. Generally, a TSO by mandate cannot own plants to produce active power. This means that as far as active power is concerned, the TSO must limit itself to installing resistors for regulating frequency and power flows. As regards plants for the production of reactive power, there are no particular limits.

It should be noted that this trend due to economic needs to reduce network management costs is due to particular incentives created ad hoc and directives in regulatory bodies.

In Italy an interesting dynamic has started between ARERA [33] (the regulatory authority for energy networks and the environment) and Terna [34] (the TSO of the Italian network) regard the use of the ancillary service market. Following increasing expenses on the Ancillary Service Market, ARERA has created an incentive mechanism to encourage Terna to reduce its use of the dispatching services market. In particular, Terna is entitled to a variable bonus depending on the savings in expenditure compared to a base year, which in this case is 2019 [31]. The basic annual expenditure is therefore 2 billion euros [32].

HVDC Special Necessities

A trend that has been seen, and continues to continue, in the European electrical system is the increase in direct current connections [24]. These systems are being installed with increasing frequency for the following reasons:

- TSOs have a mandate to expand the grid to make it more reliable and improve market conditions. In particular, TSOs must spend part of the revenues from surcharges during market splitting phases to eliminate grid bottlenecks to foster competition in the energy market. The construction of long HVDC links helps to increase transmission capacity between different parts of the grid.
- Increasing the energy transmission capacity of electricity networks also contributes to the decarbonization of the electricity system [20–22] given the uneven availability and non-synchrony of non-programmable renewable sources.

- Ease of authorization due to smaller footprint for the same transmittable power and fewer constraints regarding electromagnetic pollution always in comparison to AC lines of equal capacity.
- Lower cost in long cable connections, especially submarine ones, for connecting offshore wind farms to the coast.

For these reasons we are witnessing an increase in HVDC connections. Although there are still no solutions on the market that allow the construction of a direct current mesh network, many entities expect, with technological advancement, to be able to create a mesh infrastructure superimposed on the current alternating current network, which transmits power in direct current. To this end, it will be necessary to build numerous AC/DC conversion stations. These conversion stations, whether built with LCC or VSC technology, require a minimum short circuit current to operate, and this is a requirement that must be satisfied by the alternating current network and therefore by the TSO.

There are several projects for the expansion of electricity networks that are based on direct current connections. In Italy alone, considering the Terna hyper grid project [25], which considers an investment of approximately 11 billion euros distributed between various terrestrial and marine connections for a total of five new direct current backbones [33]. In this vein, the new project for the connection between Italy and Tunisia, recently authorized by the competent Italian ministry, should also be considered [34].

New Trends

Important changes are taking place in European networks. The push towards non-programmable renewable sources, in particular wind and photovoltaic, is changing how energy is fed into the network.

As regards this thesis, emphasis will be placed on only some of the problems that this entail and will be discussed:

- The reduced possibility of regulating the voltage that can derive both from the absence of an adequate control system and from the reduced capability compared to synchronous generators.
- The very low contribution to the fault current.

Some specific considerations will be made on the change in typology of some loads and on the new directives that come from the authorities regarding exchanges between TSO and DSO.

A third element that is considered is the increase in direct current connections.

The studies conducted in this thesis aim to develop and verify a methodology that allows TSOs to cope with the new needs due to these transformations. For the current functioning of European Electrical Systems, depending on their structure and the political directions that are being pursued, it is necessary for TSOs to pay new attention to the planning and management of the means of regulating voltage, frequency and short-circuit power. This thesis aims to provide a methodology for identifying essential investments for the safety of the electrical system verified both on theoretical case studies and on real infrastructures.

Chapter 3 – Electric Power Systems Model and Computation

This chapter will discuss briefly the mathematical models used to represent the electrical grid and the methods for calculating permanent regimes in large networks and the most common optimization models related to power-flow calculations. Regarding the computational models, starting with load-flow calculation as a fundamental method for solving power grids will be seen next:

- DC-loadflow approximation and its potencies and limitations.
- The causes and effect of active and reactive power flows in network components.

Next we will deal with power flow optimization methods, then the Optimal Power Flow (OPF) and its approximation in "direct current" the DC-LoadFlow. These tools have been used extensively in the development of this thesis.

Then will be shown the calculation of the short-circuit power, a feature of the electric systems central in this thesis.

Finally, mention will be made of the Monte Carlo method as an effective tool for reducing the complexity of some optimization problems.

The state of the network is considered known if the voltages in all nodes and the currents in all branches, both active and passive, are known. In this thesis we will focus solely on the calculation of steady-state regimes and some fault regimes.

From the study of electrical engineering, we know that the steady-state behavior of an electrical network, which is described by a linear system of differential equations, can be represented and solved by a complex linear algebraic system obtained by the Maxwell node method [35,36]. This system of equations is linear with respect to the quantities of voltage and current and from it we can obtain the admittance matrix and subsequently its inverse, that is, the short circuit matrix.

Therefore, once the voltages of the generators are known in modulus and phase, it is easy to calculate the state of the network. From a practical point of view, however, the quantity of greatest interest is the active power. The electrical infrastructure was, in fact, created to transmit power from one point to another. The method for solving electrical networks starting from the powers is called load-flow calculation.

Loadflow

To verify how the network behaves, given that the power supplied by the generators and absorbed by the loads is known, it is necessary to start from the representation of the network with the admittance matrix constructed with the Maxwell node method and add the power equation to the nodes. The steps and considerations reported below refer to the representation in polar coordinates of the electrical quantities of voltage and current. The matrix and vector quantities are marked in bold, while the complex quantities are underlined.

$$[\bar{\mathbf{I}}] = [\bar{\mathbf{Y}}][\bar{\mathbf{E}}] \qquad 3.1$$

$$\overline{\mathrm{N}}_{\mathrm{k}} = 3\overline{\mathrm{E}}_{\mathrm{k}}\overline{\mathrm{I}}_{\mathrm{k}}^{*} \qquad 3.2$$

$$\overline{\mathrm{N}}_{\mathrm{k}} = 3\overline{\mathrm{E}}_{\mathrm{k}}\sum_{\mathrm{i=1}}^{\mathrm{n}}\overline{\mathrm{Y}}_{\mathrm{ik}}^{*}\overline{\mathrm{E}}_{\mathrm{i}}^{*} \qquad 3.3$$

$$\overline{N_k} = 3E_k\sum_{i=1}^{n}Y_{ik}E_{ik}e^{j(\theta_k-\gamma_{ij}-\theta_i)} \qquad 3.4$$

$$\begin{cases} P_k = \sum_{i=1}^{n} 3E_kE_iY_{ki}cos(\theta_k-\gamma_{ij}-\theta_i) \\ Q_k = \sum_{i=1}^{n} 3E_kE_iY_{ki}sin(\theta_k-\gamma_{ij}-\theta_i) \end{cases} \qquad 3.5$$

$$\begin{cases} P_{gen,k} - P_{load,k} - \sum_{i=1}^{n} 3E_kE_iY_{ki}cos\left(\theta_k-\gamma_{ij}-\theta_i\right) = 0 \\ Q_{gen,k} - Q_{load,k} - \sum_{i=1}^{n} 3E_kE_iY_{ki}\sin\left(\theta_k-\gamma_{ij}-\theta_i\right) = 0 \end{cases} \qquad 3.6$$

Equation (3.1) reports the relationship between nodal currents and nodal voltages via the network admittance matrix. This matrix has dimension n with n equal to the number of nodes in the network. Equation (3.2) is the equation of the complex power at a generic node k that comes from the network components (without loads and generators). In (3.3) the current at node k is replaced with the corresponding row of the system in (3.1). In this equation, we see how the power injected at the single node depends on the elements in derivation at the node and on the transits on the branches that converge on it. In (3.4) we move from the representation in complex quantities to the representation in modulus and phase of the electrical quantities and in (3.5) the power is divided into active and reactive power. Finally, the power injected by the generators and absorbed by the loads is added to the node balance. The system represented in (3.6) is a system of 2n equations in the 4n unknowns of active power, reactive power, voltage modulus and voltage phase. For each node, two quantities are therefore fixed to solve the system. The quantities fixed at the node depend on whether this is a generation node (active power and voltage module imposed), a load node (active and reactive power imposed) or the balance node which fixes the reference phase (modulus and voltage phase imposed) [35].

Once the specific quantities of the various nodes are fixed, this system allows the state of the network, or its operating point, to be determined. The resolution of this system of nonlinear equations occurs numerically. The most common system is the Newton-Raphson method. This iterative method, using the partial derivative matrix of the system of equations, starts from an arbitrary initial solution and converges towards one of the possible solutions of the system. When using the Newton method, starting from an initial solution as close as possible to the solution of the problem is of great importance. In this regard, it is important to keep in mind some characteristics of the electrical system. The electrical infrastructure has been designed and built so it could operate in a wide range of voltages. Nevertheless, it is a common objective for the TSOs to guarantee a really stable voltage in non-emergency conditions in a narrow range (for the transmission network +- 5% around the nominal value). So, the problem is generally well conditioned, and it is sufficient to initialize all phases to zero and voltages to the nominal voltage. A second aspect to consider regarding high and very high voltage networks is that the network components have a predominantly inductive rather than resistive behavior. As for transmission lines, these easily have a resistive part that is about 1/10 of the inductive component.

DC-LoadFlow

Returning to the load-flow equations, this information allows us to make some useful approximations from which t the DC-LoadFlow derives. This method allows to have a good approximation of the active power flows around the grid neglecting the system losses and the reactive power balance.

Regarding the grid's model, if the network admittances are strongly inductive, then:

$$|Re(\overline{Y_{ij}})| \ll |Im(\overline{Y_{ij}})| \qquad 3.7$$

$$Arg(Y_{ij}) \sim -\pi/2 \qquad 3.8$$

$$\begin{cases} P_k \sim \sum_{i=1}^{n} 3E_k E_i Y_{ki} sin(\theta_k - \theta_i) \\ Q_k \sim \sum_{i=1}^{n} 3E_k E_i Y_{ki} * (-cos(\theta_k - \theta_i)) \end{cases} \qquad 3.9$$

Turning to the powers transiting on individual branches..

$$\begin{cases} P_{ij} \sim 3E_j E_i Y_{ji} sin(\theta_j - \theta_i) \\ Q_{ij} \sim 3E_j E_i Y_{ji} * (-cos(\theta_j - \theta_i)) \end{cases} \qquad 3.10$$

Now, assuming that the voltages are all the same as the nominal voltage (precisely because they vary within a narrow range):

$$\begin{cases} P_{ij} \sim 3E^2 Y_{ji} sin(\theta_j - \theta_i) \\ Q_{ij} \sim 3Y_{ji} E^2 * (-cos(\theta_j - \theta_i)) \end{cases} \qquad 3.11$$

And considering the phase variations between adjacent nodes to be small, we can write:

$$sin(\theta_j - \theta_i) \sim (\theta_j - \theta_i) \qquad 3.12$$

$$cos(\theta_j - \theta_i) \sim 1 \qquad 3.13$$

And finally:

$$\begin{cases} P_{ij} \sim 3E^2 Y_{ji} * (\theta_j - \theta_i) \\ Q_{ij} \sim 3E^2 Y_{ji} \end{cases} \qquad 3.14$$

These equations reported in 3.14 compose the approximation of the so-called DC-Load-flow. It is important to notice that the reactive power contribution of the branch is constant, and it elides in the nodal reactive balance.

$$Q_k = 3E^2 Y_{kk} + \sum_{i \neq k} 3E^2 Y_{ki} \qquad 3.15$$

$$Q_k = 3E^2 y_{shunt,k} \qquad 3.16$$

In the end with the DC-loadflow approximations:

- The power transfer through the network is linear with the phase difference between the nodes. This Linear approximation implies that the DC-LoadFlow is a linear problem that can be solved in closed form.
- In order to linearize the active power flows across the grid, the reactive power at the node depends only to the shunt admittance at the node. This implies that there is no reactive balance due to the lines and no reactive power flowing across the network.

These approximations do not consider losses or flows of reactive power through the network. The DC-load-flow is in fact widely used in studies that want to focus on active power such as planning studies for the expansion of transport capacity or generation park. It is also widely used in market simulations where the focus is mainly on the economic aspect and less on the electrical one.

In this thesis work the approximation of the DC-load-flow will be used precisely for this purpose. In more detail it will be used to simulate the operation of the energy market and produce various active-power scenarios.

This method is also used to obtain a starting solution for the complete LoadFlow problem. The voltages are initialized at the nominal voltage and the phases at the solution of the simplified DC-LoadFlow problem. This is particularly recommended for large grids that have big phase differences among the nodes.

Active and Reactive Power Flows in Transmission Networks.

As we have seen from the LoadFlow equations the transmitted powers depend primarily on the angles of the voltages at the nodes. At the same time if the voltages are equal at all nodes there is no transmission of reactive power through the network. To better understand some of the phenomena discussed in the thesis we will go into more specifics of these behaviours by distinguishing between overhead and cable lines. Two lines of common configuration for the Italian network were considered, the data for which are shown in Table 3.1.

Line type	Conductor	Z' [Ω/km]	C' [nF/km]	Sz [MVA]	Pc [MVA]	Length [km]
OHL	ACSR-31.5 three conductors bundle	0.023+j0.266	13.5	2000	640	100
Cable	2500 mmq Copper	0.0133+j0.172	234	1240	3308	60

Table 3.1 – Test Lines features

The configuration of conductors, impedance and capacitance per unit length, power at the thermal limit and characteristic power are shown, the latter quantity being discussed in more detail later. We can first see how the resistive part of the series impedance is less than one-tenth of the inductive part. Now through the laws of electrical engineering we go on to see the trend of the active power transmitted as the phase difference between the two nodes changes.

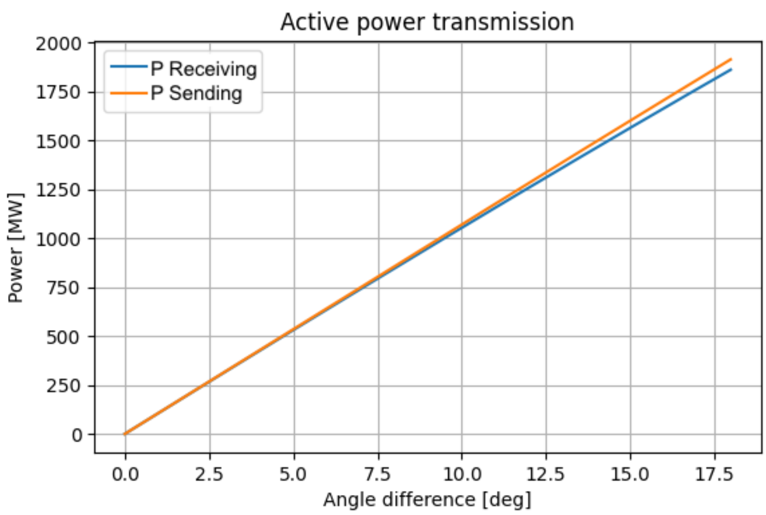

Figure 3.1 – Active power transmission OHL

It can be seen that the Transmitted Power is definitely linear with the phase difference between the voltages in the considered operating range. At the same time, we can see how considering the line to be lossless is a reasonable approximation in many cases. For completeness fine reported the transmission efficiency as a function of phase difference.

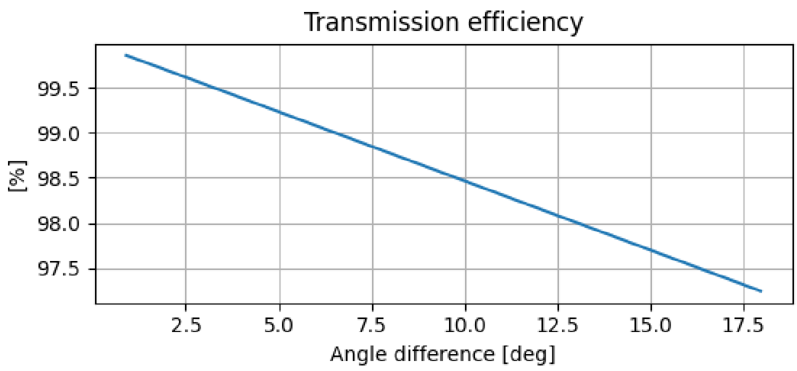

Figure 3.2 - Transmission efficiency OHL

Turning to the power transmitted by the cable line.

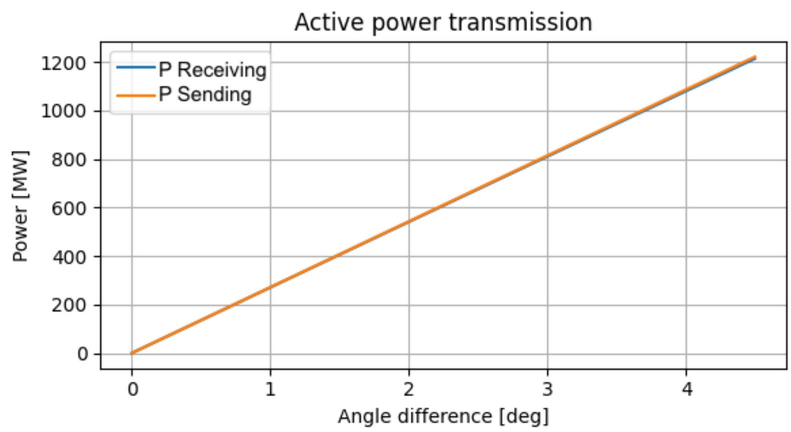

Figure 3.3 - active power transmission cable line

Here again the behaviour is totally linear given the smaller phase difference between the voltages at the terminals. Here the losses are even less and remain contained under 0.5 percent.

As for reactive power, let us look at the reactive power output of the lines under consideration as the power at the arrival node varies.

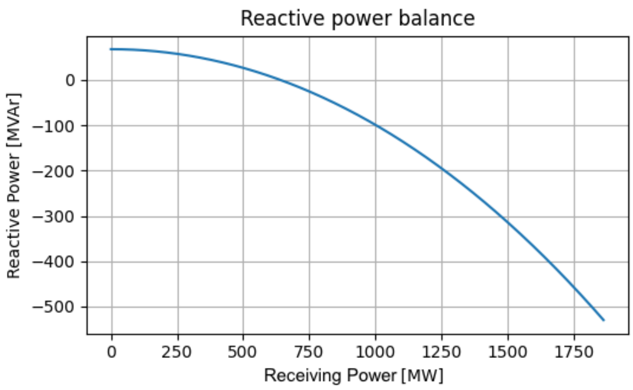

Figure 3.4 – reactive power production OHL

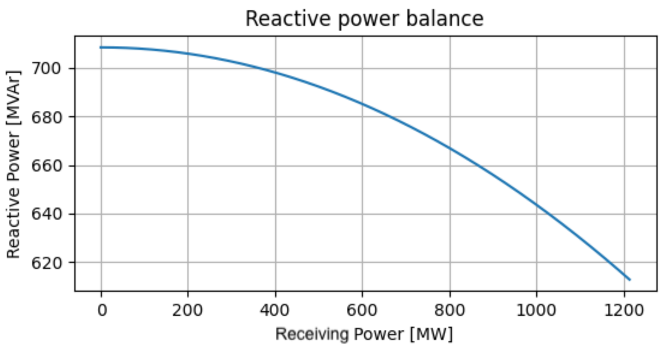

Figure 3.5 – reactive power production Cable Line

From Figures 3.4 and 3.5 it can be seen that the two curves have the same trend the values are very different. In both cases, the increase in transmitted power results in a greater absorption of reactive power by the series reactance of the line. This offsets the capacitive reactive power output produced by the cross capacitance of the line. Both no-load lines produce reactive power but having arrived at a critical value of transmitted power, the reactive power produced by the overhead line cancels out and then begins to become negative. This value of equilibrium power at which the line absorbs the same reactive power it produces is called characteristic power and can be calculated by formula 3.17 and is shown in Table 3.1 with Pc for both lines.

$$P_c = \frac{3E_n^2}{Zc} \quad 3.17$$

While the overhead line can carry the characteristic power, for the cable line the Pc is greater than the maximum transmissible power at the thermal limit and therefore the cable line will always be capacitive. Since the cable line always remains capacitive and even at maximum load continues to produce large amounts of capacitive reactive power, it is technical practice to compensate cable lines over a certain length with shunt reactors at terminals between 90 and 98 percent of the cable's rated capacity.

Moving on from the reactive balance of the line we go to see how this can be transported. When we have no voltage imbalance and no power is transmitted, reactive power comes out of both terminals equally, as the transmitted power increases, more reactive power "comes out" at the start and less at the finish.

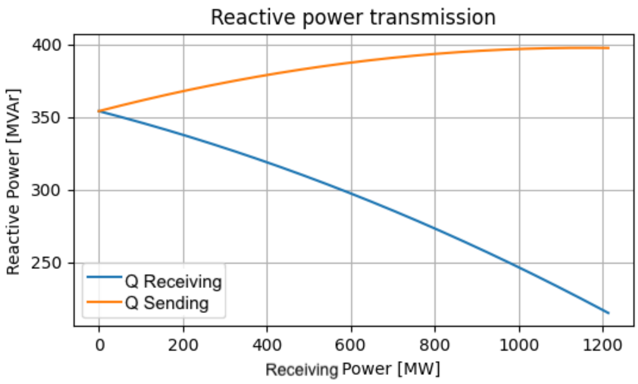

Figure 3.6 - Reactive power at cable line terminals.

In a lossless situation, the reactive power produced would remain the same at both ends of the line.

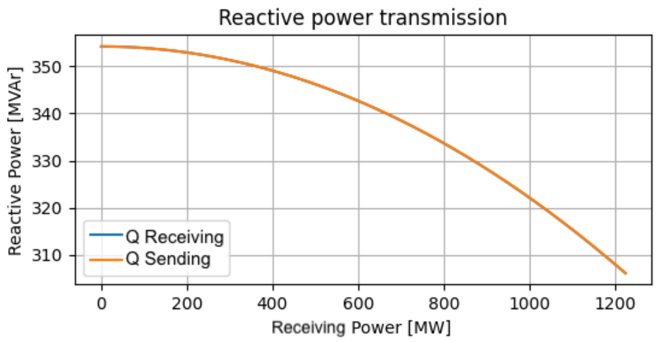

Figure 3.7 - Reactive power at cable line terminals no losses scenario.

When you is introduced an imbalance between the voltages at the terminals instead, the reactive power flow at the ends of the line changes considerably.

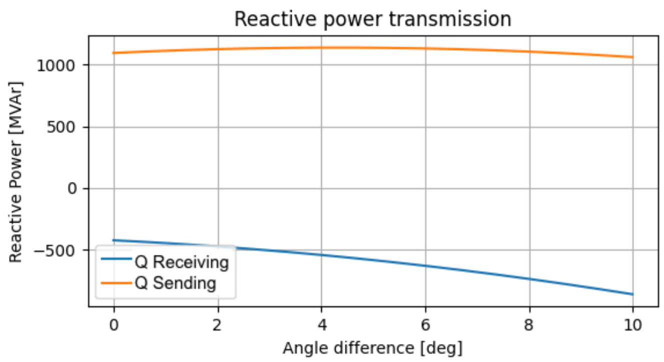

Figure 3.8 - Reactive power at cable line terminals with 5% voltage unbalance.

In Figure 3.8 we can see how a 5% voltage imbalance between the terminals results in a large transit of reactive power. A voltage was set at 0.975 p.u. at departure and 1.025 p.u. at arrival. In this case we see how reactive power is absorbed at arrival and delivered at departure. The reactive power then flows from the highest to the lowest voltages. Interestingly, a voltage imbalance of this magnitude results in a reactive power outflow almost equal to the rated capacity of the cable. In this situation there is no margin left for active power transport. Voltage regulation is therefore also necessary to prevent cable lines from carrying only reactive power that would be better delivered locally. Moreover, it should be noted that, while for active power by putting several lines in series the phase can continue to increase indefinitely, for reactive power the voltages cannot get out of a reasonable range of ± 5 %. Finally we see that this imbalance of reactive power is little affected by the phase difference between the voltages.

For the sake of brevity, the behaviour of the overhead line is not reported, which has the same dynamics but less pronounced due to the higher series impedance of the link. From this analysis we can infer the following:

- Active power flow depends on phase differences between voltages.
- The reactive demand of the lines depends on the transiting active power.
- The reactive power flow depends mainly on the modules of the voltages.
- For long cable lines, voltage control at the terminals is essential to prevent their active power carrying capacity from being further reduced by reactive power.

OPF

Once the behavior of a network has been solved, given the measured or desired power flows, further considerations can be made. From the moment it was possible to calculate the behavior of the networks starting from the injected and absorbed powers and the voltages of the generators, the next step was to apply objective functions that, respecting the constraints of a good operation of the electrical network, minimized certain quantities.

A first example, given the maximum power that can be supplied by the generators, is to find the dispatching that minimizes the losses. That is, by associating different costs for the production of electrical energy to the generators, one wants to find the dispatching that minimizes the production cost. All these optimization problems constrained by the network equations and the operating constraints of the various components are called Optimal Power Flow.

The generic formulation of an OPF in polar coordinates can be summarized as follows:

min	$F(\mathbf{x})$	3.18
Subject to	$G(\mathbf{x}) = 0$	3.19
	$H(\mathbf{x}) \leq 0$	3.20
	$\mathbf{x}_{\mathbf{min}} \leq \mathbf{x} \leq \mathbf{x}_{\mathbf{max}}$	3.21
with	$\mathbf{x} = \begin{pmatrix} \boldsymbol{\theta} \\ \mathbf{V_m} \\ \mathbf{P_g} \\ \mathbf{Q_g} \end{pmatrix}$	3.22

Where Eq. 3.18 is the objective function: generally, it is a cost function dependent on the active and reactive power. Eq. 3.19 represents the system of network equations in the form of the balance of nodal powers as in equation 3.6. Eq. 3.20 is the system of constraints of the network quantities calculated as a function of the vector of variables, for example, the flow rate constraints of the lines fall here. Eq. 3.21 represents the system of inequalities that limits the domain of the problem and of the network variables. $\mathbf{x}$ is precisely the vector of variables that is usually composed of:

- the angles of the voltages,
- the moduli of the voltages, and
- the unknown active and reactive powers.

The most classic formulation of an OPF is therefore aimed at minimizing the costs of energy production.

Regardless of the representation that is made of it, the structure of the problem categorizes it as a nonlinear programming (NLP) problem, and it is almost always also non-convex. Over the years, many variants of OPF have been developed, both to simplify the model and make it easier to handle, and to enrich the representation of the network and network constraints for various purposes. As regards more complex representations of the problem, we can briefly mention the most common ones [37]:

- Security-constrained OPF: These OPFs are structured in such a way that in addition to the case of a healthy network there is a specific system of equations for each fault considered. For single faults the size of the system grows linearly, while it is exponential in the case of multiple faults. These OPFs are widely used both for the verification of the safety of the system in real time and for defining the operational safety limits for the robustness of the system.
- Reserve-constrained OPF (generation reserve): these OPFs are intended to ensure that there is always an adequate generation reserve both for imbalances and for any sudden outages of the generation units. These conditions are inserted with additional constraints on the active power.
- Unit commitment constrained (multi-hour-OPF): this category of OPF was created to consider some constraints of the generation plants such as the maximum load ramp that they can sustain, or the times needed for re-ignitions. For each instant of time considered there is a system of equations that describes the network at that instant and therefore the number of equations that make up g(x) grows linearly with the time that is considered. For the power constraints, different constraint equations are added for each generation node and each instant of time.
- Voltage-stability security-constrained: This category of OPFs adds auxiliary equations to estimate how close a given node is to voltage collapse. Although the exact calculation of the power that can be transmitted before a voltage collapse occurs is not straightforward and often involves the calculation of subsequent load flows, there are several indicators to estimate the proximity to it. Some simplified formulations have been included in OPFs to verify both a margin towards power increases and a robustness to failures towards voltage collapse.

Some of these formulations involve the introduction of binary variables, bringing the complexity of the problem towards MINLP (Mixed-Integer Non-Linear Programming). An example is the unit-commitment problem where binary variables define the state (in service or off) of the generator. Subsequently, equations are defined between the binary variables to respect the restart limits.

The Generation Expansion Planning and Reactive Power Planning problems also have a MINLP formulation very similar to the unit-commitment-OPF. Each expansion intervention is associated with a binary variable that multiplies the power that can be supplied by the systems to "cancel" or "allow" the injection of power into the grid.

These models can be combined with each other to obtain increasingly accurate, but complex formulations. Very often the size of the system grows linearly with the scenarios or with the models, but the complexity of solving these NLP and MINLP problems grows more than linearly with the size of the system. Furthermore, as we will see in the chapter dedicated to the review of the scientific literature, very often very accurate models had several equations and variables such that they could only analyze very limited networks.

DC-OPF

This category of OPF simplifies the system of equations with the same approximations as DC-PF (null resistances of the network components, unit voltages at all nodes, small angular differences). These assumptions are often acceptable on the transmission network, especially if it is highly meshed and composed of short lines. This greatly simplifies the system of equations 3.24 which becomes linear. A further simplification occurs in the calculation of the capacity limits of the lines which under the approximations made are directly constraints in active power and the series of inequalities 3.25 is also simplified.

min	$f(\mathbf{x})$	3.23
Subject to	$P_{gen,j} - P_{load,j} + \sum_{i=1}^{n} Y_{ij}\left(\theta_j - \theta_i\right) = 0 \ \forall j$	3.24
	$Y_{ij}\left(\theta_j - \theta_i\right) \leq P_{ij,limit} \ \forall i \neq j$	3.25
	$\mathbf{x_{min}} \leq \mathbf{x} \leq \mathbf{x_{max}}$	3.26
with	$\mathbf{x} = \begin{pmatrix} \boldsymbol{\theta} \\ \mathbf{P_{gen}} \end{pmatrix}$	3.27

As mentioned, this simplification is more than acceptable under certain conditions and this model will be used in this work to emulate the behavior of the electricity market.

Short-circuit Power Calculation

The short-circuit power of an electrical network is essential for the selectivity and safety of protection systems and the containment of voltage variations within the permissive values. It is defined by the short-circuit current and can be easily calculated from the nodal admittance matrix. According to the DIN/IEC EN 60909 standard [38] the equivalent model is calculated at the failure point. To correctly evaluate the short-circuit currents, the nodal admittance matrix $[\boldsymbol{Y}_{\boldsymbol{bus}}]$, must be modified including the sub-transient reactance of the synchronous generators in order to obtain the nodal short-circuit admittance matrix $[\boldsymbol{Y}_{\boldsymbol{bus,SC}}]$.

Starting from the nodal short-circuit admittance matrix $[\boldsymbol{Y}_{\boldsymbol{bus,SC}}]$, we can write the following:

$$\begin{bmatrix} \overline{Y_{11}} & \cdots & \cdots & \overline{Y_{1n}} \\ \cdots & \cdots & \cdots & \cdots \\ \cdots & \cdots & \cdots & \cdots \\ \overline{Y_{n1}} & \cdots & \cdots & \overline{Y_{nn}} \end{bmatrix} \begin{bmatrix} \overline{E_1} \\ \vdots \\ \overline{E_{QJ}} \\ \vdots \\ \overline{E_n} \end{bmatrix} = \begin{bmatrix} 0 \\ \vdots \\ \overline{I_J} \\ \vdots \\ 0 \end{bmatrix} \qquad 3.28$$

Where I_j is the fault current at node j and the voltages at the network nodes are unknown. To solve the system, the nodal admittance matrix is inverted, and we obtain the following system:

$$\begin{bmatrix} \overline{E_1} \\ \vdots \\ \overline{E_J} \\ \vdots \\ \overline{E_n} \end{bmatrix} = \begin{bmatrix} \overline{Z_{11}} & \cdots & \overline{Z_{1J}} & \cdots & \overline{Z_{1n}} \\ \cdots & \cdots & \cdots & \cdots & \cdots \\ \cdots & \cdots & \overline{Z_{JJ}} & \cdots & \cdots \\ \cdots & \cdots & \cdots & \cdots & \cdots \\ \overline{Z_{n1}} & \cdots & \overline{Z_{nJ}} & \cdots & \overline{Z_{nn}} \end{bmatrix} \begin{bmatrix} 0 \\ \vdots \\ \overline{I_J} \\ \vdots \\ 0 \end{bmatrix} \qquad 3.29$$

The fault current can then be written as:

$$\overline{I_J} = \frac{\overline{E_J}}{\overline{Z_{JJ}}} \qquad 3.30$$

Where E_j is the Thevenin voltage before the fault. The short circuit power at the node j is obviously given by:

$$P_{cc,j} = \left|3\overline{E_J}\overline{I_J}\right| = \left|\frac{3\overline{E_J^2}}{\overline{Z_{JJ}}}\right| = \left|\frac{V_n^2}{\overline{Z_{JJ}}}\right| \qquad 3.31$$

The Monte Carlo Method

The Monte Carlo method is a particular method of numerical resolution [39]. The Monte Carlo approach can be applied to various fields and aims not to solve a problem in a closed form or in its entirety, but to numerically approximate the result through a series of statistically relevant calculation attempts. This approach is useful when a problem cannot be tackled in its entirety, but one tries to reduce it to a representative subset. This type of calculation is more precise the larger the space of solutions investigated and its effectiveness for functions that have good behavior is ensured by the Central Limit Theorem [40]. This methodology was developed in the 1940s by scientists of the Manhattan Project for neutron collision problems [41].

This is an approach that is used in many different fields and was born from the need to solve stochastic and combinatorial problems where the number of variables and the size of the problem make an exact resolution of the problem computationally too expensive. In the field of electrical engineering, it is used for system reliability studies and planning studies. In both cases, these are studies that involve many stochastic variables and their complex interaction. As regards reliability studies, a Monte Carlo approach allows simulating the overall degree of system reliability, given that the reliability of the individual components and the probability of certain failures occurring are known or estimated. As regards planning studies, Monte Carlo methods are used by both manufacturers and TSOs. Manufacturers must consider the evolution of loads, raw material costs and the availability of non-programmable sources [42,43]. Transmission network operators, in addition to considering the evolution of loads, must also consider the availability of producers dependent on raw materials, the availability of wind, solar and hydro sources, and the investments made by producers [44–46]. These analyses aim to obtain various load and generation scenarios that the TSO will have to face.

Although in this thesis a formally rigorous Monte Carlo method has not been strictly used, the philosophy of reducing the problem to a representative subset of cases has been applied several times, in different phases of the study.

Chapter 4 – Reactive Power Planning in the Scientific Literature

In this section, we will discuss planning techniques for securing reactive power requirements for the grid. As early as 1989, CIGRE published a report with guidelines for reactive power resource planning [47]. Given the lower cost of reactive power control equipment, RPP always came after a planning phase more focused on active power. Already in the CIGRE report, several techniques were identified to model and solve the RPP problem such as: sequential load-flow, optimal-power flow, linear-programming techniques, non-linear-programming techniques, and mixed-integer-nonlinear-programming. These various formulations of RPP have different levels of complexity, different network representations and different boundary assumptions. In the following, we look at the most interesting approaches and case studies over the years with a closer look at the most recent publications.

Let us briefly recall that the problem of reactive power planning is a MINLP programming problem where:

- For each possible installation is used a binary variable that determines its construction, this variable multiplies the reactive power delivered (also a variable to be identified) increasing the complexity of the problem.

- Wanting to make robust optimisations, it is necessary to test the effectiveness of the regulation means on various scenarios, which linearly increase the number of equations and constraints.

- These types of problems are very complex to be solved, and the computational complexity always increases more than linearly.

By taking account these topics, the approaches used have been varied over time as the knowledge about them, the technologies available and the boundary conditions have changed.

- In [48] (1987) a Benders decomposition approach has been used to reduce the complexity of the problem. As already mentioned, the RPP problem belongs to the category of the MINLP problems. The Benders decomposition transforms a mixed-integer nonlinear programming problem in a sequence of nonlinear continuous problems and mixed-integer linear problem [49][50]. Since then, this method has been widely used for the RPP. This approach allows a considerable reduction in the problem's complexity without compromising the correctness of the result. This was way more fundamental when there was less computational power available. Applying the Benders decomposition to the RPP transforms the whole problem into a first problem and a second problem. The first one is a nonlinear continuous problem which represents an optimal power flow. The second problem corresponds to a linear mixed-integer problem which aim is to determine the installation of the reactive power sources minimizing the cost. This second problem has constrains known as “Benders Cuts” which derive from the first problem analysis. Also, it’s interesting to note that the cost function of the reactive power sources can have a fixed cost and a variable one, this well represents the reality of the problem where the fixed costs represent the auxiliary systems for connecting the equipment to the busbar and the linear cost is linked to the rated power of the equipment. The authors also included an analysis of the most severe fault cases. The proposed strategy has been applied two times to the IEEE 118 case grid and to a 1079 bus case grid. Nevertheless, different simplifications were performed to execute the calculations. The representation of the grid where simplified linearising the load-flow equations and decoupling the active and reactive power. This is a well-known technique is called Carpentierr’s method [51] and it is used to reduce the computational time of Load-Flows and optimal power flows calculation accepting a small error. Also, an important limit was that the study took in account a single generation-load scenario.

- A second interesting approach has been performed in [52] (1988). Here the authors approached the problem differently with successive Linear problems. After an initial load-flow analysis they built a linearised model of the grid without decoupling the active and reactive power. Also, the integer variables were linearized. This allowed a massive speedup in computational time at the cost of a considerable post-process to discretize the linearized variables. This system was applied to the IEEE 30 and a practical 224-bus network. Also, this study has the limit of the single load-generation scenario.
- In [53] (1997) an Evolutive Programming algorithm[54] has been used to solve the reactive power dispatch problem. In this study the authors compared the performance of a EP algorithm with the Broiyden’s method[55] in solving a reactive OPF. The EP algorithm belong to the meta-heuristic optimization algorithms and are the precursors of the genetic algorithms. The Broiyden’s method on the other hand is a gradient-based algorithm like the Newton-Raphson one used in nonlinear continuous problems. The

two methods were applied to the IEEE 30-bus gid with interesting results, the EP method showed a better convergence than the analytical method, paving the way for a more abundant application of meta heuristic algorithms in the reactive power dispatch problem. The study has two main limitations: it considered different discrete constants as though they were continuous and resolves a single scenario.

- In [56] (1995) an interesting study has been done upon the Italian Power grid. In this paper the authors proposed a new approach to the reactive power flow to consider two different types of faults: the loss of transmission capacity and the loss of generation capacity. The problem has been faced developing two consecutive ORPF by linearising the fault condition around the steady state condition before the fault. The main ORPF problem has not been linearised and has been solved with the Han Powell algorithm. The system has been tested on a small CIGRE test network and the full 400/230 kV Italian network. The main limitation of this study is that the method proposed were more a tool for verifying the effectiveness of a certain reactive power configuration in a single active-power scenario. Although it has been an interesting algorithm then used for on-line grid security verification in the Italian national control system.
- In [57] (1999) has been proposed a three-level strategy for reactive power planning. The first stage aimed to the creation of different scenarios. The second stage performed the optimization were:
  - the upper level was a binary-encoded GA with a particular mutation operator (Lamarque operator) which determined the optimal position of the reactive power sources.
  - The lower level was composed by a sequence of linearized, decoupled load-flows which computed the size of the reactive power installation.
  - The lower level computed the performance o the solution, which was the investment and operational cost.

  This study was also applied to an interesting network. The case study was a Venezuelan 63 network portion composed of three different voltage levels 765/400/230 kV. The study proved the efficiency of the GA in a multi-level optimization procedure has a tool for reactive power planning.
- In [58] (2004) a hybrid evolutive algorithm has been used to tackle the RPP problem. In this case the method was tested on the IEEE 30-bus network. The peculiarity of the method has been the introduction of a penalty function to guide the optimization algorithm without limiting the domain. In order to simplify the problem, only four

locations were available for the installation of the reactive power problem and the method is more suited for a ROPF than for a RPP problem.

- The review made by Zhang et al. in [59] (2007) contains an interesting perspective on the work done so far. It can be seen that the majority of the approaches to the RPP problem were based on mathematical programming than on meta-heuristic algorithms or a combination of the two approaches. This means also that the reactive power planning problem are actually reactive OPF. The approaches were different from a simpler linear programming representation of the problem to a complete MINLP. Almost all the works focused on a single objective with around many constrains. The most common objective function is the minimization of the cost in different forms: variable VAR sources use cost, fixed VAR sources cost, fuel cost. In Fewer cases the objective were linked to electrical magnitudes such as a specific voltage schedule, the maximization of the voltage stability margin, or the voltage deviation. According to the objective, to the constrains and if there are fault scenarios, we can have a simple OPF, Security Constrained OPF (SCOPF), or Voltage-Stability Security-constrained OPF(VS-SCOPF). The two main used meta-heuristic algorithms for RPP have been so far evolutive Algorithm and tabu search. Furthermore, there are some papers that make use of fuzzy decision-making logic in order to address load and costs uncertainties. The authors ended concluding that more research was needed on the meta-heuristic algorithms since they allow to pursuit different objectives at the same time and reduce the problem complexity.
- In this regard the authors in [60] (2012) use a Genetic algorithm to tackle the RPP problem. According to the authors the main advantage of the genetic algorithm is the coding simplicity and capability to handle more objectives at the same time. Although they wanted to consider three different non-homogeneous objectives (voltage stability, voltage deviation and the SVC installation cost) they made a linear combination of objectives. The most interesting part of the work is that the authors considered a 140 bus System with many wind turbines. They focused on the modelling of the Double Fed Induction Generators (DFIG) of the wind turbines to highlight their limited contribution to the voltage regulation. The optimization procedure was a two-step process where the upper optimization algorithm was the GA. The GA's optimization variables were the site an size of Static Var Compensators (SVC) then a lower OPF was used to obtain the best control variable for the power grid in different active power scenarios. This has been one of the first papers to consider the implication on reactive power planning of

renewable energy systems in the transmission system. Also, the use of this optimization scheme allowed the consideration of many load and power generation scenarios.

- In [61] (2013) has been highlighted the need to reconsider some aspect of the transmission expansion planning. In this review has been noted as the shift from a regulated power sector to a de-regulated one brought new hypotheses an uncertainty on the Transmission expansion planning problem. The main aspect is the evolution of the production sector which can't actually be programmed but brings new uncertainty. This also influences the RPP problem.
- In [62] (2014) a multi objective differential evolution algorithm with self-tuned parameter has been used to face the reactive power problem. The study proposes a single stage optimization where the meta-heuristic algorithm has to optimize the installation position and size with all the control variables of the power grid. This approach allows the authors to use a representation of the grid really complex and precise. The OPF had full control over the generator's voltage, the transformers' tap ratio, and the reactive power of the SVC. Since they are performing a multi-objective optimization, they introduced a selection operator based on rank (see Chapter 7) and solutions' density to obtain a smooth and continuous Pareto frontier. The voltage stability is evaluated through the L-index and used as a constrain. Since the number of variables handled by the only optimization layer was vast, the computational time was considerable and had to examine only few load and fault scenarios.
- In [63] (2015) the reactive power planning problem has been treated again with a mathematical programming approach but with different conditions. The study has been conducted to take in consideration the effect of high wind penetration. It has been developed a multi-scenario (VS-SCOPF) to face multiple aspects of the problem. First of all, a great attention has been posed to the generation of many generation and load scenarios according to the wind conditions. Then, to reduce the problem's size, the active power scenarios have been reduced to a representative set. From these representatives' active power scenarios, the worst fault for each scenario has been considered. Then has been taken in to account the voltage stability of the faut scenario. This scenario generation and then reduction approach allowed to consider different load conditions. The problem has then been modelled as a MINLP problem with a minimum cost function and a voltage stability constrained. The problem has then been solved through the Bender's decomposition. The new focus on the renewable energy sources is becoming more and more common through the years.

- Also, in [64] (2020) has been used a mathematical programming approach: the authors created a modular model called LEGO to study the impact of different hypothesis on the optimization result. The model can consider many aspects of the electric grids as: the generation expansion, the reactive power compensation expansion, the energy storage, the frequency stability and the unit commitment. The problem in its general form should be a MINLP problem but under some assumption has been transformed in a MIQP (Mixed Integer Quadratic Problem) which can be resolved with the *second-order-cone* approach. The model has been developed to consider all these aspects at the same time to see how facing these problematic at the same time or separated influences the costs. A great attention has been posed to the impact on the system inertia. Due to the complexity of the model has been possible to analyse a grid that was composed by only 9 busses and for a time horizon of 7 days. A system so small and with this time horizon led to a MIQP problem with 168.000 variables. At first they used the transmission expansion module to see the impact of the inertia on the renewable penetration. According to their study to maintain an acceptable ROCOF (rate of chance of frequency) the renewable penetration in their grid can't exceed the 80% of on-line generation. This threshold can be overcome only installing synchronous condensers or accepting to rely on *virtual inertia*. Another interesting aspect has been the investigation of the effect of considering the reactive power requirements in the generation expansion planning. From their research emerges that considering the two aspects in two distinct optimization phases instead of in the same single-stage optimization leads to a total cost increase of only 1.5%. This is an interesting insight that told us that the active power planning and the reactive power planning can be decoupled with little harm. This is mainly due tu the great difference in investment costs between the power plant and the reactive power sources. One last interesting information is that according to their model and their costs the minimum-cost energy mix leads to a 33% percent share of renewable energy. This means that any increase in the renewable energy installed sources brings extra costs for the system. The market has its balance point at 33% renewable share and any modification needs external incentives. The major problem in this study is that the short-circuit power is not considered.
- In [65] (2020) a new hybrid approach has been used. In this approach there is a preliminary study of the grid before using a crow search algorithm to obtain the most economical set of reactive power compensation measures. At first the authors select the nodes that have the biggest power consumption with no generators in the location. Then

they individuate the nodes with the major loss of sensitivity and finally they analysed the Jacobian of the load-flow to see the nodes where the voltage is more sensible to the reactive power injection (a.k.a. least short circuit power). After they spotted the most critical nodes, they used this information to reduce the number of candidate nodes for reactive power compensation. They used a multi-objective function trying to minimize: the shunt reactor cost, reactive power cost and the line charging cost. The limitation is that the position of the on-line generators is not known a-priori in a free-market context, and this leads to substantial changes in the Jacobian matrix.

- In [66] (2020) a different mathematical programming approach has been proposed using the epsilon-constrained method. This approach allows to solve multi-objective problems through mathematical programming without using any meta-heuristic algorithm. With this approach the problem is recursively resolved through different linear combinations of the different objective as thought is a single objective problem. They also considered the uncertainty o renewable energy production and use the L-index to estimate voltage stability and the loadability factor. The method has been applied to the IEEE 30 bus system. Once obtained the Pareto frontier a fuzzy decision maker has been used to select the best solution.
- In [67] (2021) the RPP problem has been tackled with an hybrid PSO-virus colony algorithm. The case study was referred to a grid with high wind penetration. Major attention was given to the lower capability of wind turbines with a power factor between 0.98 in advance and 0.96 in retardation. The pre-posed reactive power compensation means are TCSCs and SVCs. Again, a preliminary analysis was conducted on where to install the means for compensation by study of L-index and voltage volatility. The optimization conducted was multi-objective type aimed at minimizing losses, voltage fluctuations and voltage stability. As the last step of the method, a fuzzy decision maker was used to choose the final solution.
- In [68] (2021) has been used a new hybrid algorithm based on differential evolution and crow-search. The authors proposed a method to find candidate nodes for compensation base on: loss of sensitivity analysis, power-flow analysis and modal analysis. They then developed multiple load scenarios and searched for a minimum cost solution.
- In [69] (2021) an approach that is becoming commonplace was presented: preventive network analysis followed by actual optimisation. Candidate nodes were chosen with multiple criteria: the fast voltage stability indicator, the line stability factor, the line stability index, the voltage collapse stability indicator, the L-index and the modal

analysis. The optimization algorithm used is a hybrid between PSO and crow search. A comparison of multiple optimization algorithms is also performed. These algorithms act on both the interventions and control variables network by de facto solving an OPF. The adopted networks were IEEE 30 and IEEE 57.

- In [70] (2022) two new algorithms have been used: the imperial colonist algorithm and the gravitational search algorithm. The authors built different scenarios to cope with the real-time uncertainties. The two algorithms have been used on the IEEE 24 and 118 bus systems.
- In [71] (2022) the Harris Hawks algorithm has been used for the RPP problem. The optimization carried out has been multi-objective trying to minimize the power losses, the operating costs and the voltage profile. The algorithm has been used on the IEEE 57 grid in a 100 hours scenario.
- In [72] (2022) a probabilistic hybridization between the crow search algorithm and the JAYA was made to solve the reactive power planning problem. The method involves the detection of weak nodes through loss of sensitivity analysis, power flow analysis, modal analysis, fast voltage stability index and collapse proximity indicators. The algorithm was used to optimize the cost losses, the Var source costs, the var generation cost and the line charging cost. The authors studied different scenarios un two different networks: the IEEE 30 bus system and the 75 bus UPSEB power grid. The installed components were various types of FACTS.
- In [73] (2022) the authors used the moth-flame algorithm. They used the L-index indicator to detect the weak nodes and the reactive power flow analysis to detect sensible lines to install TCSC. In this case, the installation is done on this analytical analysis and the optimization algorithm determines only the control variables. The method is tested on the IEEE 57 bus system.
- In [74] (2023) a transmission expansion planning problem is considered. In this work the system is modelled in AC with the second order cone relaxation. The authors claim that the reactive power is poorly considered in the transmission expansion planning problem. This is true but is a good practice to set a limit to the problem complexity. Nevertheless, their work is interesting because they considered also HVDC links and storage systems in the TEP problem. They divided the problem in two layers: the first aims to determine the HVDC connection and the storage entity. They studied various scenarios for the graver’s six bus system and the Jiangxi power grid in China. In their study most of the final cost is determined by the HVDC systems and the storage systems.

- In [75] (2022) a security-constrained AC dynamic transmission expansion planning with reactive requirements has been developed. The Authors used a complex hybrid algorithm mostly based on the Differential evolution algorithm but with contamination from the random search algorithm, the chaos theory algorithm and local search. To handle the complexity of the reactive phenomenon and the dynamic ones a hierarchical bi-level strategy has been adopted to contain the system complexity. The upper layer tried to optimize the transmission expansion intervention and the lower optimized the gird setpoints. They studied only few dynamic events and studied three different power grids: the Graver's 6 bus network and the IEEE 24 and 118 bus grids.
- In [76] (2023) the authors used a grey wolf algorithm to determine the optimal location of capacitor banks in a radial distribution grid. The model of the grid is greatly simplified by its radial structure. The most interesting aspect is the use of the Monte Carlo approach to consider the renewable energy sources and load variability. They used a multi-step approach with the sensitivity analysis. The grid used was the IEEE 33 bus system.

The following are the most widely used networks:

- Graver's 6 bus grid: [75]
- Custom: 9 bus [64]
- IEEE 14 [63]
- IEEE 24: [70] [75]
- IEEE 30 [52] [58] [62] [66] [69] [72]
- IEEE 33: [76]
- IEEE 39 [65]
- IEEE 57 [62] [65] [69] [71] [73]
- IEEE 118 [48] [65] [70] [75]
- Cigre test network: [56]
- Real networks: 1079 bus [48], 224 bus network [48], Italian network (1994) [56], Venezuelan 63 bus network [57], existing 140 bus network with many wind farms [60] [67], 62 and 191 bus Indian networks [68], 75 bus UPBEB power grid [72]

Methods used are shown below:

- Mathematical programming:
  - Benders decomposition [48] [63]
  - Broiyden's method [53]
  - Successive linear programming [52]
  - Linearized loaf-flows [52] [56] [57]
  - Secon order cone: [64]
- Meta-heuristic optimization:
  - Evolutive programming [53] [58]
  - Genetic algorithm: [56] [60]
  - Differential Evolution [62] [68] [75]
  - Crow Search algorithm: [65] [68] [72]
  - JAYA: [65] [72]
  - Sine-cosine algorithm: [65]
  - Particle Swarm: [65]
  - Virus colony [67]
  - Hawk Algorithm: [69]
  - Imperialist competitive algorithm: [70]
  - Gravitational search algorithm: [70]
  - Harris Hawks [71]
  - Moth-flame algorithm [73]
  - Grey wolf Algorithm [76]
- Fuzzy decision making: [66] [67]

The most common objective functions are the following:

- Single objective
  - Investment cost [48] [52] [53] [56]
  - Min total cost (losses+investment): [57] [58] [63] [64] [68] [75]
  - Minimize losses: [73]
- Multi objective:
  - Linear combination of objectives [60]
  - Two objectives: [62]
  - Three objectives: [65] [67] [60] [72]

Other features:

- Articles that consider the effect of faults: [56] [63] [75]
- Articles that consider high renewable penetration: [63] [67]
- Articles that use the sensitivity analysis: [65] [67] [68] [69] [72] [73]

Main limits:

- Single scenario [48] [52] [56] [57] [60] [65] [69]
- Two load scenario: [58]
- Limited VAR sites: [58]
- Grid Linearization [52] [57]
- Integer variables linearized [52] [58]
- More a reactive OPF than a reactive power planning [53] [56] [62] [69] [73]
- Linear combination of different objectives with arbitrary weight [60]
- Model too complex for a large grid [64]

In conclusion, we can observe several trends:

- The increase in computing power over the years has led to more and more varied and elaborate algorithms adding analysis of certain faults and more and more scenarios. The use of mathematical programming techniques makes it possible to consider several objectives at the same time because of great complications and simplified models. The use of meta-heuristic algorithms has made it possible to both pursue multiple objectives and use larger models. The division of the problem into several levels reduces its complexity.
- A critical reading of the literature shows that short-circuit power is never considered, whereas over the years TSOs have seen a constant reduction in fault current and an extension of disturbances and voltage-drops until it was necessary for them to install synchronous compensators.
- Where it is done, the use of sensitivity analysis does not consider the change of position of the generators and their actual capability, which for wind and photovoltaic sources are dependent on the power output. This needs at least to re-think the use of this technique by using chronological series.

This led us, on the one hand, to a necessary inclusion of short-circuit power and, on the other hand, not to use the sensitivity analysis but rather the analysis of the duration time curves of the voltages at the nodes.

Considering the short-circuit power evaluation involves the inversion of the admittance matrix for each generator configuration, this excludes the use of mathematical programming techniques.

From these considerations, it was decided to opt for a multi-level method structure to reduce the computational complexity. At the same time, it was decided to create a multitude of different generation and load scenarios to represent the greater variability introduced by non-programmable renewable sources. In order to be able to handle all these cases, it was decided to treat them individually by running a series of hourly ACOPFs. To handle the two-level strategy and the inability to use mathematical programming techniques a meta-heuristic approach has been chosen.

Among the test networks, the IEEE case 24 was chosen. Although the IEEE 30 network has been more widely used, case 24 has a higher voltage level and is more similar to the transmission networks in the focus of our attention.

Chapter 5 – Measures and Installations for Voltage Regulation

The components of the electrical system that can contribute to the grid's reactive balance are manifold. Since, as seen in Chapter 3, the active power flow alone alters the reactive balance of the lines, and thus of the grid, all components can contribute to voltage regulation. In the following, we will only briefly mention the least impactful measures and go into more detail about the other most effective resources a TSO can resort to.

As already mentioned, altering active power flows changes the reactive requirements of lines; this can be done by a TSO in different ways and with different associated costs:

- By connecting its own resistors in a station: this measure, easily implemented by the TSO, involves both the cost of the resistors and the energy associated with their use. Due to the increase in active power flowing through the network, there is a slight increase in the reactive requirement of the lines. This measure has a minor effect on the grid and in fact the resistors are installed in the transmission grids and operated for other purposes. They are usually used as a means of frequency regulation, to counteract the formation of ice sleeves on low-load mountain lines, and to limit wind power failures. Nevertheless, it is an inexpensive means if resistors are already available to alter the reactive balance of the lines.
- Change of active power dispatch: this measure involves buying down and up power services from producers or consumers at strategic points in the grid in the ancillary services market. This makes it possible to both load and unload lines by altering their relative active balance. This measure is rather expensive and again not very effective. In fact, the change of dispatch is generally used to solve congestion rather than to alter the reactive balance of the network.
- - Use of series capacitors (also Tyristor Controlled Series Capacitors) TCSC: this measure, by changing the series reactance of the line where compensation takes place, causes both a change in the power flow of the network and the insertion of a series capacitive component. This measure, as series capacitors are handled entirely by the TSO, does not entail any additional operating costs and is quite effective.

- In-phase and framing boosters: These are systems consisting of transformers with ratio converters that have windings both in shunt and in series to the lines. Depending on the internal structure of the transformer, this can add either a phase or a quadrature component to the line voltage. This results in both the possibility of varying active power flows and absorbing or delivering reactive power. However, these components are very difficult to operate and are little used.
- Use of UPFCs: Unified Power Flow Controllers are particular systems of transformers and converters that allow the active power flow at the ends of the line to which they are installed to be varied. This involves both a change in the power flows on the network, in particular on the line ‘controlled’ by the UPFCs, and the inductive elements of the UPFCs themselves.
- Transmission network degaussing: this measure allows the reactive energy produced by the lines to be reduced at low loads. For reasons of safety and continuity of service, it can only be implemented at low loads and in moderation in order not to lose robustness to faults and safety in n-1.

Direct action on reactive power:

- Change of voltage setpoints: this measure involves changing the voltages imposed on the generators and the associated change in reactive power produced. This is a cost-free measure if left to the active generators that are obliged by the grid code to provide the voltage regulation service [77].
- Switching on a generator to contribute to the reactive balance: a TSO can request the switching on of a generator in an area that requires regulation of reactive power, and therefore voltage, via the ancillary service market. This measure allows a very effective timely intervention but entails an exorbitant cost by having to resort to offers from the ancillary services market for the switching on and commissioning of a generating unit.
- Tap staggering: this measure is implemented by the TSO using autotransformers and transformers in parallel. Tap staggering involves the parallel operation of two regulated transformers on different sockets. By setting the voltage on the primary side and using different voltages on the secondary side, a circulating current is determined which, as it passes through the transformer windings, results in reactive power being absorbed. This measure is only feasible under low load conditions when the transformers work far below rated power but allows reactive power absorption in the order of a hundred MVAr.
- Use of the TSO's own resources for the injection or absorption of reactive power: If the TSO possessed elements in its stations capable of absorbing or supplying reactive

power, it could make use of them without paying third parties. Within these components we find both rotating machines, static converters and other network components and their various combinations.

Having now given an overview of the various operational measures that a transmission system operator can resort to, we will go into detail on the technological aspects of the most effective and economic measures:

- **Synchronous condensers**:
  - These components are in fact synchronous machines with excitation windings that run on no-load, i.e. they are connected neither to a prime mover nor to an operating machine. Thanks to the rotor windings, these machines generate a magnetic field which, due to the laws of electromagnetism, aligns with the rotating magnetic field induced by the mains voltage on the stator when the machine is connected without a prime mover. The rotating magnetic field of the rotor, in phase with that of the stator, generates an induced electromotive force in phase with the mains voltage. Knowing, therefore, that the electromotive force is in phase with the mains voltage, the complex phasor equation of the equivalent circuit of the infinite power generator-mains system can be reduced to a real equation.

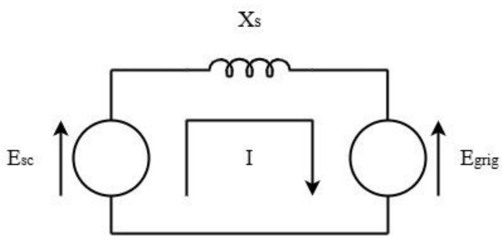

Figure 5.1 - Simplified scheme for synchronous condensers behaviour

$$Q = 3\, E_{grid} \frac{E_{sc} - E_{grid}}{X_s} \qquad 5.1$$

  - *Over and Under excitation Behaviour*. From the expression of reactive power, we divide the generator's operating plane into two zones: overexcitation and underexcitation respectively. In over-excitation we have that the internal machine voltage is higher than the terminal voltage and then the generator delivers reactive power (it therefore behaves like a capacitor). The operating limit is imposed by the limits of the rotor and stator currents.

In underexcitation behaviour, the internal voltage is lower than the terminal voltage and the compensator absorbs reactive power (thus behaving as an inductor). The maximum under-excitation operation is when the excitation voltage is zero and the generator consists in a synchronous reactance alone. The fact that the value of the reactive power that can be absorbed by the generator depends on its synchronous reactance imposes an important choice in the construction technique of synchronous compensators. These, in fact, can have either a smooth rotor or a salient pole rotor. Due to the greater presence of air inside the machine, salient pole rotors have a smaller synchronous reactance and can therefore absorb more reactive power under overexcitation.

- *Stabilising effect on the voltage*: as is well known, synchronous compensators exchange reactive power with the grid because they can impose an electromotive force at their terminals. This mode of interaction with the grid results in a stabilising effect for the voltage, i.e:
    - As can be seen from equation 5.1, when there is a voltage drop on the grid side, the reactive power delivered by the synchronous compensator increases. Since the Thevenin equivalent impedance of the transmission grid is inductive, the increase in inductive power delivered by the compensator ‘sustains’ the voltage.
    - Similarly, when there is a rise in mains voltage, the synchronous compensator absorbs more reactive power and this counteracts the rise in mains voltage.
- *Short-Circuit Power*: An intrinsic characteristic of rotating machines that is fundamental to the proper functioning of the network is their contribution to short-circuit power. The special behaviour during electromagnetic transients of these machines means that during faults they support voltage. This has two beneficial effects for the network:
    - They increase the short-circuit current, which is necessary both for the proper behaviour of the system protections and for reducing the spatial extent of disturbances due to faults.
    - A high short-circuit power value leads to less propagation of voltage harmonics in the network.

- *Increased inertia*: Since the rotor of these machines rotates synchronously with the mains and the electromagnetic torque is proportional to the angular difference between the rotor and stator magnetic fields, the mechanical inertia of the rotor helps to stabilise the frequency. In order to increase the frequency-stabilising effect, the inertia of the rotors can be increased by fitting flywheels to the shaft.

It is evident from the above features that synchronous compensators are indispensable components of the electrical system.

- **Voltage Source Converters**: VSCs are static AC/DC converters that can regulate the voltage both in phase and in quadrature to the mains voltage. They are usually connected to the grid via an AT/MT transformer that interposes its short-circuit reactance between the grid and converter voltages. The equation that determines the reactive power delivered by the VSC is the same as 5.1, but the reactance interposed between the VSC and the grid depends on how it is connected to the grid and has values far less than the synchronous reactance of the compensators, so they can absorb as much reactive power as they can deliver. These converters, like the synchronous compensators, have a stabilising effect on the mains voltage. Being electronic components, they can be controlled very quickly and have a very fast response. Unlike synchronous compensators, these converters do not 'naturally' contribute to short-circuit power and frequency stabilisation but must be specifically controlled to contribute to network stability. In the event of a short-circuit near the converter, it can be commanded to increase the voltage at its terminals; however, this contribution must be very limited in time and a voltage above 1.4 p.u. cannot be commanded. This is due to the very low thermal inertia of static converters, which leads to a rapid rise in temperature of the semiconductor junctions where most losses are concentrated. During a frequency transient, in addition to a specific control system, the converter must have an adequate energy reserve. This can be provided by means of a storage system at the DC bus of the converter. In this way, the converter can both feed power during an under-frequency transient and absorb it during an over-frequency transient. This contribution to the frequency transient can be made in different ways depending on the control system implemented. Either a proportional-integral contribution can be made as for primary frequency regulation, or a 'derivative' contribution proportional to the frequency variation as for the inertia torque of synchronous compensators. This second behaviour, much studied in recent years, is known as ‘synthetic inertia’.

In addition to the cost associated with accumulators, this implementation of ‘synthetic inertia’ entails several technical difficulties in the control that must measure the variation of a quantity, namely frequency, which is very difficult to define during a transient. A notable advantage of VSCs is the possibility of controlling them to ‘absorb’ specific harmonics. This is undoubtedly an advantage when one is in the vicinity of specific harmonic sources (such as arc furnaces or older converters) that one wants to counteract without increasing the short-circuit current.

- **Shunt reactors**: these are inductive components that are widely used in high and medium voltage. By absorbing reactive power, they are widely used for compensating cable lines and long overhead lines. From a constructional point of view, they consist of either a single three-phase component with a five-column core or three single-phase units. This is necessary to avoid transformer coupling between the phases. This is not detrimental in symmetrical regimes but leads to various problems in dissymmetrical regimes. In particular, during a single-phase opening, the healthy phases would continue to energise the faulty phase, preventing a fault from being extinguished. Another design feature is the possibility of having a ratio variator. This component by varying the number of turns of the reactor would change the impedance and thus the reactive power absorption. Variators usually allow power steps of 5%, up to 40% reduction of the reactive power absorbed by the reactance. As with the synchronous compensator, the effect on the voltage of the shunt reactor is stabilising, because following an increase in mains voltage it would increase its reactive power absorption, thus counteracting the increase in mains voltage.
- **Tyristor-controlled Reactors**: Tyristor-controlled shunt reactors are possible. By varying the switching angle of the tyristors and by biasing the voltage, it is possible to fine-tune the reactive power absorbed by the reactors. As above, tyristor-controlled reactors also have a ‘stabilising’ effect on the voltage. A major advantage over reactors with an underload ratio variator is the rapidity of control afforded by tyristors: the absorbed power can be varied within a few mains periods.
- **Shunt capacitors**: Shunt capacitors are the most economical means of producing reactive power for the grid. In the HV grid they are mainly used at high loads to supply reactive power to lines or to supply reactive power to LCC-type HVDC links.

Being shunt components, their reactive power depends on the square of the voltage. This leads to an anti-stabilising effect. This is because as the mains voltage increases, they would tend to produce more reactive power and thus, given the inductive behaviour of the mains, support the voltage increase. Conversely, as the mains voltage decreases, they would produce less reactive power, thus decreasing their contribution to the voltage increase. These components cannot be biased, but only switched in steps.

- **Static Var Compensators**: SVCs are systems consisting of a controlled reactor tyristor with a capacitor bank in parallel. The two elements can be operated separately and due to the biasing of the reactor tyristors, it is possible to switch seamlessly between purely capacitive and purely inductive behaviour. Along with these main components, there is usually also a bank of filters to reduce harmonics due to the switching of the reactances. The maximum capacitive and inductive reactive powers are the nominal powers of the capacitor bank and the reactance. This system can be equipped with a control loop which, in capacitive operation with biased reactance, reduces the ani-stabilising effect of the capacitors.

Chapter 6 – Methods and Instruments

In order to ensure a secure and stable transmission grid, both from the point of view of short-circuit current and voltage stability, the following methodology is proposed in this chapter. This methodology aims to identify the most effective set of investments to guarantee TSOs the adequacy and security of the grid considering the major changes the electricity sector is undergoing.

The methodology consists of two main parts, the first is aimed at creating generation scenarios that are intended to be as representative as possible of the evolutions of the electricity system as a generation park and transmission system. This first phase is basically an active power planning where only the change of the generation park or even grid developments can be considered. In fact, it is intended to generate the generation and grid structure scenarios to be exercised by the TSO.

The second part of the methodology takes as input the production scenarios and network structure identified in the first phase and identifies the best set of measures to ensure voltage stability and protection selectivity while making as little use as possible of the ancillary services market

This procedure was mainly developed in the Python programming language. In addition to the code produced for this study, various libraries were used, both for data analysis such as Pandas, matplotlib and NumPy and specifically for modelling and analysing electrical systems such as Pandapower and PyPower.

Python

Python [78]is a versatile programming language widely used in scientific calculations and research due to its simplicity, readability, and extensive ecosystem of libraries. is a high-level, general-purpose programming language [79]. Its design philosophy emphasises code readability with the use of significant indentation.

Python is dynamically typed. It supports multiple programming paradigms, including structured (particularly procedural), object-oriented and functional programming. It is often described as a "batteries included" language due to its comprehensive standard library.

With libraries such as NumPy and SciPy, Python provides powerful tools for numerical computing and scientific calculations, enabling researchers to perform complex mathematical operations and data analysis efficiently [80].

Additionally, Python's data visualization libraries, like Matplotlib and Seaborn, allow scientists to create insightful visualizations, helping them interpret their data more effectively.

The language's interoperability with other programming languages and its strong community support further enhances its suitability for scientific research, making Python a popular choice among researchers for tasks ranging from data manipulation and statistical analysis to machine learning and artificial intelligence applications.

Pandapower

Pandapower [81] is a Python-based open-source library specifically designed for the analysis and optimization of electric power systems.

It provides a user-friendly, high-level interface that simplifies the process of modelling and simulating electrical grids, making it particularly valuable for researchers, engineers, and analysts in the field of electrical engineering.

Pandapower integrates seamlessly with Python's rich ecosystem of scientific libraries, allowing for robust data analysis and visualization.

The library supports a wide range of power flow calculations, short-circuit analysis, and optimal power flow solutions, both distribution and transmission networks. It was tested with many CIRGRE [82]and IEEE [83]networks which are included in the default library[84,85].

Additionally, pandapower's modular architecture and extensive documentation make it an accessible tool for users of varying expertise, facilitating the study of power systems from both a theoretical and practical perspective. Its popularity and continuous development[86,87] made it suitable for the study. Pandapower has also a module for the short-circuit power calculation [88] which uses the model contained in the DIN/IEC EN 60909 [38] standard. The modelling of the load-flow problem and the OPF are in polar coordinates as shown in Chapter 3.

The Developed Methodology

The final aim of this work was to develop and test a methodology that would provide TSOs with the optimal set of investments to ensure proper voltage regulation and sufficient short circuit power. To this end, an attempt was made to reproduce as closely as possible the mechanism and context in which a TSO operates.

The aim was to create a simulation of grid operation by distinguishing between 'cost-free' actions that can be performed by the TSO and actions that require an operating cost.

During the real-time operation of a grid, the TSO must guarantee active power dispatch over which it has no direct control. At most, this active power dispatch can be determined in such a way that it meets certain security and reliability requirements. As seen in Chapter 3, real-time active dispatch is only subject to a verification of the transit limits between zones, which are imposed by the TSO. Once the active dispatch is determined, the TSO can only change it by using its own resistors (paying for the consumed energy) or the ancillary service market. With regard to reactive power and voltage regulation, the no-cost operations that a TSO can do are:

- Manoeuvre transformers tap ratios.
- Operate its own reactive power control equipment such as: shunt reactors, series capacitors, shunt capacitors, SVCs, FACTS, UPFCs, synchronous compensators etc.
- Imposing a certain voltage setpoint or reactive power supply on production facilities within the limits of their control and capability. With regard to this point, an increasingly frequent trend must be mentioned. The spread of small-scale renewable generation plants (below 10 MW) means that they are less able to regulate voltage, as they are usually connected to the sub-transmission grid and therefore have less impact on the voltage regulation of the transmission grid, and very often do not have either an appropriate control system or a connection to the grid operator through which they can receive information on the voltage setpoint and reactive power output.

If the grid operator has insufficient resources available for voltage regulation, it must resort to the ancillary service market to request the switching on of a generating unit that can contribute to voltage regulation where required.

An ACOPF with the following characteristics was therefore set up to simulate these conditions:

- A very rigid active power dispatch around a predetermined dispatch value.
- Constraints for voltage values at the nodes consistent with the safe operation of the transmission grid.
- An availability of reactive power regulation of generators connected to the grid dependent on generator technology and dispatching.
- The TSO's means of voltage regulation.

This ACOPF is used to evaluate, in relation to a given dispatch, the effectiveness of the voltage regulation means owned by the TSO. When the ACOPF cannot find a grid operation that meets the voltage and capability constraints of the generators, this means that the TSO must resort to the ancillary service market. This module will be called the 'operation simulator'. Solving the operation simulation problem in this formulation involves solving an NLP-problem.

To use this tool effectively, two boundary components are required. The first is an optimisation algorithm that searches for various configurations of means for voltage regulation owned by the TSO. The second is an abundance of active power dispatching that considers as many scenarios as possible.

It should be noted here that it would be possible to integrate the choice of means of reactive power regulation into the ACOPF by switching from an NLP formulation to a MINLP formulation. As seen in Chapter 4, this would entail three problems. The first is a major complication of the model that would prevent it from dealing with extended networks or many scenarios. The second is the impossibility of considering more than one objective at a time. The third is not being able to consider the short-circuit power problem, since its calculation involves inverting the network admittance matrix.

As far as the optimisation algorithm is concerned, it must have the following characteristics: it must be able to follow at least two objectives at the same time and it must optimise substantially discrete variables (the position and size according to the size of the network and the manufacturers' standard sizes). It is true that the sizes could be considered as continuous variables, but in an economy of scale where the TSO must install numerous components, it is advantageous for these to be of the same size both for economy of production and reserve management.

As far as the two mandatory objectives, these are:

- The solution of an NLP that has constraints dependent on the position, type and size of the compensation means.
- The inversion of a matrix where all diagonal elements can change depending on the position of the compensation means.

Given the computational complexity of these two problems and the presence of multiple objectives, it was decided to resort to a meta-heuristic optimisation algorithm.

Given the combinatorial nature of the problem involving a large number of variables where each can assume a very limited range of values, it was decided to resort to the most suitable algorithms for this type of problem, namely genetic algorithms.

Having set the problem to be optimised and the chosen optimisation algorithm, we now briefly look at scenario creation. For reasons of organisation of the research group and in relation to the other active projects and the skills of the individual group members, this part has been given secondary attention. The creation of various generation and load scenarios can be seen as an active power planning problem. This problem accepting the reasonable approximation of modelling the network with DC-LoadFlow becomes a linear programming problem where the variables to be optimised are the installed at the individual nodes of the various technologies and the generation at the individual node's hour by hour by technology. These modelling approaches were extensively developed in the research group I was part of during my PhD so instead of replicating them this stage was developed differently by emulating and verifying the reactive power planning configuration.

In particular, a genetic algorithm was used in pursuit of two objectives: the first was to decarbonise the electricity grid, the second was to minimise cost, producing a variety of dispatching scenarios to be used. This available installed power was combined with photovoltaic and wind power output data to produce a series of DC-OPFs determining hour-by-hour dispatching at minimum cost. This procedure only serves to produce realistic displacements for the grid under consideration on which the optimisation of reactive power generation means can then be carried out. At this stage, it would also be possible to consider possible expansion plans for the transmission grid, but this would not lead to a substantial change in the second stage of optimisation. Let us recall as seen in chapters 3 and 4 that the problems of active and reactive power are both easily decoupled from a mathematical point of view and from a cost point of view [64].

To recapitulate, the procedure consists of two phases as shown in Figure 3.1. In the first step, the following are taken as known: the grid topology, the nodal load (time-varying), the nodal producibility (mainly dependent on wind and photovoltaic producibility) the location of conventional generation plants. These have been kept fixed to simulate current trends in the electricity sector, most new power generation plants are from non-programmable renewable sources and at least in Europe, there is little construction of conventional plants (fossil fuels, hydro, nuclear). This information is used for an active power planning operation performed by a meta-heuristic algorithm that determines the sizes and a series of least-cost DC-OPFs that dispatch the producible energy hour by hour. In the second stage, the previously calculated active dispatch and grid topology are taken as input. Here, a second algorithm determines the location and size of reactive power generation installations and through a series of active-constraned Reactive-OPFs the effectiveness of the installations is determined. The effectiveness of the compensation is determined by assessing how often the ancillary service market must be used to regulate the voltage.

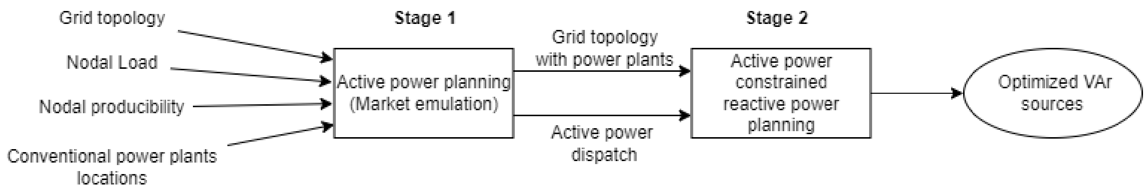

Fig 3.1 - Structure of the procedure

Chapter 7 – Optimization Algorithms

In this chapter, the two optimisation algorithms used for choosing the position of the reactive power compensation means will be presented. Two multi-objective evolutionary algorithms were chosen, which were created for solving combinatorial problems. In particular, two algorithms that are often used as benchmarks were used: the NSGA-II [89,90] (Non Dominated Sorting Genetic Algorithm) and the SPEA2 [91] (Strengthen Pareto Evolutive Algorithm). Wanting to use, for reasons of economy of scale, plants all the same size, the problem domain becomes practically binary. For this reason, two algorithms were chosen which were born to deal with discrete problems. Since there is no algorithm that works better than the other on all problem types, both were implemented. Remembering also the no free lunch theorems for optimization [92].

These two algorithms both belong to the category of evolutionary algorithms and particularly of genetic algorithms (GA).

These algorithms draw inspiration from the mechanisms of natural selection and the Darwinian evolution of species. They treat the solutions under consideration as real individuals characterised by a certain genetic heritage. This representation of solutions has made them widely used in the world of research, especially in combinatorial problems precisely because of their ability to find the best 'combination' of genes.

Before the actual explanation of how genetic algorithms work, it is necessary to preface this with the fact that they readapt certain terms from biology, which are listed here for the sake of clarity:

- Chromosome: a representation of a solution in the 'domino' of the problem. It is generally encoded with a vector of bits or characters.
- Population: a set of solutions related to the problem under consideration.
- Gene: part of a chromosome. Generally, consists of one or more parts of the vector of bits or characters encoding the chromosome.
- Fitness or performance: the values achieved by the solution, basically it is the image of the chromosome in the 'codomain' of the problem. Evaluation takes place according to a specially designed function called the *evaluation function or evaluator*.

- Crossover: generation of a new solution by mixing existing solutions.
- Mutation: random alteration of a part of a chromosome.

The purpose of these algorithms is to emulate the process of natural selection and evolution of species by treating the solutions as individuals in a population. The genes of the best individuals are then combined to obtain a statistically better performing next generation. To this end, a genetic algorithm acts by performing these operations:

1. a population of individuals with random genes is initialised;
2. the performance of the solutions is evaluated;
3. parents are chosen to initialise a new generation;
4. crossover of the genes of two parents takes place to initialise a ‘daughter’ solution;
5. a random mutation of some genes of the new generation takes place;
6. the evaluation in step 2 is repeated with the new generation.

We reproduce in figure 7.1 the flowchart of the algorithm, from which it emerges that the operation of the algorithm can be summarised in four fundamental operators: the evaluator, the selector, the mutation operator and the crossover operator.

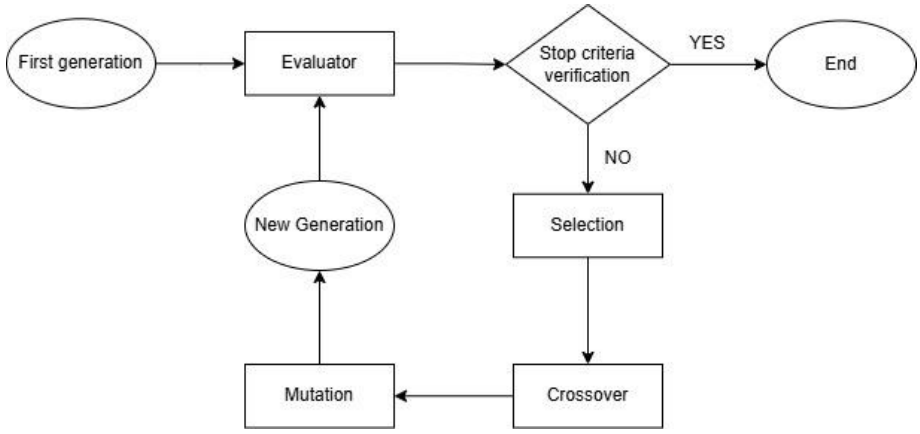

Figure 7.1 Flowchart characteristic of genetic algorithms

The four operators (in the rectangular boxes in the figure) are the entities that actually act on the population and determine its evolution. Each of these agents, which are the true heart of the algorithm, can perform its task in many ways, contributing in different ways to the evolution of the population. The iterative process stops at a stopping criterion or after a certain number of generations and allows evolution towards optimised solutions to the problem under consideration. The convergence of this iterative process towards optimised solutions of the problem is ensured by an important theorem of computer science briefly given below.

The Schema Theorem, or Fundamental Theorem of Genetic Algorithms, was formalised in 1970 by John Henry Holland and is today considered one of the most important theorems to show the potential of genetic algorithms. Based on the fact that during the execution of a genetic algorithm, by evaluating the strings related to the vector coding of the solutions of the problem under consideration, the fitness value of the different information contained in the chromosomes is implicitly evaluated, a formula can be deduced that allows us to approximate the expected number of the fitness value of the next chromosome. The formula derived (not shown for ease of discussion) shows an increasing trend in the fitness value of the solutions, which assures us of the convergence of the algorithm.
The four operators of the algorithm used in this study are briefly described below:

- The Evaluator: this operator performs the cost and short-circuit power calculations, thus evaluating the two optimisation objectives, i.e. obtaining a minimum short-circuit power and minimising the cost. The two objectives to be minimised are therefore: the number of nodes with insufficient short-circuit power and the overall cost of installing the synchronous compensators.
- The crossover operator: this operator deals with combining two ‘parent’ solutions to obtain ‘daughter’ solutions. In particular, each gene of the daughter solution has an equal probability of receiving the gene from either parent.
- The mutation operator: each gene has a certain probability of spontaneously mutating and changing value, which is decided during the initialisation phase of the algorithm.
- The selection operator: this operator is the one that defines the type of genetic algorithm. In both cases, a binary tournament is performed by selecting two solutions at random and choosing only one according to certain criteria. In the case of NSGA-II. The criterion on the basis of which the best solutions are selected is based on two quantities, rank and crowding distance. In the case of SPEA2, a fitness function is calculated that takes into account both how much better the solution is than the others and how far it is in a ‘little explored’ codomain zone.

See below the two selection operators of NSGA-II and SPEA2.

NSGA-II Selection Operator

The selection of the solutions used to give rise to the next generation takes place via a binary tournament on two quantities: rank and crowding distance. The first value represents how close the individual is to minimising the problem's objectives in relation to others, the second represents how close the individual is to a codomain zone with few neighbouring solutions.

Rank Computation

The NSGA-II uses the concept of the Pareto frontier to 'sort' solutions in order to select them by assigning them a *rank*. Given a population, the algorithm calculates the Pareto frontier: solutions belonging to this first frontier are assigned *rank 1* and set aside.

Then the algorithm calculates the pareto frontier again without considering the solutions that were given *rank*: these new solutions are assigned *rank 2*. The process is repeated until all solutions have been labelled according to their order of belonging to the various frontiers, as in Figure 7.2.

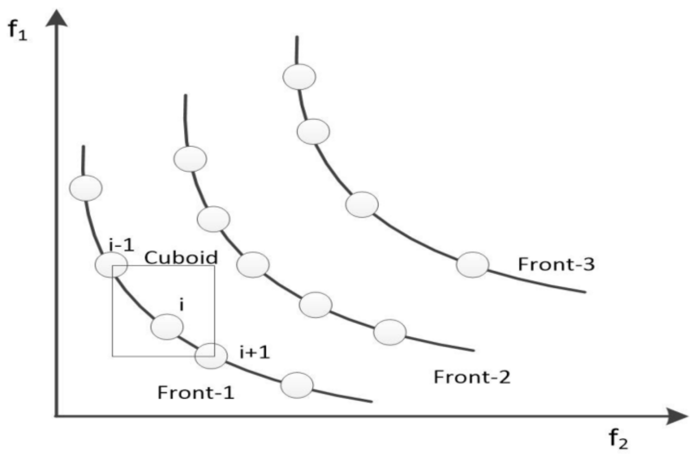

Figure 7.2 - Division of the population into Pareto frontiers

In Figure 7, solutions belonging to the first frontier have *rank 1,* those belonging to the second frontier *rank 2, and* so on.

To complete the selection process, the algorithm needs a second fundamental parameter, namely the *crowding distance* (CD).

Crowding Distance Computation

The crowding *distance* aims to give a measure of the crowding of solutions in a certain area of the output space. In this algorithm, the CD of a given solution is calculated by considering only those solutions that have the same *rank*. In fact, CD is a measure of the crowding at various points on a given Pareto frontier. For example, see Figure 8 for a two-objective optimisation.

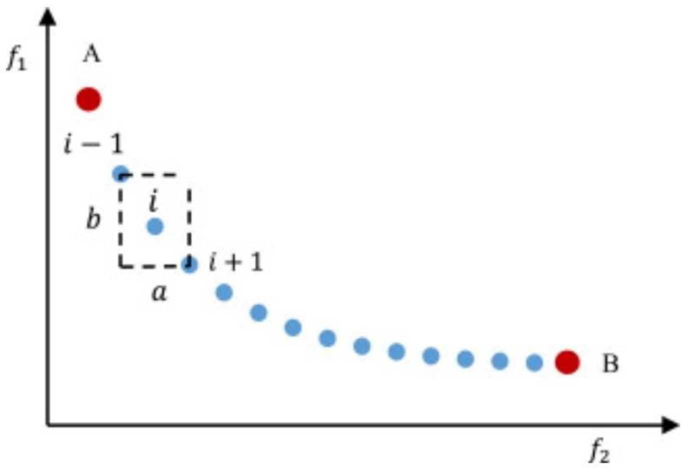

Figure 7.3 Representation of the cuboid for computing the crowding distance

As a first step, solutions must be represented in a normalized target space between zero and one, since targets are often not homogeneous in units and may have reference scales that differ by several orders of magnitude.

Secondly, these must be ordered according to one normalized target at a time, for example *f1*..Having done this, the *crowding distance* of solution *i on* target *f1* is equal to the normalized distance between the solutions spanning it, *i-1* and *i+1*.So summarizing in a formula:

$$CD(i)_{f1} = |\, f1(i-1) - f1(i+1)| \qquad 7.1$$

Where *f1* is the normalised performance of the solutions. Thus in Figure 4.4 the is equal to segment *b*. In a multi-objective optimisation, the total *crowding distance* for a given solution is:

$$CD(sol) = \sum_{k=1}^{n} CD(sol)_{fk}/n \qquad 7.2$$

Where n is the number of targets.

In Figure 7.3, for example, the CD of solution *i* is *a* + *b*. The only exception for this calculation are the 'extreme' solutions of the distribution, i.e. those that lie at the two extremes of the frontier. Since they have no solutions to constrain them on one side, they are assigned the maximum CD, i.e. equal to 1. This assignation has the consequence that the solutions at the extreme of the distribution are always kept for reproduction. Their peculiar position is derived from their genes that generally don't want to be lost in the selection process.

During the binary tournament the solutions are then first compared by rank, where the solution with the lowest rank is taken. This is because it minimises all objectives better. In the event of a tie, the solution with the greatest crowding distance is taken, in order to investigate less explored areas and have a more compact Pareto frontier.

SPEA2 selection operator

Here, the binary tournament is performed on a single quantity: the fitness function

The fitness function contains information both on and about the solution. The procedure for calculating fitness involves the following steps:

- calculation of "strength" of a solution
- calculation of raw fitness
- calculation of distances between individuals
- calculation of 'density' between solutions

The strength of a solution is the number of solutions it dominates. The raw fitness of a solution is the sum of the strengths of the solutions that dominate it. Thus

$$Raw_i = \sum_{j=1}^{n} \begin{cases} Strength_j & if\ j\ dominates\ i \\ 0 & else \end{cases} \quad 7.3$$

Where Raw_i is the raw fitness of the i-th solution and $Strength_j$is the strength of the j-th solution. Non-dominated solutions have raw fitness 0.

Next, the solution space is normalised so that targets with different magnitudes can be compared. Secondly, the Euclidean distance between all individuals is calculated and stored in a matrix. The density estimation is calculated using the following formula:

$$D_i = \frac{1}{\sigma_i(k)+2} \quad 7.4$$

Where D_i is the density estimation of the i-th solution and $\sigma_i$is the vector ordered in increasing order of the distances of the other solutions from solution i. $\sigma_i(k)$is the k-th distance. The parameter k is usually dependent on the size of the population participating in the optimisation or alternatively can be set to 1 by default.

Given the raw fitness and density estimation, the fitness of the solution is simply the sum of the two:

$$F_i = Raw_i + D_i \quad 7.5$$

Both algorithms aim to maintain the diversity of the solutions by means of density estimation. This operation is slightly more expensive for SPEA2, but since the calculation of the objective function of the various solutions is considerable, the increase in calculation time to determine the parent solutions is negligible. In addition, both algorithms, when the population grows, begin to set aside the less performing solutions by excluding them from the mating pool.

Chapter 8 –Case 24 IEEE Method Application

The IEEE Case 24 was used as the first test network. [93], chosen for its structure and size. In particular, it has two voltage levels 220 and 138 kV, which are currently used in sub-transmission networks. The limited number of nodes allows reduced calculation times, thus enabling the methodology to be tested in different scenarios. The IEEE 24-bus reliability test system was developed by the IEEE reliability subcommittee and published in 1979 as a benchmark for testing various reliability analysis methods. The objective was to define a system sufficiently broad to provide a basis for reporting on analysis methods for combined generation/transmission (composite) reliability methods[93].

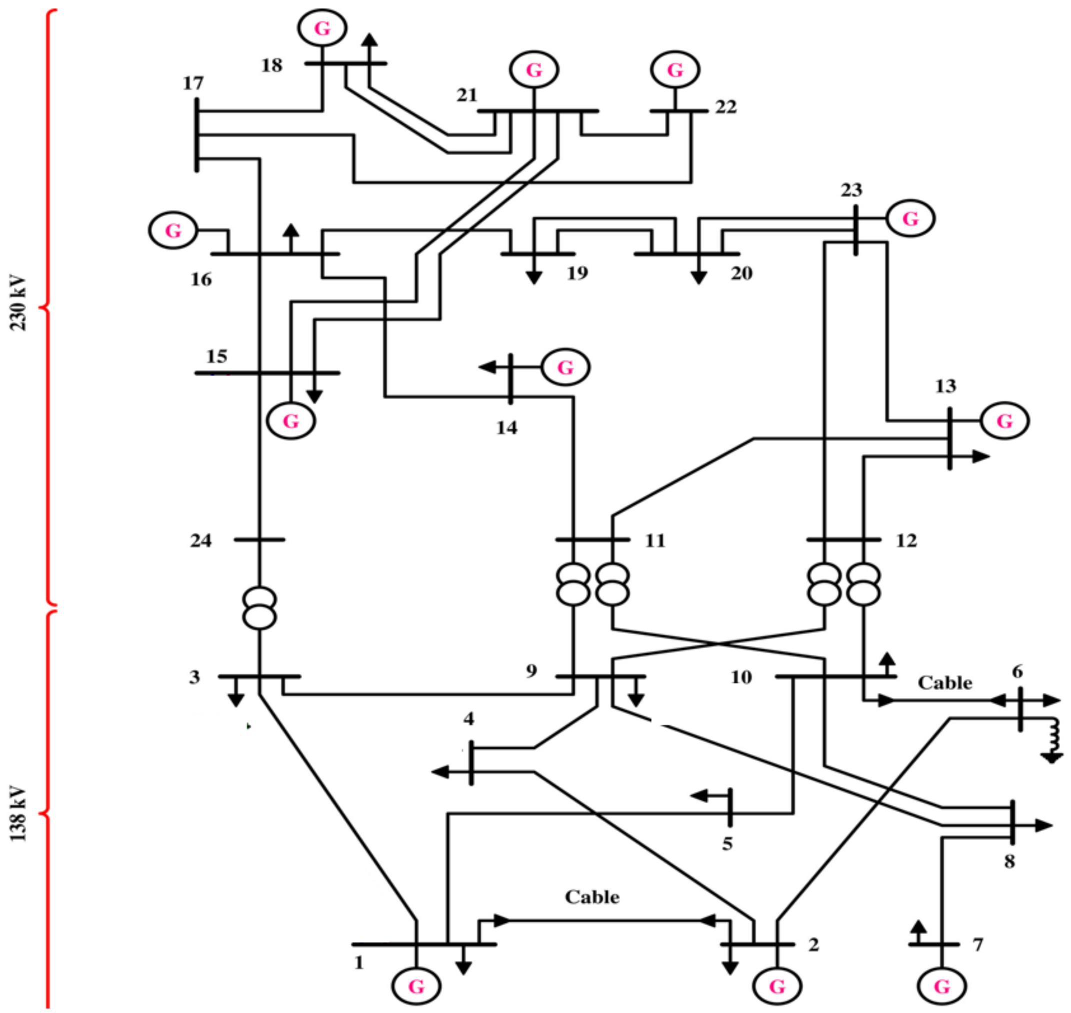

Figure 8.1 – IEEE Case 24 test system

All scenarios were modelled on two weeks of dispatching: a winter week and a summer week to assess the effect of different availability of energy from renewable sources.

As explained in Chapter 6, the first part of the procedure involves the creation of an active dispatch and a realistic generation park. For this purpose, two different optimisation tools were nested. The first 'external' optimisation sought the best size and positioning for the construction of new wind and photovoltaic generation plants. The second, 'internal' optimisation is linked to the first, and aims to simulate the energy market in order to imitate the processes of current European grids and to evaluate the goodness of the plant positioning calculated by the 'external' optimisation.

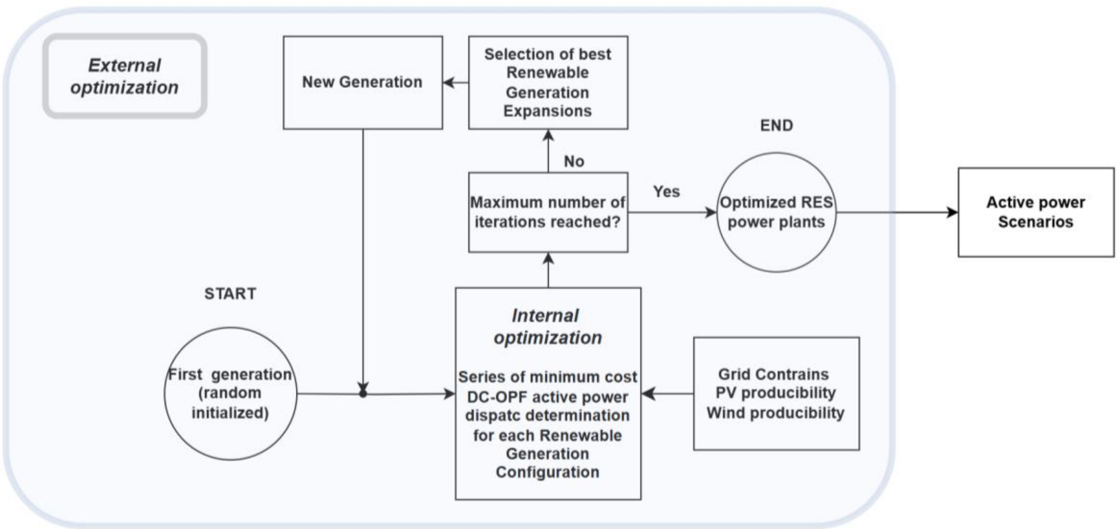

Figure 8.2 - Active power scenario generation procedure

Grid Consistency

The system is composed by 24 busses system with two voltage levels: 220 kV and 138 kV. There are 14 nodes at 220 kV and 10 at 138 kV. The nodes are connected by a total of 29 lines and 5 transformers. There are loads on each bus and several generators both conventional and static. The peak annual load is 2850 MW and an hourly load demand profile has been obtained according to the hourly load variation described in [93].

Since the scope of the study is to simulate and assess the necessities due to a shift from a system based on conventional power plants to a distributed RES-based system, the many generators present on the case study has been replaced with fewer, more powerful gas power plants. In particular the original generators have been replaced with the ones in table 8.1.

Bus Number	Bus Voltge kV	Generator power [MW]
1	138	200
2	138	200
7	138	200
13	230	400
18	230	400
21	230	400
22	230	400
23	230	400

Table 8.1 - Power and position of the conventional generators

First simulation step – Active Power Planning

As mentioned above, the active dispatching scenarios were obtained by means of two different optimisation systems nested together.

In particular, the external optimisation was performed with an NSGA-II algorithm, and we will refer to it as 'active power planning'.

The internal simulation, on the other hand, is done by a sequence of DC-OPFs that simulate the operation of the energy market considering the loadability limits of the grid lines. We will refer to this internal optimisation as 'market simulation'.

The external algorithm is an NSGA-II and has to optimise node by node the installed power from wind and photovoltaic sources. Nodal productivities were taken from [94][95] taking nodes in southern Italy at realistic distances compatible with the structure of the case 24 network. The load was derived with the formulas given in [93]. It was chosen to simulate a winter week and a summer week to see the different contributions of the renewable sources considered.

In each 138 kV node, PV and wind power plants with power from 25 to 150 MW could be installed in steps of 25 MW, and in 230 kV nodes from 100 to 600 MW in steps of 100 MW. The aim of this optimisation is to find optimal sizes and locations for renewable generation plants. The function to be optimised is 'market simulation'. The optimisation was of a bi-objective type where on the one hand one wanted to minimise costs, at the same time one wanted to maximise the energy produced from renewable sources.

Market Simulation

This optimisation aims to recreate the conditions of the energy market. Many European markets used to have dispatch priority for non-programmable renewables. This dispatch priority has been removed, but renewable resources are currently the most competitively priced for various reasons, which differ from country to country. However, in order to consider scenarios strongly based on inverter-based production in the dispatch simulations, priority was given to the use of wind and photovoltaic sources. Conventional sources were all considered gas-powered.

Overall, the DC-OPFs followed the following constraints:

$$I_{line,i,DC,h} \leq \alpha_{DC} I_{line,i,Max} \quad \forall\, i,h \tag{8.1}$$

$$P_{genTG,k,DC,h} \leq P_{genTG,k,Max} * \mathrm{S_m} \quad \forall\, k,h \tag{8.2}$$

$$P_{genWind,k,DC,h} \leq P_{genWind,k,Max} * \mathrm{PF}_{genWind,k,h} * \mathrm{S_m} \quad \forall\, k,h \tag{8.3}$$

$$P_{genPV,k,DC,h} \leq P_{genPV,k,Max} * \mathrm{PF}_{genPV,k,h} * \mathrm{S_m} \quad \forall\, k,h \tag{8.4}$$

$$\min\left(C_{gas} * \sum P_{genTG} + C_{wind} * \sum P_{genWind} + C_{PV} \sum P_{genPV}\right) \tag{8.5}$$

In the above equation:

i is the subscript for the lines;

k is the subscript for the generators;

h is the subscript for the hour/scenario.

Eq. 8.1 describes the limit in line capability;

$I_{line,i,DC,h}$ is the line current for the *i-th* line in the *h-th* hour;

$I_{line,i,Max}$ is the line's maximum capacity;

α_{DC} is the lines' capability factor for the DC-OPF to mimic both the operating strategies that do not involve loading the lines to the maximum for safety reasons, both serve to leave the margin for reactive power transit. In this simulation, α_{DC} was set at 0.7.

The Eq. 8.2 represents the active power limit on conventional power plants considering the Stability Margin factor (SM) set to 0.9.

Equations 8.3 and 8.4 represent the active power limit on the renewable energy sources dependent on the Producibility Factor (PF) which is time dependent.

Equation 8.5 represents the cost function which aims to be minimized and determines the priority in the renewable sources use. For the gas-powered power plants has been considered only the gas cost for a total of 9 c€/kwh while for the PV and Wind a production cost dependent on the maintenance both at 1 c€/kwh. These numbers are in indicative and serve primary to set the priority among the energy sources. The total cost of the system has been calculated considering 26 summer weeks and 26 winter weeks. The annualized capital cost for the RES is 80 €/MWi for the PV and 175 €/MWi for the wind power plants.

Active Power Planning results

The parameters of the NSGA-II algorithm were:

- A first population of 100 individuals
- 50 new solutions are calculated on each iteration
- The mutation probability is 5%

The population obtained by the optimization is reported in Fig. 8.3.

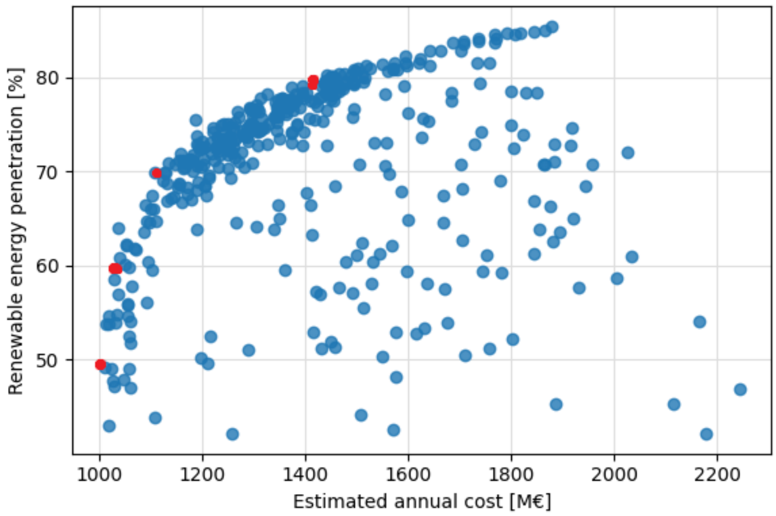

Figure 8.3 – Active power planning solutions (1200)

Although active power planning is not the focus of the work some interesting considerations can be drawn from it.

The percentage of renewable source penetration that results in the lowest overall system cost is around 50%. This is despite the fact that the grid is of a limited size and therefore with a very high contemporaneity factor of renewables that results in moments of high overproduction and the absence of pumped storage plants that would facilitate the integration of renewables. That said, to achieve higher penetration rates, the costs for the system increase.

This is consistent with what was found in [64] where to achieve high penetration of renewables it was necessary to move away from the natural equilibrium of the least-cost market.

From this spectrum of possible generation parks, four solutions with different penetration belonging to the pareto frontier were chosen. The active dispatch of these solutions will constitute the active power scenarios calculated in the actual Reactive Power Plannig phase.

Table 8.2 shows the installed powers to achieve the calculated renewables penetrations.

		Power plants capacity [MW]			Installed capacity/Peak power ratio [MW]		
		Fossil	**PV**	**Wind**	**Fossil**	**PV**	**Wind**
RES production scenario	**50%**	2600	2275	1675	1.01	0.89	0.65
	60%	2600	3150	2150	1.01	1.23	0.84
	70%	2600	2850	3225	1.01	1.11	1.26
	80%	2600	3825	5300	1.01	1.49	2.07

Table 8.2 - Res scenarios installed capacity

In the following figures report the active power distribution across the various scenarios.

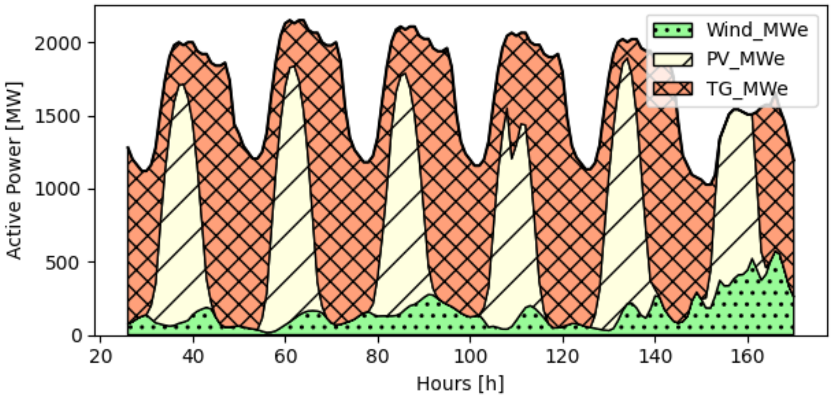

Figure 8.4 - 50% RES Scenario – Summer Week

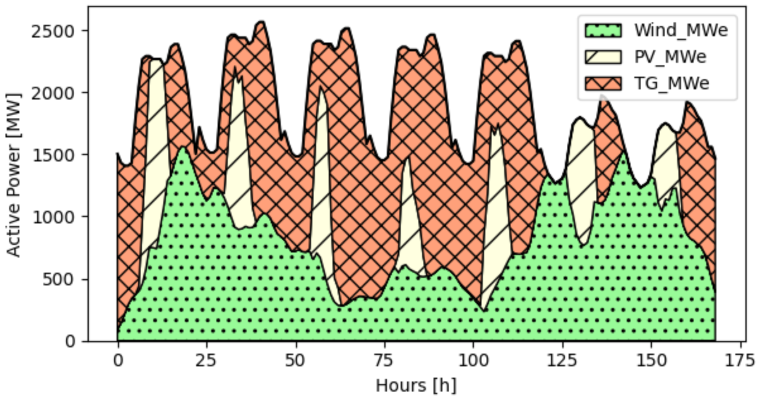

Figure 8.5 - 50% RES Scenario – Winter Week

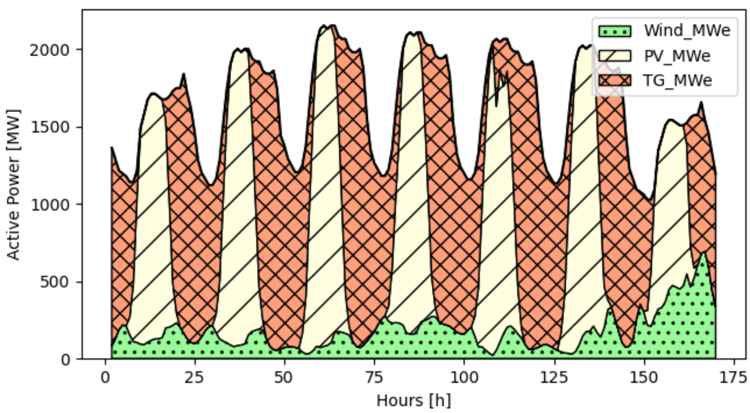

Figure 8.6 - 60% RES Scenario – Summer Week

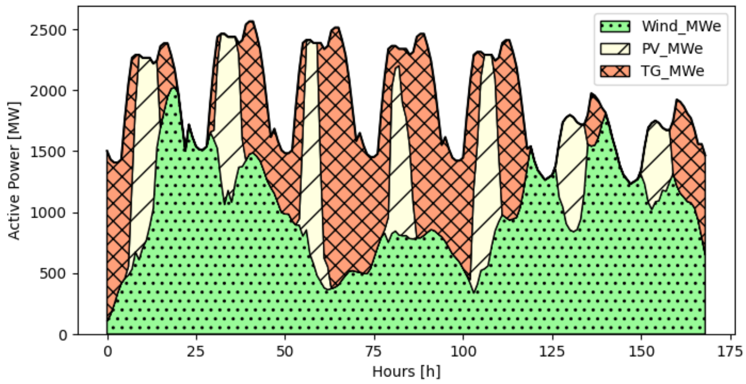

Figure 8.7 - 60% RES Scenario – Winter Week

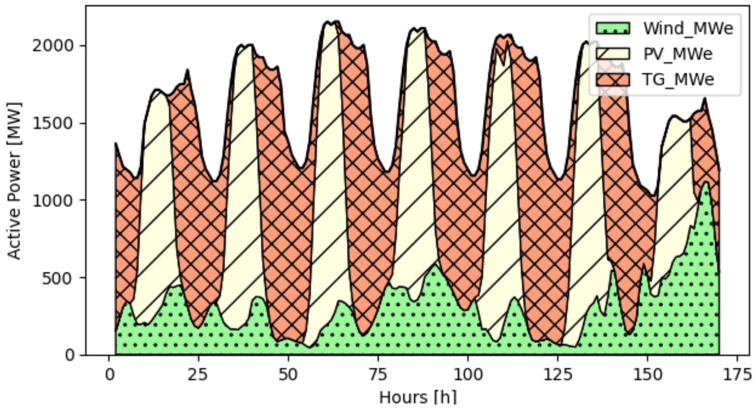

Figure 8.8 - 70% RES Scenario – Summer Week

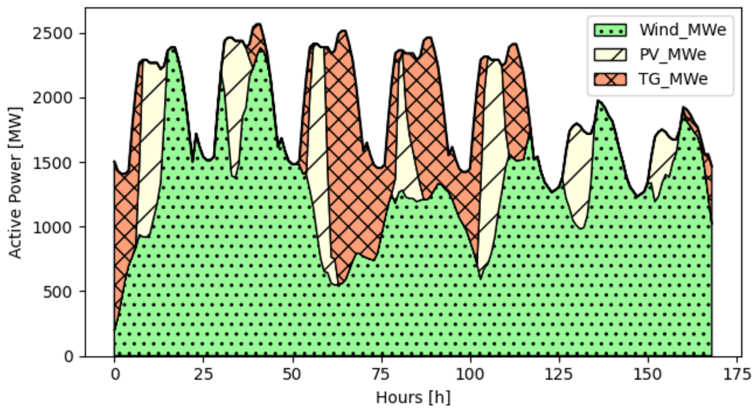

Figure 8.9 - 70% RES Scenario – Winter Week

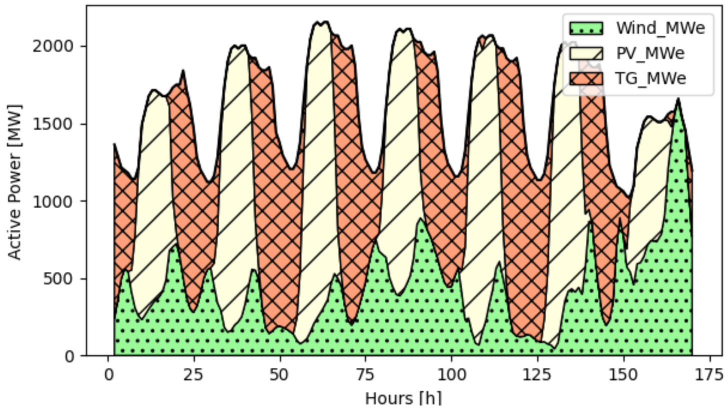

Figure 8.10 - 80% RES Scenario – Summer Week

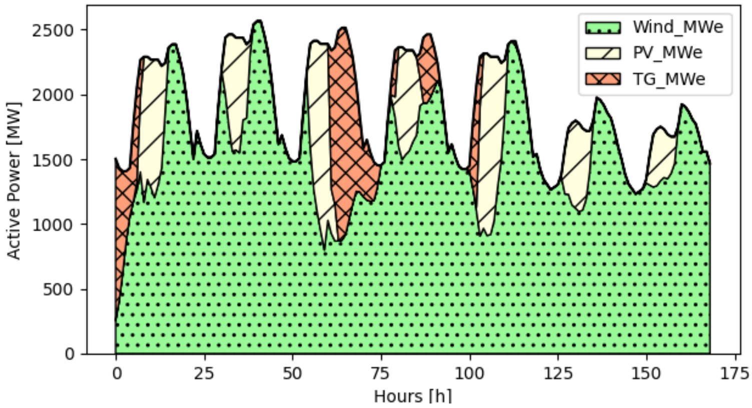

Figure 8.11 - 80% RES Scenario – Winter Week

Technology	Installed Power [GW]	Produced energy [GWh]	Equivalent hours of operation [h]	Production Share [%]	Scenario
PV	2.275	3430	1508	22	**50% RES**
Wind	1.675	4259	2543	27	
TG	2.6	7945	3056	51	
PV	3.15	4282	1359	27	**60% RES**
Wind	2.15	5238	2436	34	
TG	2.6	6114	2352	39	
PV	2.85	3685	1293	24	**70% RES**
Wind	3.225	7249	2248	46	
TG	2.6	4699	1807	30	
PV	3.825	3805	995	24	**80% RES**
Wind	5.3	8745	1650	56	
TG	2.6	3084	1186	20	

Table 8.3 - Main energy features of the produced scenarios

Table 8.3 reports different energy indicators for the produced scenarios. The total annual energy consumption is 15.635 GWh and if they were completely produced with gas-fired power plants, their average equivalent hours of operation would be around 6045 over 8760 hours of the year. It can be noted that increasing the RES share leads to a reduction in the equivalent hours of operation for inevitable overproduction.

Second Simulation Step – Reactive power planning

The second optimisation stage realises the actual reactive power planning. This is also realised with a two-level structure: an external optimisation performed with a meta-heuristic algorithm and the internal optimisation simulating the conditions under which the TSO must operate the network consisting of a series of OPFs.

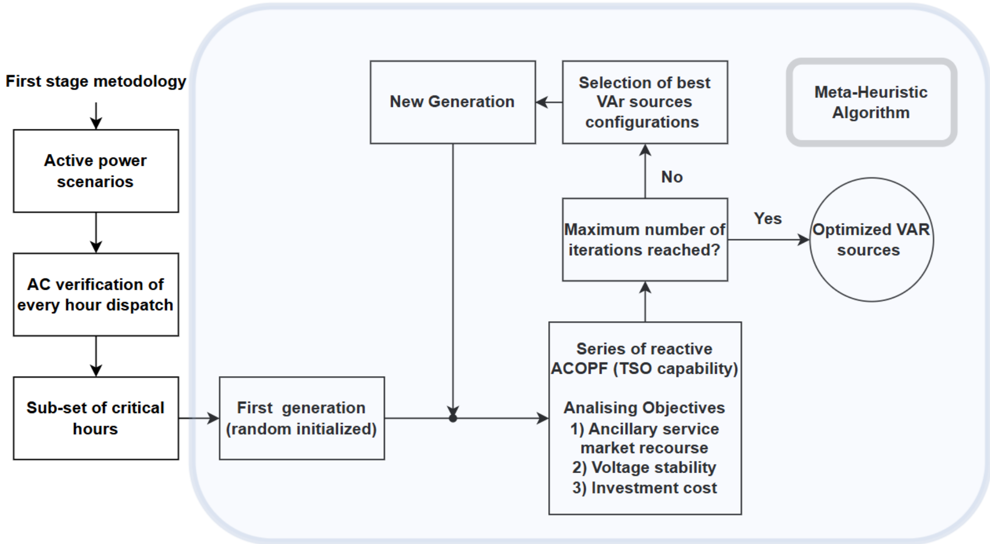

Figure 8.12 – structure of the second step

TSO possibilities and constraints

The constraints implemented in the AC-OPF to simulate the dispatching conditions within which the TSO can work without having to resort to the ancillary service market are as follows:

$$I_{line,i,AC,h} \leq \alpha_{AC} I_{line,i,Max} \quad \forall\, i,h \tag{8.6}$$

$$P_{gen,k,DC,h}\left(1-\gamma_{gen}\right) \leq P_{gen,k,AC,h} \leq P_{gen,k,DC,h}\left(1+\gamma_{gen}\right) \quad \forall\, k,h \tag{8.7}$$

$$-\ P_{genPV,k,AC,h} * \tan\left(\varphi_{PVMax}\right) \leq Q_{genPV,k,h} \leq P_{genPV,k,AC,h} * \tan\left(\varphi_{PVMax}\right) \quad \forall\, k,h \tag{8.8}$$

$$-\ P_{genWind,k,AC,h} * \tan\left(\varphi_{WindMax}\right) \leq Q_{genWind,k,h} \leq P_{genWind,k,AC,h} * \tan\left(\varphi_{WindMax}\right) \quad \forall\, k,h \tag{8.9}$$

$$-\ P_{genTG,k,AC,h} * \tan\left(\varphi_{TGMax}\right) \leq Q_{genTG,k,h} \leq P_{genTG,k,AC,h} * \tan\left(\varphi_{TGMax}\right) \quad \forall\, k,h \tag{8.10}$$

Similar to DC-LoadFlow:

Equation 8.6 represents the loadability limit of AC lines. α_{AC}has been assigned a value of 0.9 in order to always have a small margin.

Equation 8.7 was included to allow a small deviation from the active power outcome of the dispatch to compensate for losses and possible load imbalances. is set to 0.05.

Equations 8.8 and 8.9 are the reactive power constraints that can be delivered by renewable sources. They have been determined such that $\cos\left(\varphi_{WindMax}\right) = 0.95$ *and* $\cos(\varphi_{PVMax}) = 0.97$. Considering the modelling in [60,67] reasonable margins were given. For conventional generators, a $\cos(\varphi_{TGMax}) = 0.6$ (equation 8.10).

About the means of compensation for reactive power, Terna's planned measures were taken into account and in particular with the costs available in their methodological document for cost-benefit assessment [33,96].

	138 kV system		220 kV system	
	Auxiliary for busbar connection	100 MVAr component	Auxiliary for busbar connection	100 MVAr component
Shunt Reactor	452	566	958	1173
Shunt Capacitor	408	566	816	1173
Voltage Source Converter	820	13464	1250	13464
Synchronous Condenser	820	8976	1250	8976

Tab 8.4 VAr sources capital cost (U.O.M. k€)

The reactors are equipped with a on load tap changer to reach up to 40% of their rated power. The meta-heuristic algorithm had the possibility of installing a single component per node but of any type up to a power of 100 MVA in increments of 25 MVA. The cost is divided between a fixed component for the stalls and a component proportional to the installed power.

The second step in the procedure for planning reactive resources is to verify the TSO's needs to make the planned dispatch safe and practicable.

First of all, it was checked whether the calculated dispatch, with the corresponding capabilities of the generating plants, entailed any operational problems: an AC-OPF was carried out with the illustrated constraints on all hours of the various scenarios.

		Ancillary service necessity [h]	% of total
RES Scenario	**50%**	22	6.5
	60%	42	12.5
	70%	21	6.3
	80%	106	31.5

Tab 8.5 Overvoltage hours according to RES share

Table 8.5 shows the times when the generators' capabilities are not sufficient to keep the voltages within the $\pm$ 5% range typical of transmission networks. Figure 7.11 shows the trend of voltages at the nodes of the 80% RES scenario. We see that there are times when the voltages exceed the limits both above and below. This may indicate either an excessive reactive power transit problem or insufficient network capability even in the case of a single-bar network.

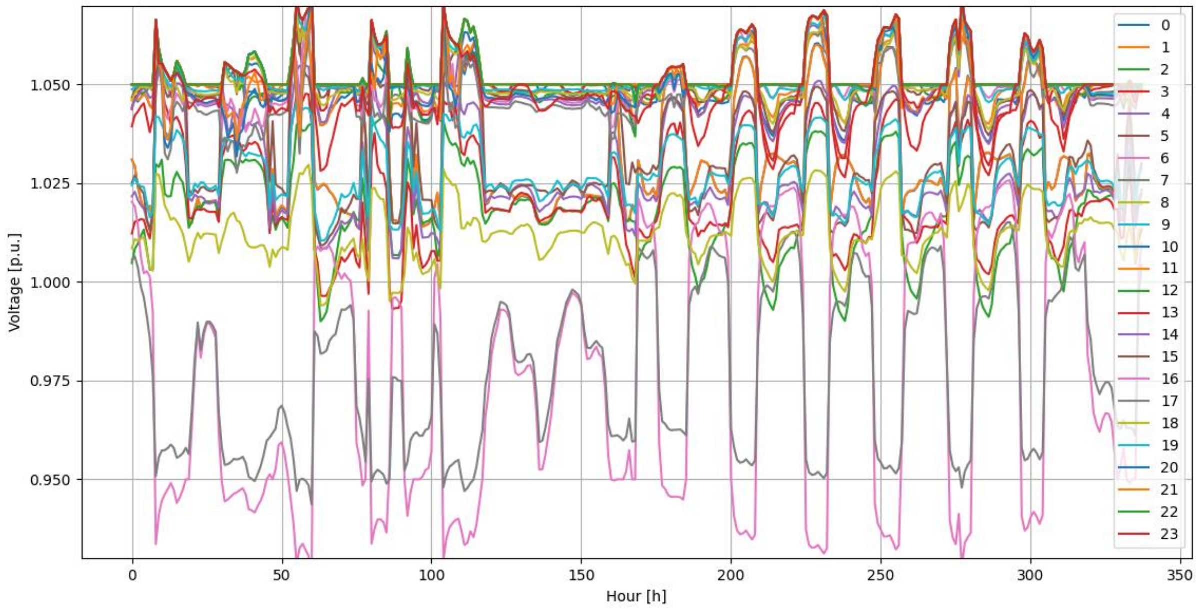

Fig. 8.13 Nodal voltage for 80% res scenario (without VAr compensation), vs. time

A comparison with the load coverage diagram in Figs. 8.10 and 8.11 shows that there are many scenarios that give problems not only with high photovoltaic production but also with high wind production. This shows the effect of the limited capability of wind generators.

These problem hours were chosen as scenarios of the AC-OPF subjected to the meta-heuristic optimisation algorithm that will try to determine the optimal set of reactive power compensation means to be installed. Both the NSGA-II algorithm and SPEA2 were tested on the four scenarios.

Reactive Power Planning – First Algorithm: NSGA-II

Optimizations with NSGA-II were performed with the following parameters:

- A first population of 100 individuals
- 50 new solutions are calculated on each iteration
- The mutation probability is 5%

The optimisation objectives set were three:

- The minimisation of investment costs for Var sources
- The minimisation of the hours in which the ancillary service market must be used
- Minimisation of the voltage variability over time: This objective was represented by first calculating the standard deviation of the voltage at the individual nodes for all simulated hours. Subsequently, the standard deviations of the individual nodes were averaged.

$$Avg\ StdDev = \frac{\sum_{n=1}^{N_{tot}} \sqrt[2]{\sum_{h=1}^{H_{tot}} \left(E_{n,h} - E_{nom_n}\right)^2}}{N_{tot}} \qquad - \qquad 8.11$$

In eq. 8.11:

- N_{tot} is the number of nodes
- H_{tot} $is\ the\ number\ of\ hours$
- E_{nom_n} is the nominal voltage of the node n
- $E_{n,h}$ is the voltage of the node n in the hour h

The inclusion of voltage volatility was done to allow one to discern between solutions that offer a complete resolution of voltage regulation problems not only based on cost but also on the margin they give to the network. More stable voltages over time indicate a greater capacity for voltage control.

Going now to check the convergence of the optimisation algorithm, we went on to graph for each generation, the lowest cost solution that would solve all scenarios with voltage regulation problems.

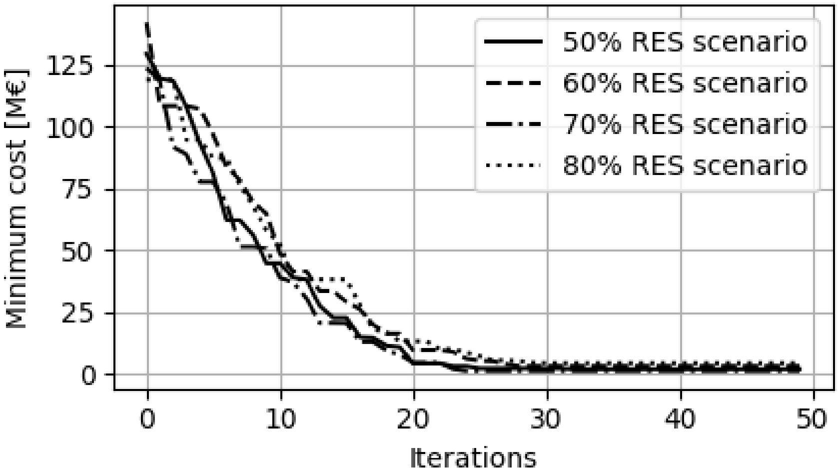

Fig 8.14 - Minimum cost solution vs the number of iterations

From the figure we can see how the algorithm found the solution at minimum cost already at the 30th iteration, i.e. after 2550 solutions and about 50 hours of calculation time on exploiting two cores working in parallel on a HP Zbook mobile workstation with an intel core i7 (7^{th} Gen) processor with 16 GB of RAM. The average time required for a Reactive OPF was about 0.45 seconds. The computational time was dependent on the OPF convergence, if there were no feasible solution the computational time was about three times higher.

Going into the details of the installed compensation means, Table 7.5 shows the powers per technology that were installed in the various scenarios and the overall costs.

	RES production scenario			
	50%	**60%**	**70%**	**80%**
Shunt reactors	25 MVAr	-	-	-
Shunt capacitors	75 MVAr	50 MVAr	100 MVAr	250 MVAr
Voltage Souce Converter	-	-	-	-
Synchronous Condenser	-	25 MVAr	-	-
Total compensation cost M€	2.083	3.310	1.382	4.470

Tab 8.6 Optimized VAr sources according to scenario.

After the individuation of the optimised Var sources, a series of Reactive-OPF is done considering the new sources. In figure 8.15 is reported the voltage profile for the 80% RES scenario after the compensation.

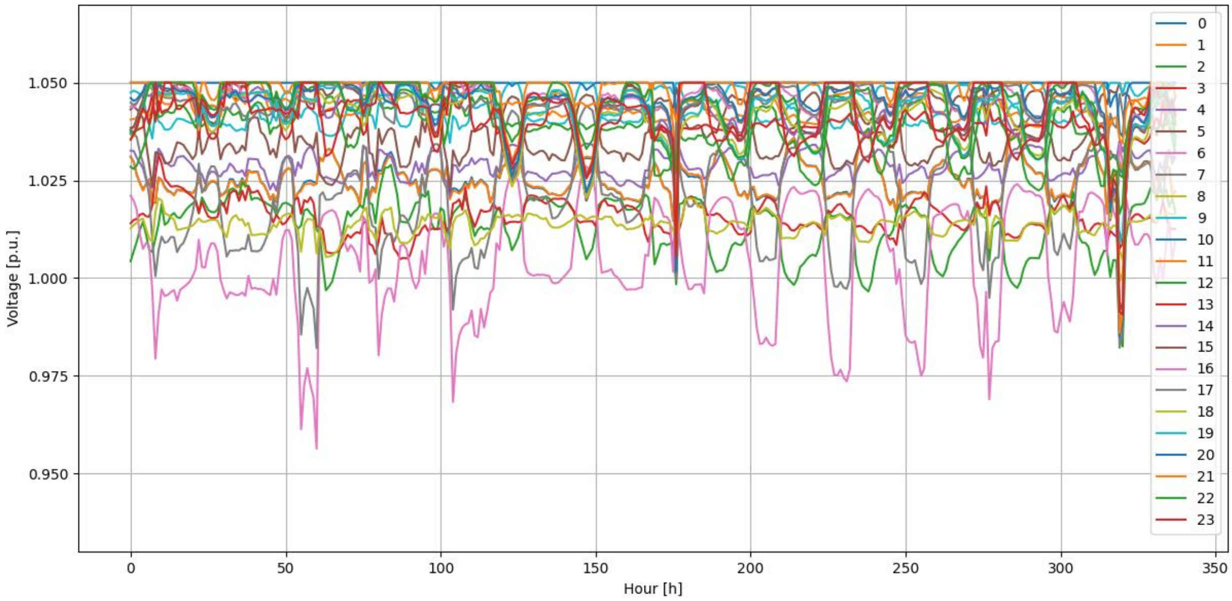

Fig 8.15 - Nodal voltages of 80% RES scenario with optimized VAr compensation.

It can be seen from Figure 8.15 that the minimum voltage is well above 0.95 p.u. of the nominal voltage and only rarely falls below 0.975 p.u. This result can be compared with the voltage profile before the optimization reported in figure 8.13 where the voltage was often exceeding the $\pm$ 5% allower range.

Reactive Power Planning – Second Algorithm: SPEA2

Optimisation with the SPEA2 algorithm was performed with the following parameters:

- A first population of 100 individuals
- 50 new solutions are calculated on each iteration
- The mutation probability is 5%

The optimised objectives were the same therefore:

- Minimisation of the cost of VAr sources.
- Minimisation of the use of the ancillary service market.
- Minimisation of the average standard deviation of voltage at individual nodes.

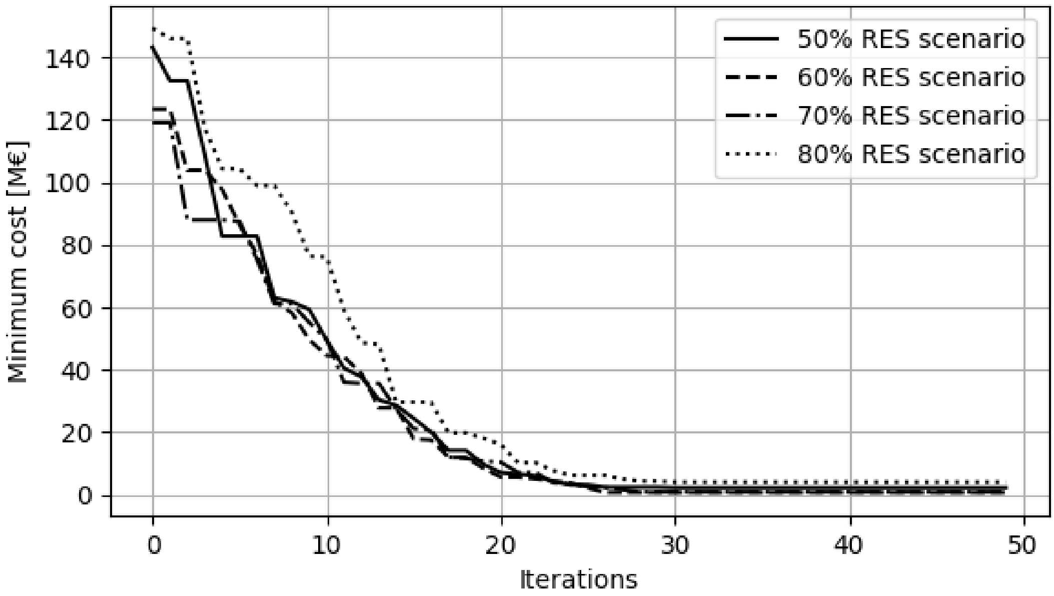

Figure 8.16 - minimum cost solution vs the number of iteration

Again, we can see from the figure that the algorithm found the lowest-cost solution as early as the 30th iteration. Entering the details of the least-cost solutions that eliminate surges, the installed powers are shown in Table 7.6.

	RES production scenario			
	50%	**60%**	**70%**	**80%**
Shunt reactors	25 MVAr	-	-	-
Shunt capacitors	100 MVAr	50 MVAr	100 MVAr	100 MVAr
Voltage Souce Converter	-	-	-	-
Synchronous Condenser	-		-	25 MVAr
Total compensation cost M€	2.225	0.690	0.8325	4.001

Tab 8.7 - Optimized VAr sources according to scenario.

Comparison Between NSGA-II and SPEA2

Table 8.8 shows the installed power and costs for the various optimal solutions.

	RES production scenario							
	50%		60%		70%		80%	
	NSGA	SPEA	NSGA	SPEA	NSGA	SPEA	NSGA	SPEA
Shunt reactors	25	25	-	-		-	-	-
Shunt capacitors	75	100	50	50	100	100	250	100
Voltage Souce Converter	-	-	-	-	-	-	-	-
Syncronous Condenser	-	-	25	-	-	-	-	25
Total compensation cost M€	2083	2.225	3.31	0.69	1.382	0.8325	4.47	4.001

Table 8.8 – Confrontation between best solutions

Comparing the results of the two optimisations, we see that:

- In each case there is a substantial need for capacitive reactive support.
- Synchronous compensators are particularly well installed while VSC are totally ruled out.
- In the 50% RES scenario, NSGA-II performed slightly better.
- In the 60% and 70% RES scenarios, SPEA2 performed significantly better and in the 80% RES scenario slightly better.

The different performance of the two algorithms is due to their structure.

There is in fact a structural randomness in the random initialisation of the first solutions, how the genes of two individuals are combined and how spontaneous mutations occur. This results in the solutions being different and the algorithms converging to local minima. To avoid this undesirable behaviour, it may be possible to either perform more optimisations or to increase the random exploration mechanisms as the generations increase so as to avoid local convergence. This can be done in several ways: either by inserting random individuals into new generations, or by increasing the mutation probability, or by hybridising the algorithm with others to acquire different peculiarities.

In this case study, the method was tested in its entirety. The first phase of scenario creation was performed with a Generation Expansion Planning executed with NSGA-II algorithm.

This phase resulted in the creation of four possible generation park scenarios each with 336 hours of dispatch. For the reactive power planning phase, all these scenarios were optimized using both an NSGA-II and a SPEA2. The procedure led to the identification of a set of means of reactive power offsets that would allow the cancellation of permanent surges and the use of the ancillary service market.

Chapter 9 – Case Study of a Modern Transmission Grid

This chapter deals with a second case study related to a portion of the future Italian grid. Note that the dispatching and active scenarios were performed externally to this thesis and for these reasons the method that has been adopted will not be analysed but will be carefully studied and verified.

The verified dispatching will be performed by three reactive power planning procedures with different objectives and different boundary conditions. All optimizations were performed with NSGA-II algorithm. Due to the problem dimension, great care has been given to the analysis of the optimization procedures behaviour.

Finally, the grid response with the new means of compensation expansions of the grid and generation fleet will be evaluated.

In this case study, a transmission network was considered, taking a portion of the Italian grid as a starting point and adding the modifications and interventions foreseen in the published development plans [25,33].

The grid structure consists of the AC and DC lines, and interconnection nodes, representing the exchange points with the rest of the Italian grid, were added in order to simulate the case of a large and interconnected grid.

In addition to the lines and interconnections, some means of reactive power regulation, such as synchronous compensators and shunt reactors, were considered as already present. Both devices are currently installed in some nodes of the Italian and other European grids. This was done to make the case study more realistic and to study how the optimisation programme interacts with existing regulation resources.

The annual dispatch was produced via a flow-based DC-OPF [97,98] for another study with the same constraints as in Chapter 6, with additional constraints regarding interconnection nodes and the presence of accumulators and resistors.

Grid Consistency

The network is similar of a portion of the national transmission grid of the southern Italian grid. The grid has three voltage levels 400 kV, 230 kV and 500 kV DC.

The most relevant is the 400 kV portion of the grid which is almost entirely made up of overhead lines.

The 230 kV lines make up the sub-transmission grid, where there are few long lines and some transmission lines. A large part of the 230 kV portion of the grid is concentrated in two zones of limited extension but with high load density. These two zones are intended to emulate the structure of the grids of large urban centres, composed of a dense sub-network, at a lower voltage than the transmission one, and almost completely in cable. This conformation of the 220 kV grid portions will be decisive in certain technical choices suggested by the optimisation procedure.

The DC portion of the network is represented by three point-to-point connections bipolar ± 500 kV both terrestrial and marine lines. They take their cue from Terna's development plan and the HyperGrid project [25].

Table 9.1 summarises the network consistency.

Voltage Level	Line Type	N° of conductors	N° of lines	Average current limit [A]
± 500 kV	HVDC	/	3	2300
400 kV	OHL	3	111	2750
		2	16	1840
	Cable	/	3	2000
230 kV	OHL	2	26	1830
		1	56	1030
	Cable	/	33	2000

Table 9.1 - Transmission Grid consistency

As can be seen from Table 9.1, almost the entire 400 kV network is composed of overhead lines, while the 230 kV portion has a more varied composition. As mentioned, almost the entire 230 kV portion is concentrated in two clusters representing two large urban areas. The two voltage levels of the AC network are connected by a set of autotransformers, whose ratings are shown below.

Rated Power [MVA]	Vcc [p.u.]	N° of autotransformers
600	0.135	2
400	0.115	20

Table 9.2 - Transformers of the transmission grid

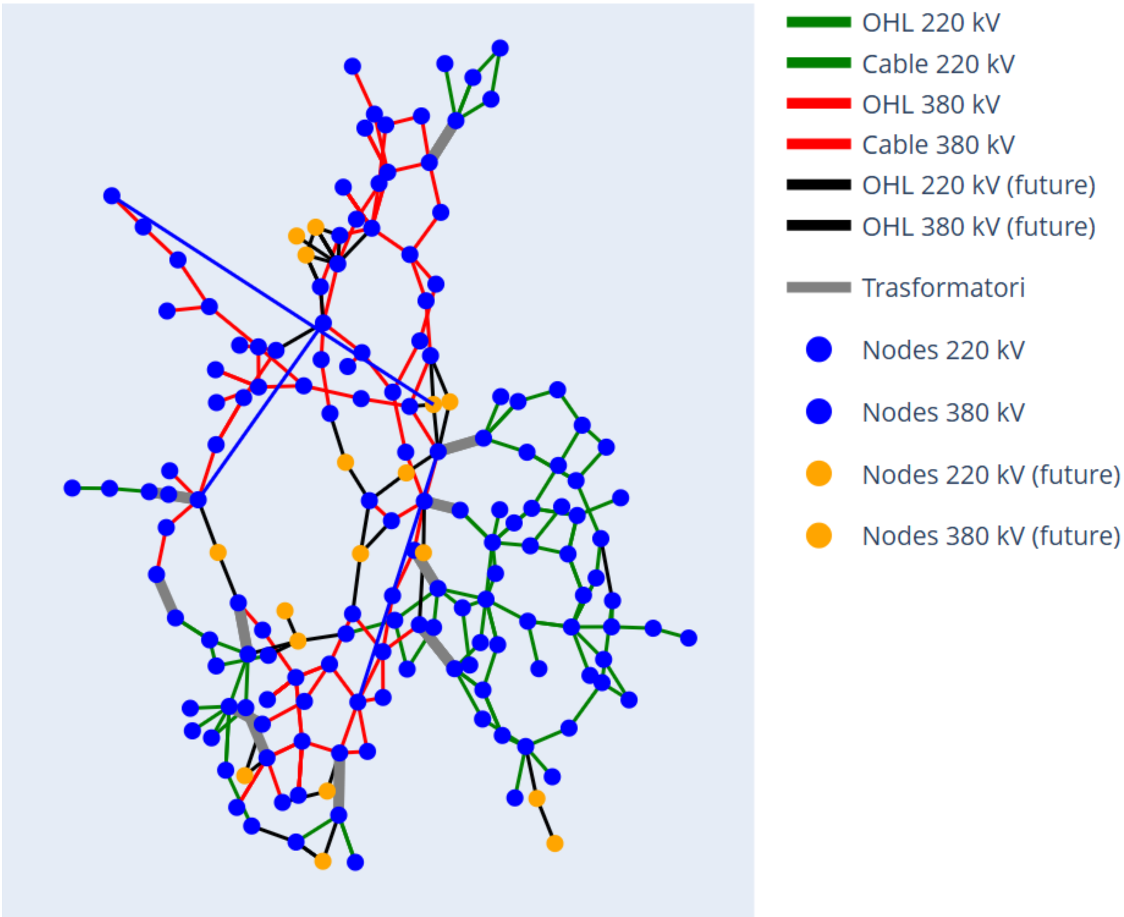

Figure 9.1 - The structure of the simulated grid (blue lines are the HVDC links)

Unlike the previous case, the active balance of the network is not zero at all the time instants considered, but there will be period of energy import and period of energy export.

A total of thirteen import nodes with different exportable powers are considered. For nine out of these thirteen interconnection nodes, it will also be possible to export energy at the times that require it.

For four interconnection nodes, only the possibility of importing energy is envisaged given a high contemporaneity coefficient of the simulated OPF-flow-based renewable production.

The planned import capacity is a maximum of 18,000 MW and the export capacity of 12,000 MW.

As far as active power is concerned, there are 31 storage nodes with a total capacity of 12,000 MW and 5 nodes where resistors are installed to be used for frequency regulation and to manage certain congestion in emergencies.

The installed capacity of resistors is 500 MW. Nevertheless, these have been considered to avoid resorting to the ancillary service market and to avoid having to pay the fee for lost wind production, which is more expensive than the cost of energy dissipated on the resistors.

Examining the specifics of reactive power, there are 25 shunt reactors of 250 MVAR, 7 synchronous compensators of 250 MVAr, 5 STATCOMs of 125 MVAr at the various nodes of the network.

Active Power Scenario

The grid is composed by 160 nodes and 196 lines and 22 380/220 kV transformers. In the simulated dispatching year, the total energy absorbed by the loads is 102 TWh. Also in the reference year, the total energy produced is 92 TWh.

Considering the average energy price of the last few years, we can derive the market volume of energy produced in this portion of the grid.

In 2019, before the energy shocks due to the pandemic and the Russian invasion of Ukraine, the average energy price was 52€/MWh, while in 2023 127€/MWh. It follows that the total value of energy managed by this network would be €4,780 million in 2019 and €11,684 million in 2023. Let us now turn to the analysis of power flows in the grid.

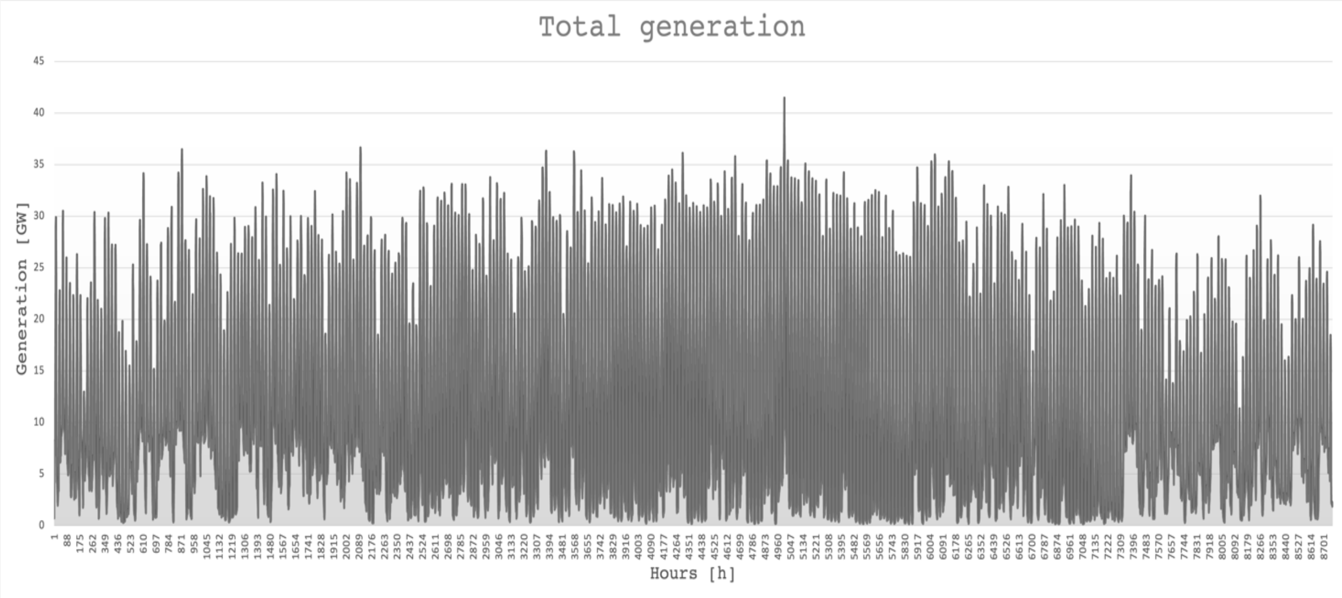

Figure 9.2 - Total active power generation through the simulated year

The power produced by the generators within the grid is highly variable over time, reaching times when generation is almost zero.

This can be explained as the dispatch envisaged a large amount of installed power from non-programmable renewable sources and consequently a large amount of energy is produced from this source. For a more accurate analysis, the generation duration curve shown below was also verified.

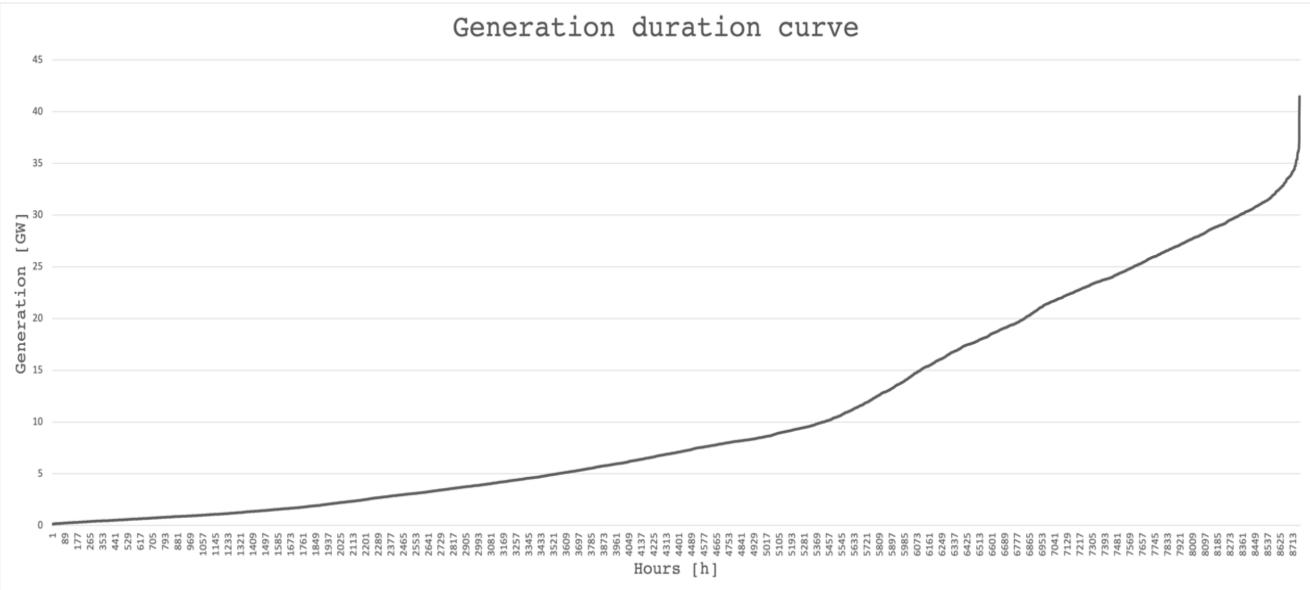

Figure 9.3 - Total generation duration curve

From the above graph, it can be seen that the grid has a very variable power output over time. In particular, there is a minimum of only 100 MW against an average load of 11,530 MW and a peak energy production of over 40,000 MW.

The chronological load curve shows a more typical pattern, with daily, weekly and seasonal trends. The average load is precisely 11,530 MW and ranges from a minimum of 6,000 MW to a maximum of 21,000 MW.

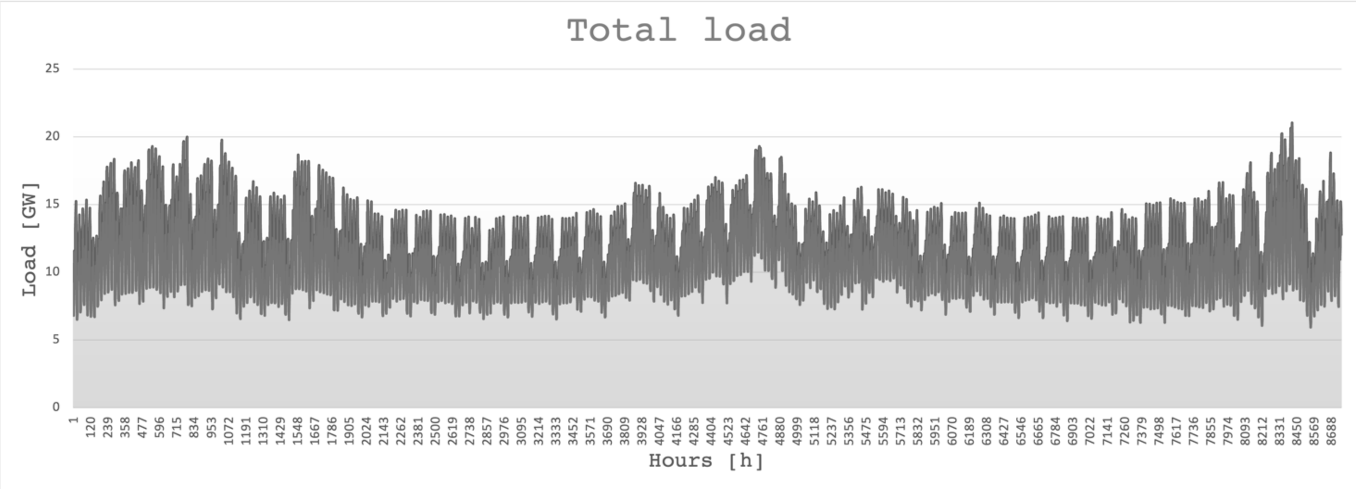

Figure 9.4 – Total load chronological curve

From the chronological load curve, we see quite a continuous trend. From this information we can expect moments of both strong import and strong export.

Relying on the active load information, the reactive load curve was also produced. The reactive load is always inductive between 1,200 MVAr and 4,000 MVAr. Clearly, the grid demand is not included.

Finally, regarding active power flows, it is very important to observe the active grid balance, i.e. the hourly difference between generation and load.

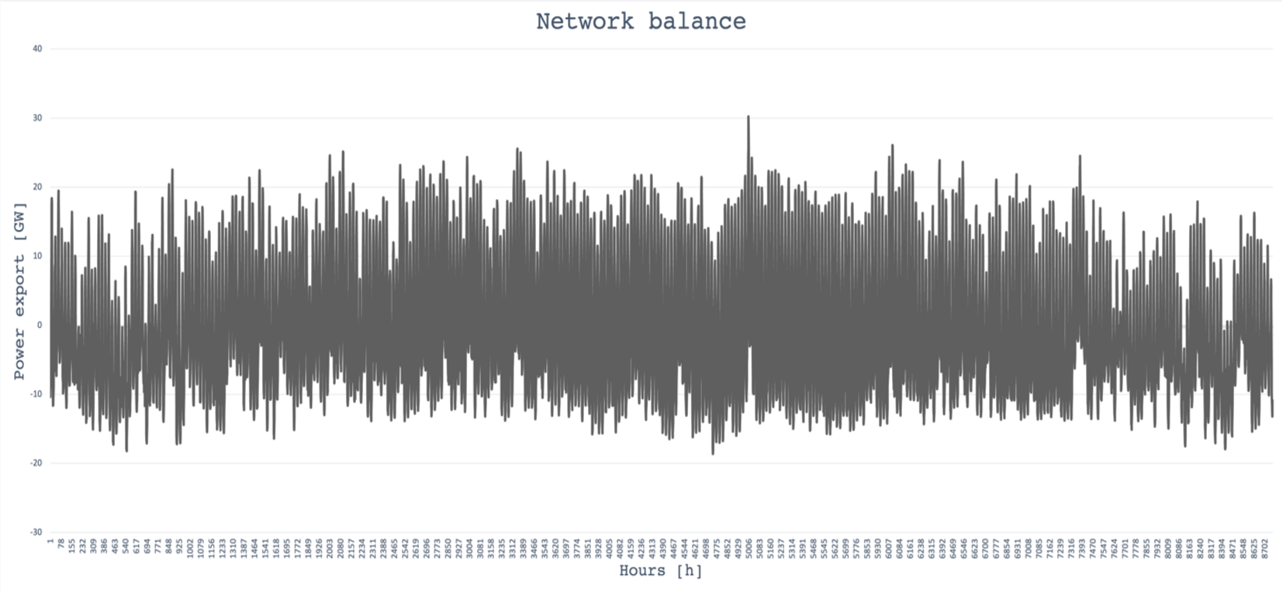

Figure 9.5 - Network active power balance

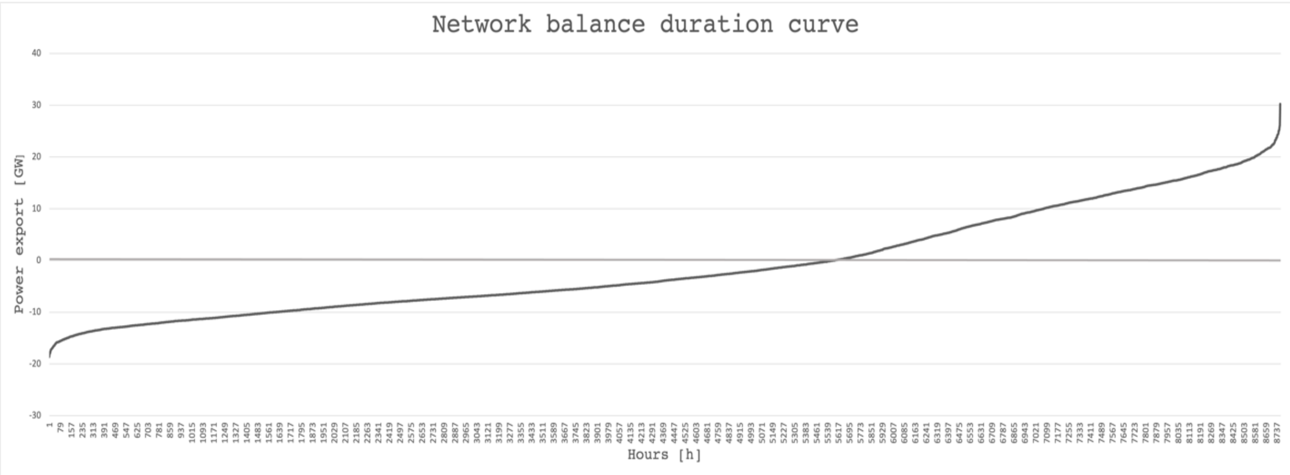

Figure 9.6 - Network active balance power duration curve

As expected, the grid moves from a need of a power import of over 18,500 MW to a need to evacuate almost 30,000 MW. The grid imports for 5670 hours/year i.e. 64.7% of the time.

Active power and storage management

With the aim of simulating a realistic behaviour of current and projected market dynamics OPFs will be set to give different priorities to export, use of storage and resistors. In particular:

- in import, internal generators will be prioritised, then the 13 interconnection nodes and finally the accumulators.
- In export, on the other hand, the local loads will be served first, then the export lines will be saturated, and finally the accumulators will be used.

Indeed, this decision to use accumulations only after the lines are saturated was made to mimic what is expected in a market environment. Storage, being operated by private entities, will have the goal of maximising profit. These could operate either in the energy market or in the ancillary service market. Since the purpose of this thesis is not to simulate the ancillary service market but to optimise the TSO's resources to use them as little as possible, the potential use of storage was considered only in the energy market simulation. Operating in this context, a private entity operating a storage plant will try to exploit the largest price differentials to return on its investment.

Making quick considerations, we can imagine that the price of energy is lower in situations of high production and higher when there are fewer generators available. However, the price differential is limited since, in absence of lines congestion, the grid under consideration is interconnected with other systems. On the other hand, this price differential between the low and high generation moments is accentuated in the event of line congestion and 'market splitting'. When the zone in question saturates its capacity to exchange power with the outside world, it separates as a market zone from the other two neighbouring zones with a consequent increase in energy costs.

Due to these costs and the fact that there are several hours when the import or export power is saturated, the OPF was set up in such a way that storage is used only when the grid can no longer exchange power with the outside world.

We summarize the main data for the network under review:

- Demand of 102 TWh
- Total generation of 92 TWh
- Reactive load between 1,200 and 4,000 MVAr
- Dispatchable power 18,000 MW
- Evacuable power 12,000 MW
- Power of storage plants 12,000 MW
- Installed capacity of resistors 500 MW
- Peak production at 40,000 MW
- Peak power to be evacuated 30,000 MW
- Peak net demand 18,000 MW

Since the active power scenario was generated by a different software than the one simulating its behaviour in alternating power, the dispatch was verified by calculating all DC-OPFs of the hours under consideration. This was done by making the powers of the loads and generators rigid and therefore not modifiable, and instead 'free' within the power limits listed above the powers of the import/export nodes, storage units and resistors.

Since no anomalies were found in the dispatch check, the AC grid behaviour was analysed without additional compensation.

Reactive Power Balance

Having ensured a correct import of the dispatch and modelling of the network, the behaviour of the network with the current reactive resources was examined.

- A series of AC-OPFs was run with the following constraints:
- Active power:
  - Power of loads is fixed.
  - Power deliverable by the generators within a range of ± 2.5% of the dispatch considered.
- Power factor of the generators connected to the grid between 0.95 early and 0.95 late. The minimum capability according to the requirements for generators imposed by Terna was considered.
- Allowable voltages between 1.05 and 0.95 p.u..

The choice of voltage range was determined assuming a 'poorly' compensated network in permanent operation. In this setting, although it is preferable to have a lower voltage limit at a higher intact grid (e.g. 0.975 p.u.) at this stage, we wanted to assess how many hours the ancillary service market would be needed to limit permanent overvoltages.

This initial analysis showed that out of 8760 simulated hours, as many as 1200 hours could not be maintained within the set limits with the current compensation resources. This analysis shows that in the planning phase of a large grid's generation park it is absolutely necessary to check the adequacy of the grid also from the point of view of reactive power, especially with the typical behaviour of non-programmable renewable resources characterised by a high volatility of availability and a limited capacity for voltage regulation.

A sample analysis of some of these hours showed that there were both times when the entire reactive balance of the grid could not be satisfied (i.e. insufficient available reactive power to meet the grid's requirements) and situations where there were excessive voltage drops along the lines and thus a non-overlapping distribution of reactive requirements and availability.

As mentioned in Chapter 3, it is precisely the transit of reactive power that determines most of the voltage variation at the ends of a HV grid component.

This means that in situations when it was not possible to meet the reactive requirements from electrically neighbouring sources, this power had to 'travel' between electrically distant points of the network, resulting in unacceptable voltage drops.

Other information can be derived from this series of simulations, particularly the reactive demand curve of the network.

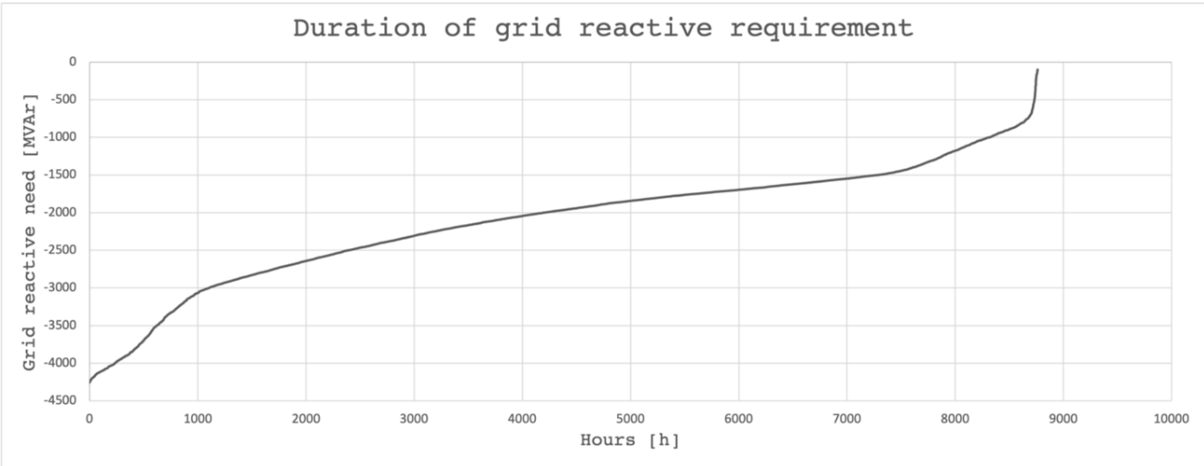

Figure 9.7 - Duration of reactive requirements

Fig. 9.7 shows the requirements of the transmission lines alone, we can see that the grid is overall always capacitive (negative reactive power according to the users' convention).

This is relevant since active dispatching involves a large production of energy from renewable sources that is unevenly distributed over the territory and between the various grid nodes. This phenomenon is well known in transmission grids which, with the increase of small and distributed plants, have seen a progressive 'unloading' of the transmission grid whose lines are therefore most of the time below their Characteristic Power and therefore have capacitive behaviour.

However, this is an overall grid behaviour, and it does not mean that there are no lines that are loaded above the characteristic power in certain dispatching scenarios, but that the overall the grid continues to have a capacitive behaviour. The power to be absorbed therefore varies between 4,800 MVAR and 1,570 MVAR.

If we check the average loading of the AC grid, we can see that it tends to be lightly loaded.

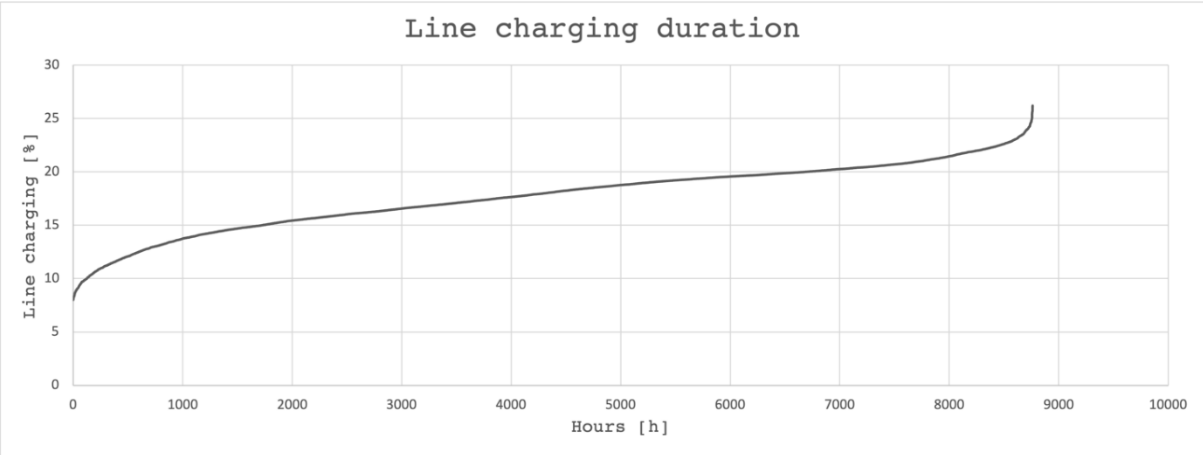

Figure 9.7 - Average line charging duration curve

As can be seen in Figure 9.8, the average loading of the AC grid is between 7 and 25 per cent of their maximum capacity, confirming that the grid most of the time can be considered 'unloaded' or at least overall capacitive. Again, as a preliminary study, the most critical load conditions for the network were checked: in particular, the number of hours in which the voltage limits were violated was correlated with the load conditions.

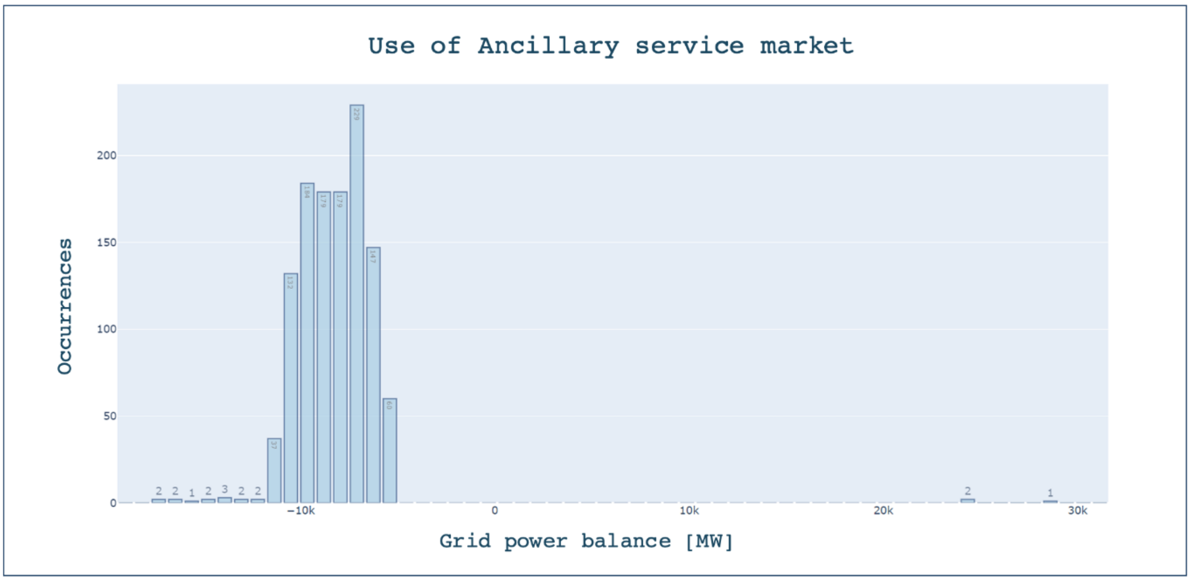

Figure 9.9 - Use of ancillary service market depending on power balance

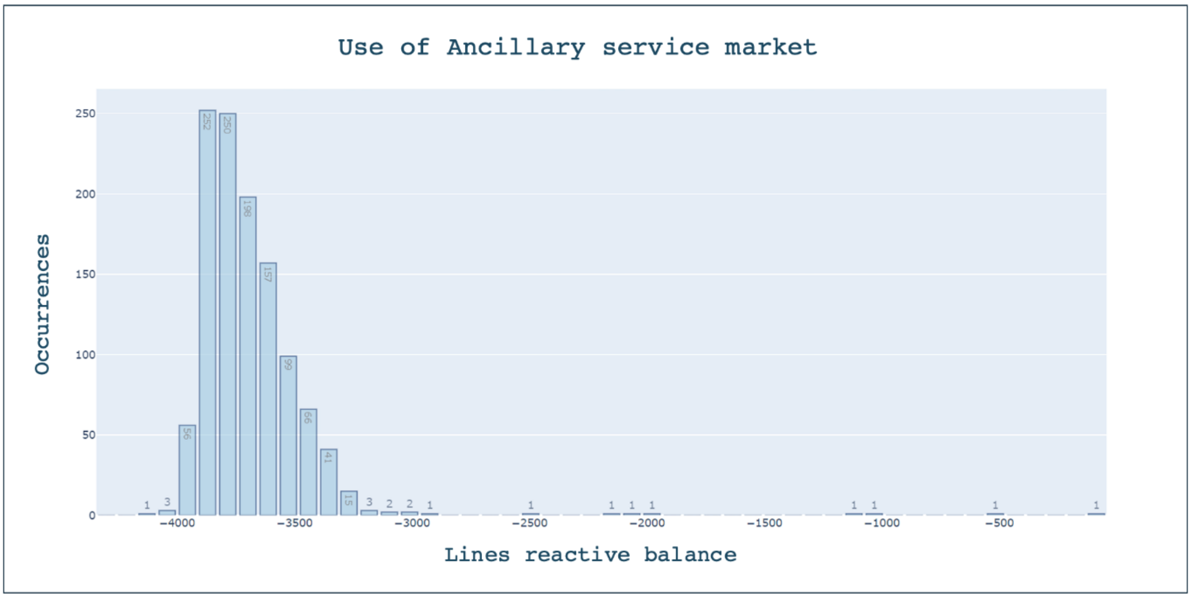

Figure 9.10 Use of ancillary service market depending on lines reactive need

It appears clearly that the system suffers mostly when the grid imports low-load condition. There are time instants when the lines are not particularly loaded and there is little generation.

Short-Circuit Power verification

As already mentioned, the containment of voltage within fixed limits also intended to ensure a minimum short-circuit power at all nodes of the 400 kV network.

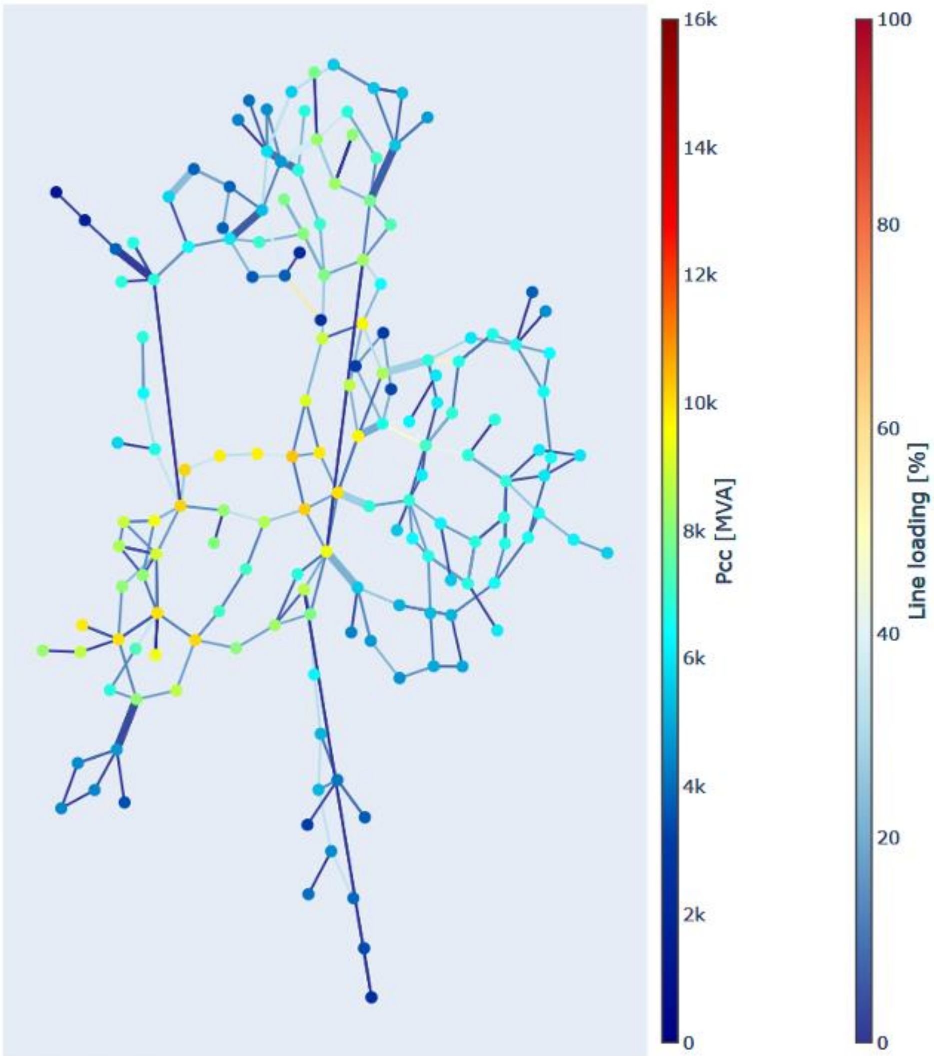

Figure 9.11 Short-circuit power on the grid

From image 9.11, in more than half of the network, the Short-Circuit Power is below the 8000 MVA threshold, which corresponds to a three-phase fault current of about 11.5 kA. This underlines how the planned synchronous condensers are insufficient to reach this threshold.

Cost Hypothesis

For each different reactive power production means the following costs have been assumed for the commercial available size from Terna's cost-benefit analysis.

- Installation of a 250 MVAr reactor bank (3.5 M€)
- Installation of a 125 MVAr STATCOM (18 M€)
- Installation of a 250 MVAr synchronous compensator (25 M€)
- Installation of a pair of synchronous compensators with a total of 500 MVAr (42 M€)

Due to the reduced extension of the 230 kV line, it was decided to install the compensators only at the nodes of the 400 kV portion. In contrast to the previous study on the IEEE 24-bus network case 24, it was permitted to install more than one means of compensation per node.

Considering that there are 75 EHV nodes the combinations of means of compensation are approximately $8 * 10^{80}$.

First Reactive Power Planning Optimization - Voltage Regulation Only

As a first improvement, an optimisation procedure was carried out with three main objectives:

1) The resolution of the hours in which the voltage constraints are violated.
2) The minimisation of the installation cost of the reactive compensation devices.
3) The volatility of the time voltage was taken into account i.e. y the standard deviation of the voltage at the various nodes in the network.

The algorithm is encouraged to choose the solution with the lowest voltage variability for the same cost, and reduction of hours with permanent overvoltages.

This measure steers towards solutions which, having more stable voltages, also reduce voltage drops and thus, in addition to pursuing the goal of a network which, overall, does not violate operating limits, which also has reduced voltage drops within it, trying to supply reactive power as locally as possible.

Given the time required to perform the Reactive-OPFs, it was decided not to simulate all hours of the year, which would have led to a calculation time of several weeks, but to choose a subset of 26 random hours from the 1200 problematic ones.

The algorithm used is NSGA-II as SPEA2 and was written after the first case on case 24 and the optimisation of the large transmission network.

Algorithm parameters

- Number of generations 40
- Initial population number 100
- New solutions per generation 100
- Mutation rate 2%

As a first analysis, let us see for each generation the minimum investment to eliminate all surges that have been considered.

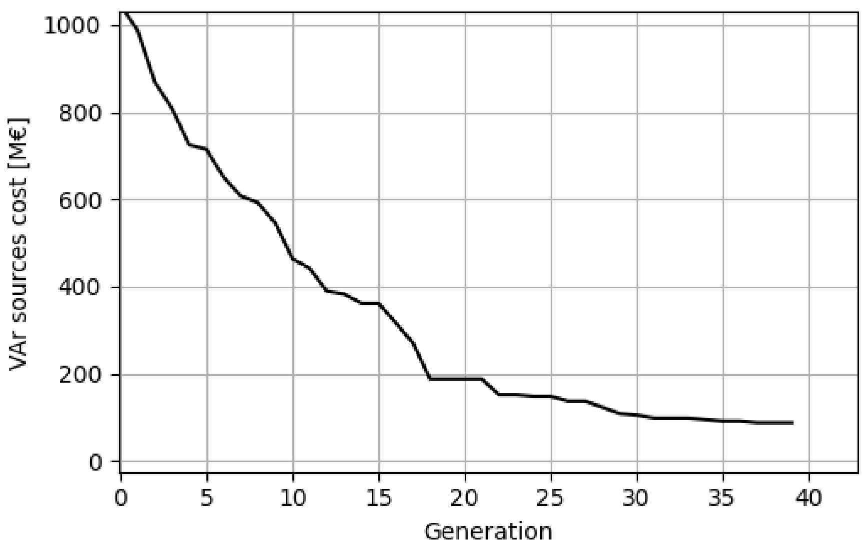

Figure 9.12 - Minimum cost solution vs the number of iterations

Fig. 9.12 shows the trend in the investment cost required to resolve the exceedances of the limits considered. Observe that by the 30th generation the cost has stabilised at 125 M€, a cost reduced by considering the dispatched energy volume of 4.780 M€ according to 2019 costs.

We now move on to an overall representation of the solutions cloud, and, dealing with tree objectives, we need a three-dimensional representation. In addition to the three spatial axes, a colorimetric axis has been added to indicate the generation to which the solution under consideration belongs.

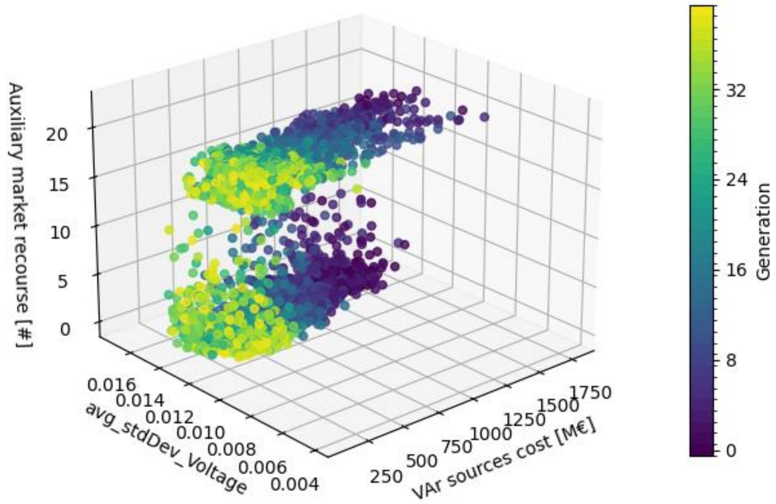

Figure 9.13 - Representation of the solution in the objectives space (4000)

Several issues can be observed from Figure 9.13. The most conspicuous is that the solution cloud is split in two clusters on the vertical axis of the hours in which the ancillary service market should be used. This indicates that many of the surges have a similar origin and once the correct interventions are identified, the number is quickly reduced. A second issue to note, but which is not surprising, is that the clearest solutions, and thus those belonging to the latest generation, are closer to the origin of the axes, showing precisely the convergence of the algorithm towards the goals.

Examining now the representation of the three optimisation objectives without the generation of the membership of the solutions, we observe the graph on two spatial axes: the hours in which to use the ancillary service market and the cost of interventions.

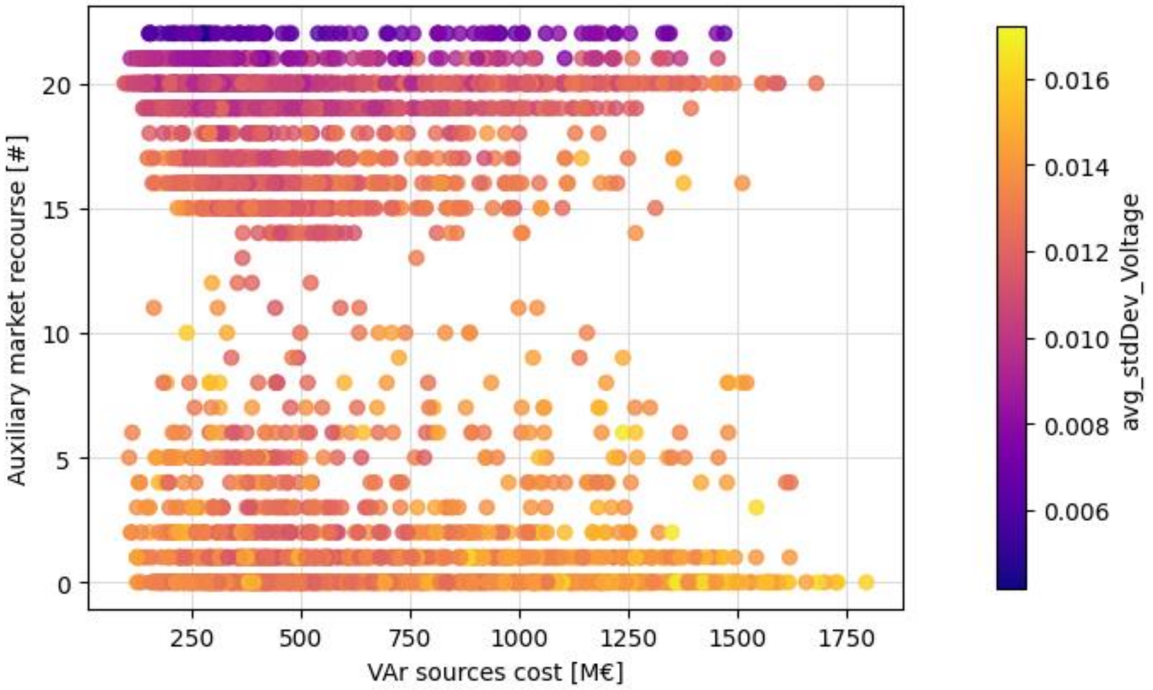

Figure 9.14 - Solutions respect to cost and auxiliary market use (4000)

In Figure 9.14 it is evident how there are two distinct zones in which the solutions are arranged in the codomain. There is an interesting phenomenon regarding these needs that is worth to be analysed and discussed. The hours with a higher non-convergence recurrence of the ACOPF have a less volatile tension: this is due to two main facts:

- First, if the algorithm converges to few hours, then it has few hours over which to calculate the standard deviation of the voltage.
- Secondly, the hours in which the TSO must resort to the ancillary service market and thus those in which voltage limits are violated, even when sufficient means are installed to avoid permanent surges these hours, will inevitably result in a greater voltage difference between the nodes thus raising the voltage standard dev.

We analyse now only the solutions with sufficient means of compensation to avoid all the permanent overvoltages under consideration by graphing them in a 2D space where in abscissas we have the compensation cost and in ordinates the voltage volatility, i.e. the average standard voltage deviation.

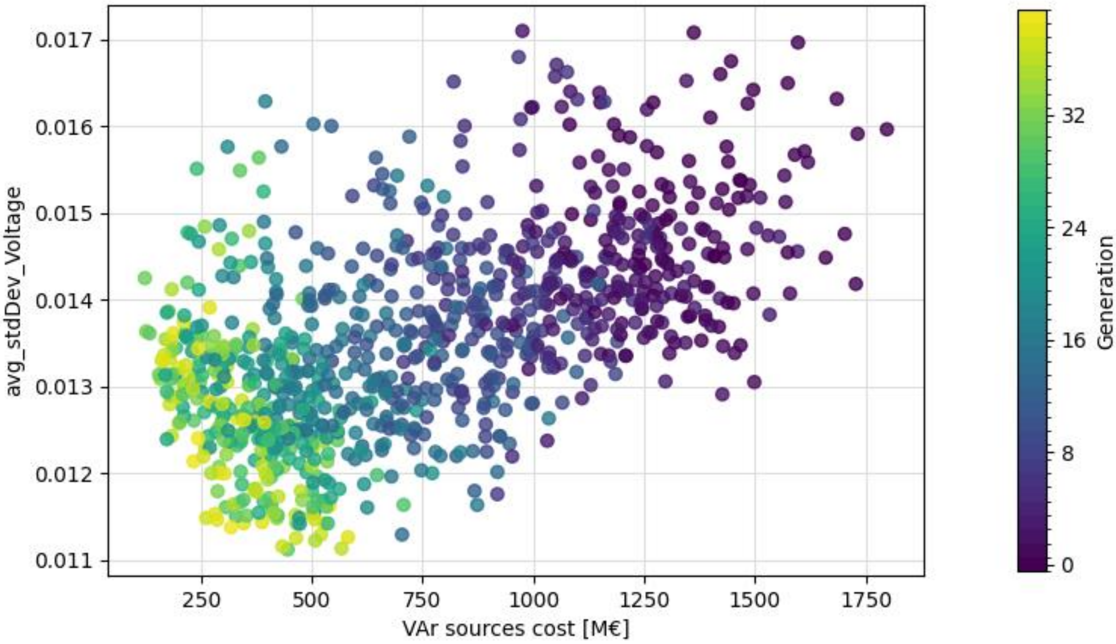

Figure 9.15 - Solutions with no use of auxiliary service market (928/4000)

In Figure 9.15, a colour scale is used to represent the generation to which the solutions belong. As above, we can see that solutions belonging to the more advanced generations perform better overall. Another interesting observation is that the problem with respect to these two objectives (cost and voltage volatility) has better behaviour, forming a compact solution cloud and not dividing into blocks as when considering hours with permanent surges.

Let us now focus only the Pareto-optimal solutions of this subset

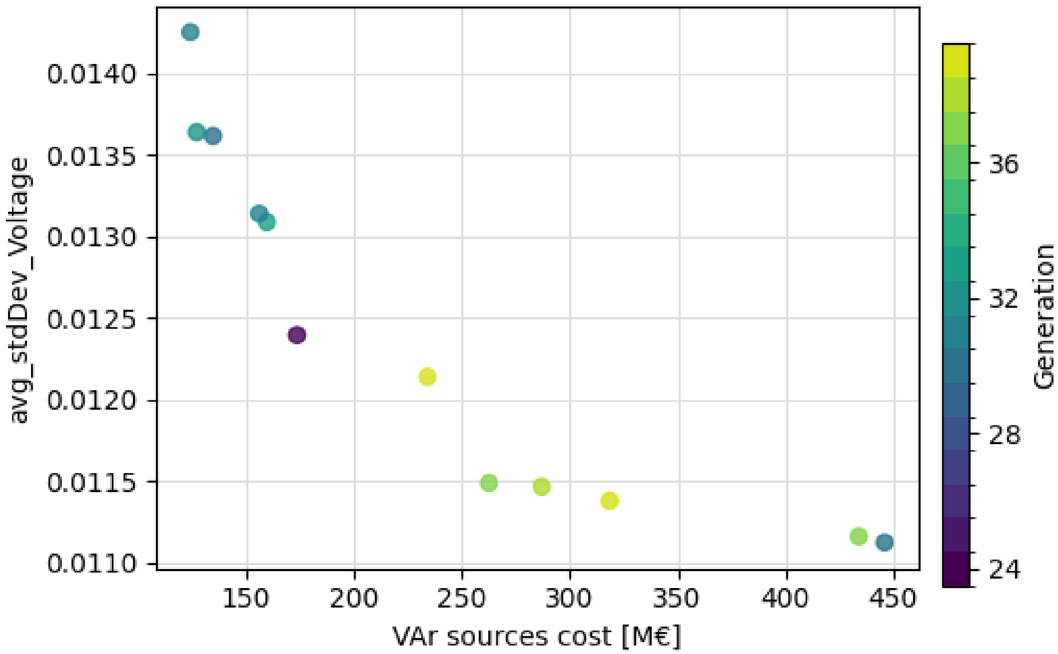

Figure 9.16 - Solutions with no use of auxiliary service market - pareto frontier only (12/4000)

From the representation in Figure 9.16 we can see the spectrum of the 'best' solutions that do not need to resort to ASM. From an algorithmic-computational point of view, we can see how the optimisation system has explored different areas of the solution space at different stages of the optimisation. We see that in the upper part there are solutions calculated around the 30th generation, while in the middle part the solutions were calculated in the earlier iterations. This shows how, even though, as shown in fig 9.12 where we note that the lowest-cost surge-free solution was found around the 30th generation (and it is precisely the solution at the top left highlighted in figure 9.16), the optimisation algorithm has continued to improve the performance of its solutions in other areas of the pareto frontier. From an engineering point of view, we see how a small investment to eliminate surges (124 M€) to reduce the voltage standard deviation from 0.0142 to 0.0112 requires a large investment (additional 320 M€). From a TSO's point of view, there is no need to resort to these extra investments as the operating constraints have already been met. Let us therefore analyse the solution shown in Figure 9.17 in more detail.

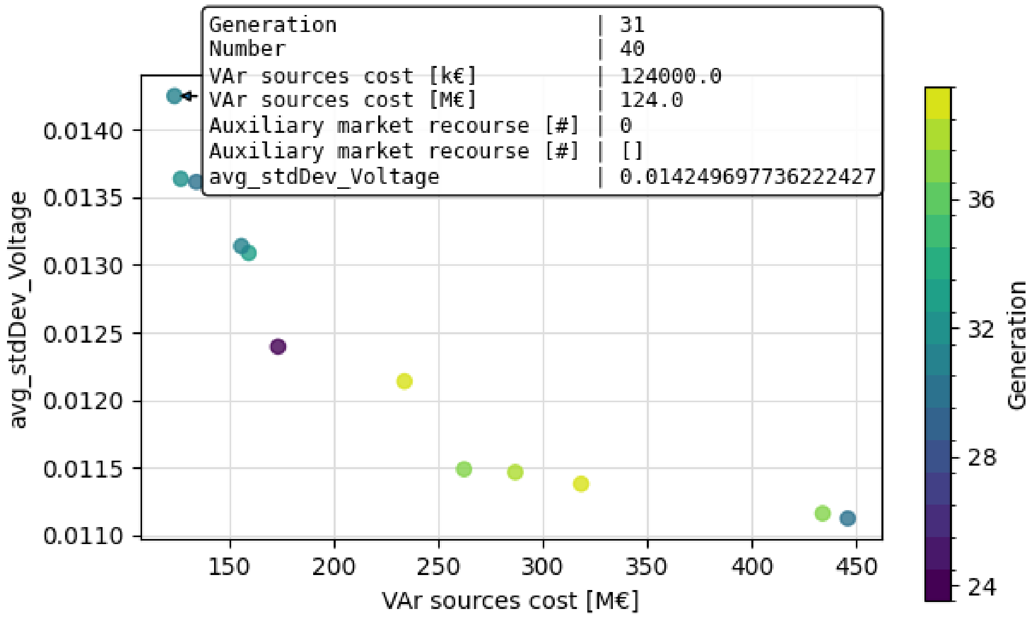

Figure 9.17 - Solutions with no use of auxiliary service market - pareto frontier only with chosen one (12/4000)

This requires the installation of three STACOMs and 18 reactors for a total of 4850 MVAr.

From the installation, it is interesting to note that the use of synchronous compensators is zero. Clearly, since the network is overall always capacitive, no shunt capacitors are installed and the only elements that can produce reactive power are the Synchronous Condensers and the STATCOMs. Given the prevailing need to absorb reactive power generated by the grid, it would not have been economically viable to do this with STACOMs or synchronous compensators, since for the same amount of absorbed reactive power, these cost about 16 times the shunt reactors.

A very important consideration follows the result of this optimisation. Wanting to reduce reliance on the ancillary service market for voltage regulation does not lead to the installation of synchronous compensators. This implies that the achievement of an adequate Short-Circuit power value requires the explicit consideration of this objective.

Second Reactive Power Planning Optimization - Voltage Regulation and Short-Circuit Power

The goal of achieving a minimum Short-Circuit power on AAT nodes of at least 8000 MVA is introduced. This is done by including a fourth target in addition to the previous three, resulting in the following list:

- Minimisation of investment costs.
- Minimisation of voltage volatility (average of the nodes' standard deviation).
- Minimisation of the ancillary service market.
- Minimisation of nodes with short-circuit power of less than 8000 MVA.

The last objective is introduced to ensure a good selectivity of the protections and a reduction of the impact of faults on the voltages of the network nodes. In addition, this minimum Short-Circuit power is necessary for the operation of the three HVDC corridors within the network.

About the assumptions made for this calculation, some clarifications must be made:

- The Short Circuit Power is calculated considering only the contribution of the synchronous compensators owned by the TSO neglecting the contribution of the generators and loads. As far as the loads are concerned, even if they were rotating machines, they would be ‘electrically distant’ from the AAT grid and the trend is increasingly towards the interposition of an inverter between the rotating machines and the grid. As for neglecting the contribution of generators, we must return to the trends that motivated this study. Namely, the ever-increasing production of energy from wind and solar sources that is almost all inverter-based. Clearly, the grid will not be powered always solely by these sources, but we want to analyse the worst case. Moreover, it must also be considered that because of the division between producers and TSOs, the location of conventional generation plants varies over time, so it would have been necessary to make different assumptions about the geographical distribution and frequency of use of these plants.
- Similarly, the contribution of interconnections is not considered. This is done in to place oneself in a precautionary and worst-case condition. In this regard, it must be considered that the area under consideration is assumed to have most of its connections to other portions of the grid via HVDC connections. This on the one hand limits the contribution

of the interconnection nodes to the short-circuit power and on the other hand requires that the interconnection nodes must be 'powerful' as they host HVDC converter stations.

- A final consideration is that Short-Circuit power is calculated when the grid is intact. Although disruptions in the transmission grid are to be avoided as much as possible and the grid is almost always meshed, the absence of a line or a TSO CS for maintenance can alter the values of fault currents and Short-Circuit power.
- Although the Short-Circuit power value may seem high because of the considerations made above, it would always be possible to disconnect the SC during operation if the fault current were to grow too high.

In contrast to the previous optimisation, the number of simulated hours was increased to 100 out of 8760. Moreover, 25 random hours were taken from the problematic ones and 75 hours that did not give rise to surges. This was done to have a closer representation of the year at hand and to direct the means of compensation not only to limiting overvoltages but also to improving the voltage of the hours considered 'non-problematic'.

Algorithm parameters:

- Number of generations 50
- Initial population number 100
- New solutions per generation 100
- Mutation rate 2%

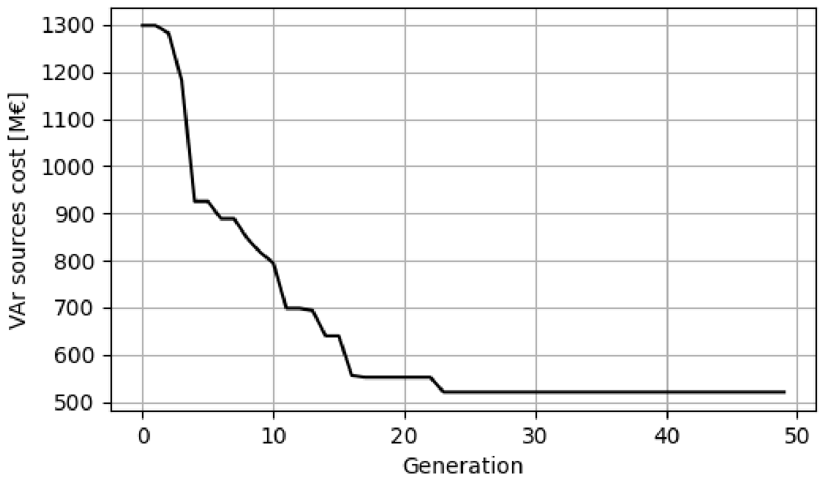

Figure 9.18 - Minimum cost solution with no recourse to the ancillary service market and one weak node vs the number of iterations

As in the previous case, the algorithm converged within 40 generations, although it only settled after the 35th. This may be due either to the different initialisation conditions of the first generation or to the presence of an additional target.

To see the convergence across multiple targets of the algorithm, we show a 2D projection in which the horizontal axis shows the cost of the compensation means and the vertical axis the voltage volatility represented by the standard deviation.

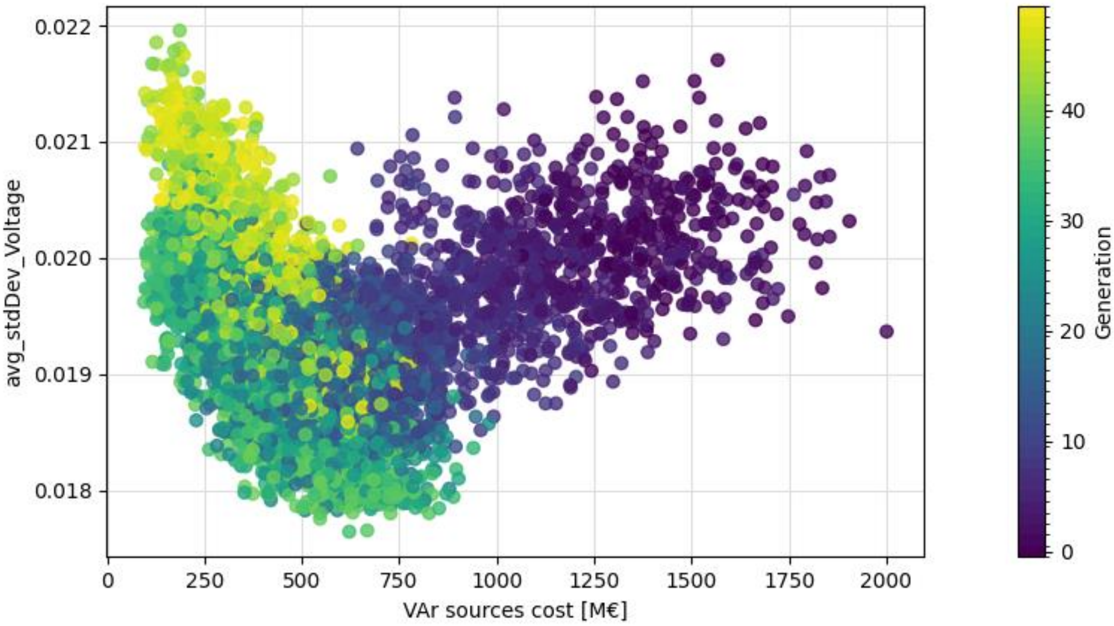

Figure 9.19 - Solutions in a cost-tension volatility plane (5000)

In Figure 9.19 it is used a colour scale to represent the generation of the solutions. We can observe how the population changes as the generations advance approaches the origin of the axes, i.e. towards the simultaneous minimisation of all the objectives.

Instead, by representing three objectives on spatial axes (ancillary service market, cost of means of compensation, number of weak nodes) and one on a colour scale (voltage volatility) we can obtain a picture of the solutions in their natural space.

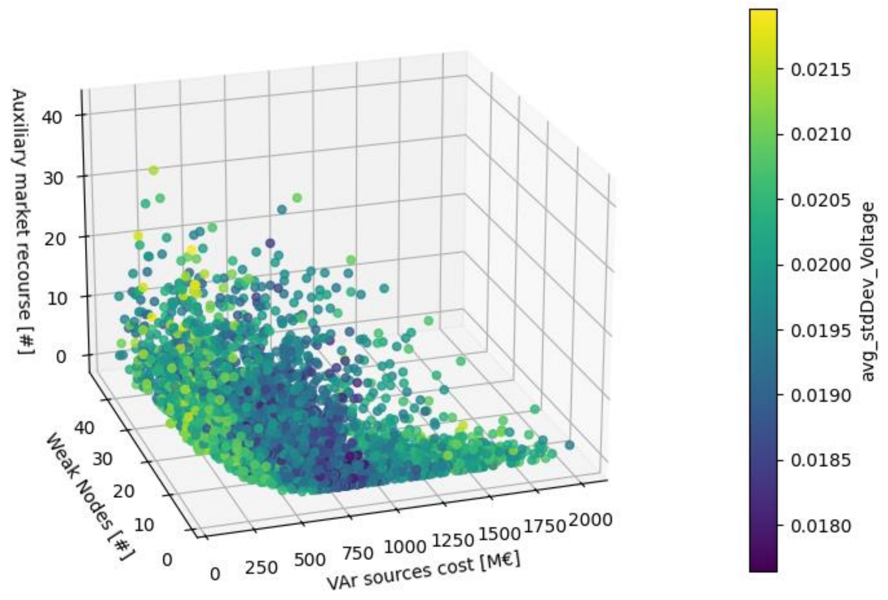

Figure 9.20 - Solutions in the 4D objectives space (5000)

From this representation, we can see how the solutions have arranged themselves in a homogeneous cloud, with a very compact pareto frontier. This, combined with convergence, indicates a good process of finding the optimum.

As we have seen in the previous optimisation, the investment cost of eliminating permanent overvoltages is low (when compared to the cost of the energy flowing through the network), we will only analyse the solutions that eliminate the overvoltages.

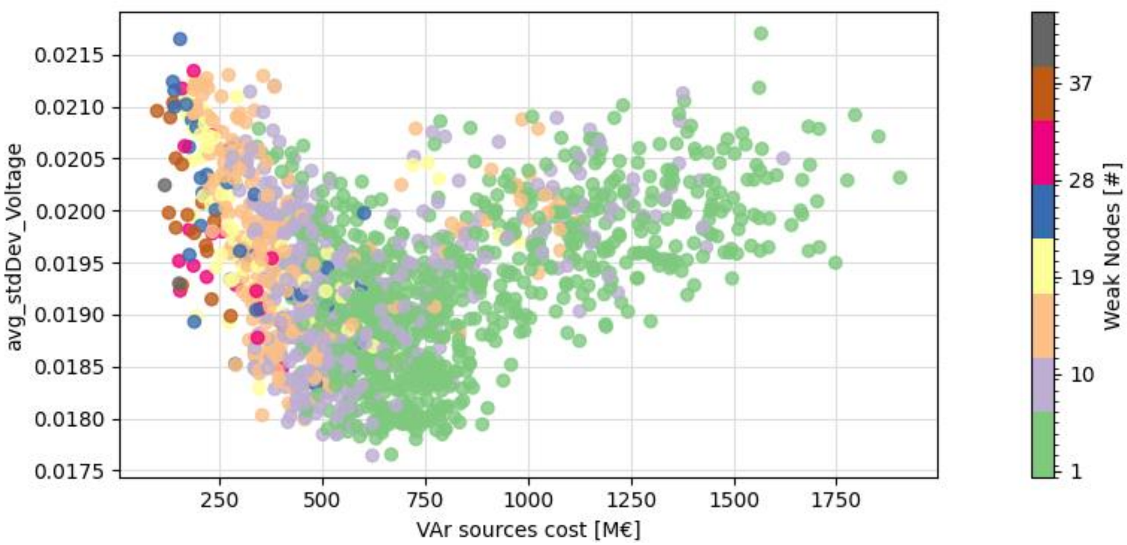

Figure 9.21 - Solutions with no auxiliary market recourse (1691/5000)

In the above figure, we can see that on the left-hand side there is a set of solutions that has no permanent overvoltages and has an investment cost of under 200 M€. These solutions are very similar to those identified in the previous optimisation in that most of the installed power is made up of shunt reactors and only to a much lesser extent of STACOMs and SC. Just as in the previous optimisation, these solutions do not meet the requirement of the minimum Short-Circuit power at 8000 MVA with a large number of weak nodes. Focusing more on the effect of the minimum Short-Circuit power constraint, let us represent in a second graph the cost on the horizontal axis and the number of weak nodes on the vertical axis to see how these two objectives are linked.

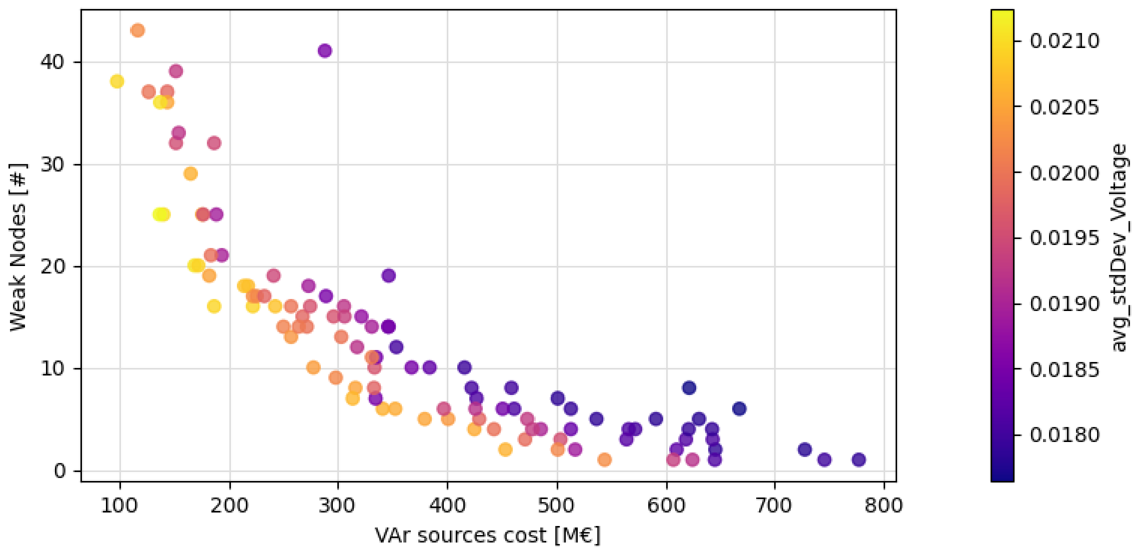

Figure 9.21 - Solutions with no auxiliary market recourse, only pareto optimal (109/5000)

The pareto-optimal solutions on the three objectives (cost of operations, number of weak nodes and voltage volatility) that do not give rise to permanent overvoltages in any of the cases considered are depicted here. The pareto-optimal solutions do not form a curve because this image represents a 2D projection of a distribution of points in 3D space.

From this figure, it is possible to see how much the desired short-circuit power is affected. The cheapest solution that does not give rise to permanent overvoltage costs, precisely 126 M€, while the solution that does not give rise to overvoltages and minimises the number of weak nodes is 544 M€.

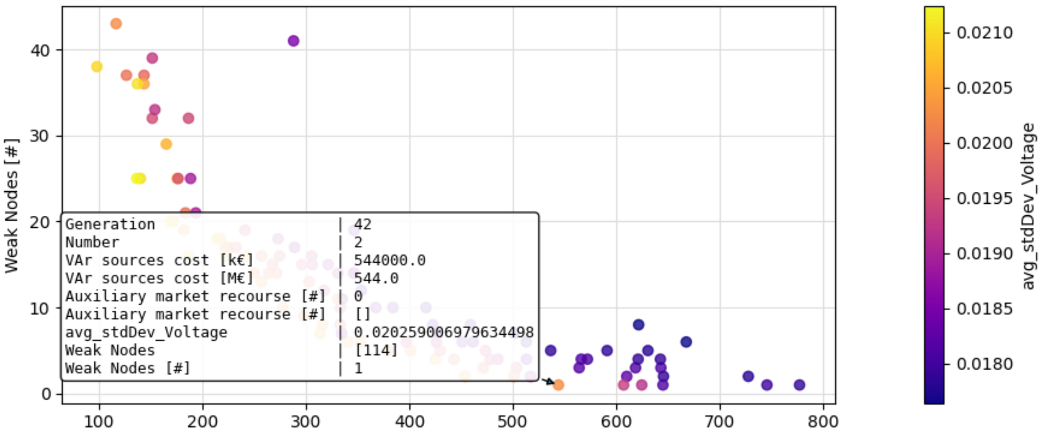

Figure 9.22 – Solutions with no auxiliary market recourse, only pareto optimal with candidate selection (109)

It should also be noted that there is no solution that brings the power of account to the desired value at all nodes. This issue will be discussed in the sequel.

Let us now analyse the solution that best satisfies all the required constraints. This involves the installation of 4 STATCOMs, 6 single synchronous compensators, 6 copies of synchronous compensators, 20 reactors. The installed power is distributed as follows.

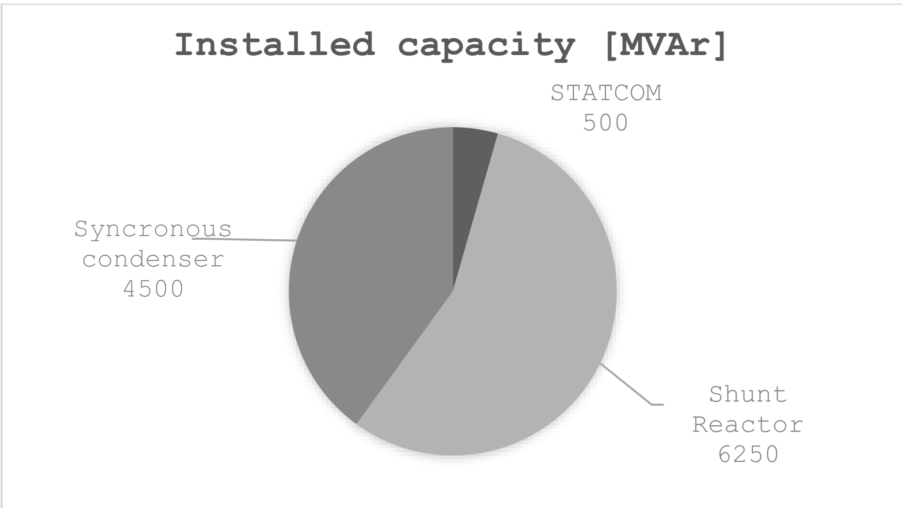

Figure 9.23 – Power distribution among VAR sources

The costs are distributed as follows:

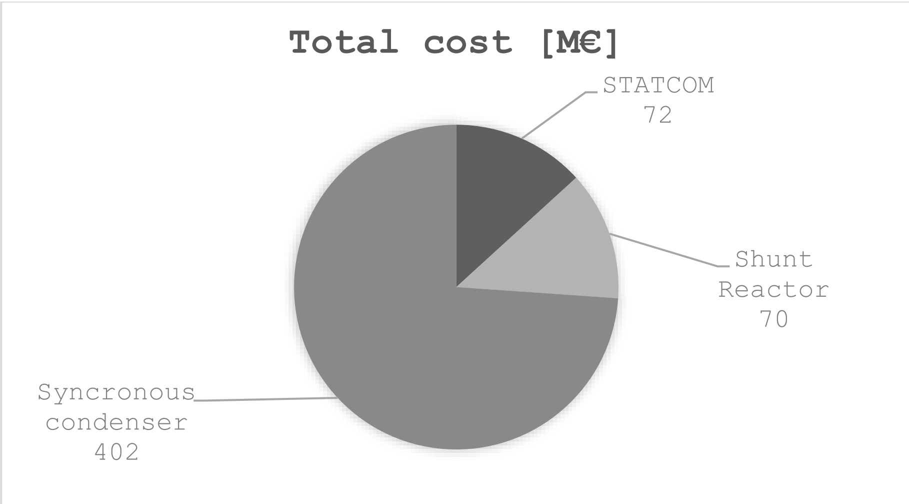

Figure 9.24 - Cost distribution among VAR sources

In Figure 9.24 the synchronous compensators, which are the most complex elements, absorb almost three-quarters of the costs. The total cost is 544 M€ and must be put in relation to both the annual energy transiting the grid from the value of 4,780 M€ to the cost of energy in 2019 or 11,684 to the cost of energy in 2023. The investment is 11.3% of the 2019 energy cost but considering that a normal lifetime for this equipment is more than 40 years, it can be distributed without problems. Another important comparison can be made with the amount of expenses incurred by Terna on the ancillary service market. These amounted to 2,600 M€ in 2021 and 2,300 M€ in 2022 (see [99]).

Indeed, this is the amount spent on the ancillary service market on a grid that in total carries three times the energy of the simulated grid, but the cost required to stabilise the voltage of the simulated portion for 40 years is less than a third of the annual expenditure on the ancillary service market. 544 M€ is also low compared to the 2024-2028 business plan, which envisages investments of over 16,500 M€.

Let us observe in more details the last weak node with a short power of less than 8000 MVA. This is due to the particular position of a specific node, which is located at the antenna at the end of a long 380 kV line where the contribution from the rest of the network is low, and even with the installation of two CS at the node (this was tested manually) it is not possible to obtain the desired current. This peculiarity does not disappear even with the assumptions on Short-Circuit power that have been made, as it is not electrically close to an interconnection node and at the same time houses an HVDC connection. It must also observe that with the two synchronous compensators installed, a short power of 7,250 MVA would be reached, so a TSO could choose either a larger synchronous compensator to achieve the required power or the addition of a third synchronous compensator to provide redundancy in the event of faults or scheduled maintenance without having to operate the HVDC connection at reduced power.

Verification of Proposed Compensation

As already mentioned, given the computational burden of the optimisation, only a portion of the available dispatching hours has been analysed. This was followed by a verification of the optimal configuration obtained by simulating all 8760 available hours with the same voltage and component loading constraints.

This analysis showed that the number of hours requiring the TSO to use the ancillary service market fell from 1200 to 58.

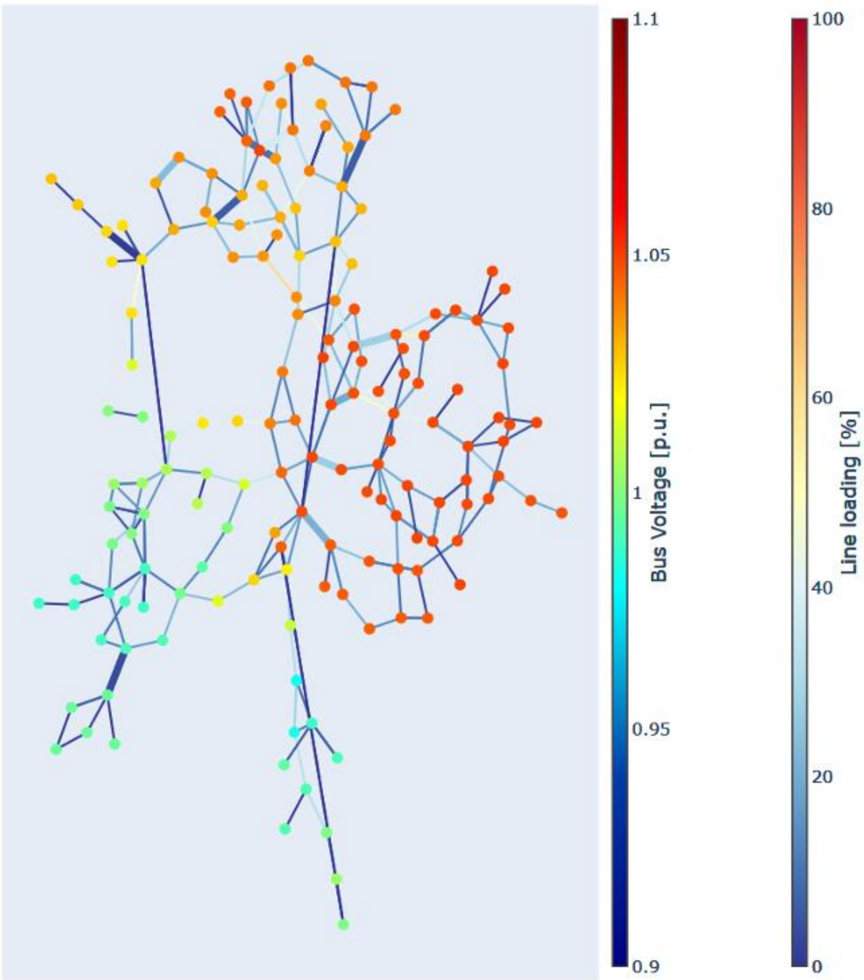

Figure 9.25 - Average voltage and line loading over the 8760 hours

From the above image, we can see that the voltage is higher in the area on the right, which is a section of the 220 kV grid in particular representing one of the two urban centres mentioned in the case study description.

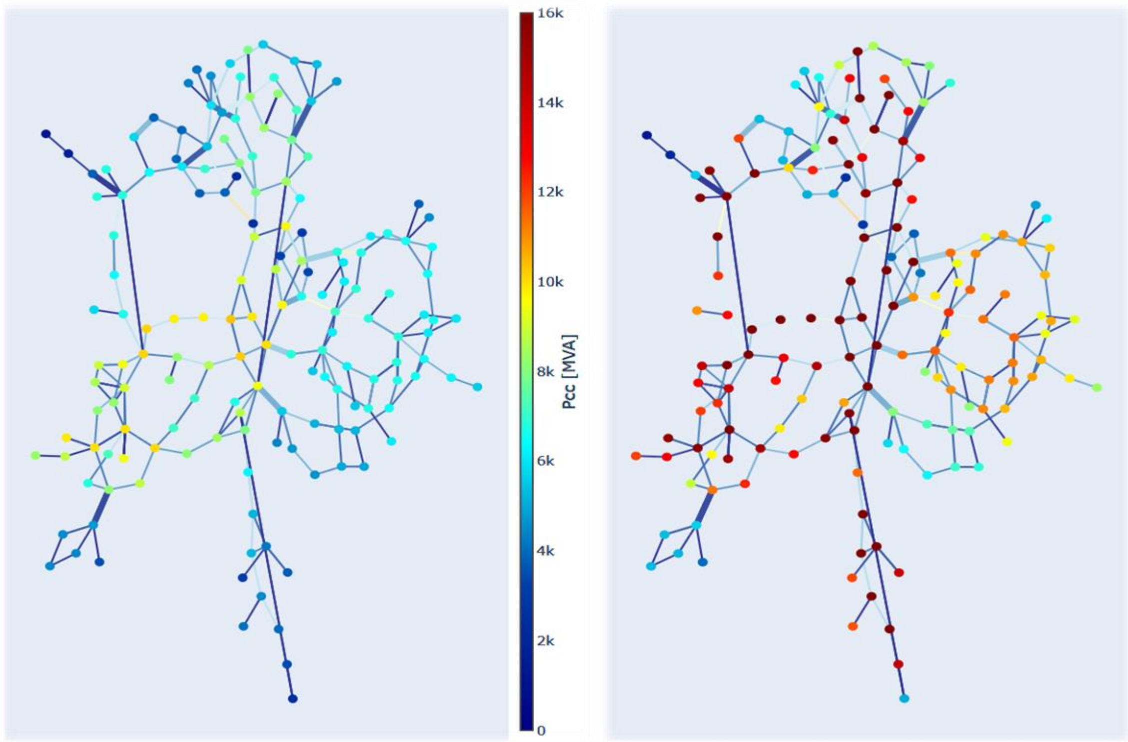

Figure 9.26 - Short-circuit power Before and after the optimization.

Finally, we focused on the 58 hours in which voltage constraints were not met. The analysis of these hours showed that in these dispatching scenarios, the overvoltages were localised in the two 220kV sub-networks representing the two urban centres. In the scenarios considered, the load was very low, and the reactive power production of the cable lines led to significant voltage drops on the 400/230 kV transformers. A quick check showed the overall extent of the cable connections in those areas and the relative reactive power produced.

Zone	Total cables length [km]	Total reactive power [MVAr]
Zone 1	103	370
Zone 2	117	332

Table 9.3 - Reactive power of 220 kV lines in urban areas

Because of this produced reactive power flowing back to the EHV grid, reactors of adequate size were placed at the transformer terminals delimiting the two urban areas in question to compensate 110% of the reactive power produced by the sub-transmission grid. This measure was suggested by the recent ARERA reactive power regulations, which provide penalties for reactive power flows back to the transmission grid.

This phenomenon was studied separately in parallel works with other colleagues in the Department. It was studied how to reduce reactive power counterflows with different mathematical techniques. Effective methodologies to reduce this phenomenon emerged. The studies also showed how the DSO can install means to reduce counterflows but in the simulated scenarios, it emerged that without precise coordination with the TSO, some problems may arise that cannot be solved unilaterally by the DSO. Particular reference is made to parallel flows of reactive power, which, since these portions of the grid are most formed by cable lines, are very sensitive to voltage unbalances (as was seen in Chapter 3).

As a result of the compensation of the 220 kV sub-transmission, all 58 hours that were causing problems were converged. The estimated cost for the reactance and auxiliaries for the installation of these reactances is an additional 21 M€ leading to a final cost of 565 M€.

Third Reactive Power Planning Optimization – Voltage and Short Circuit Power with 220kV Compensated

We wanted to check whether the effect of the 220 kV network compensation influenced the optimisation process and its final result. The parameters of the algorithm and the hours chosen for the evaluation of the compensation means are the same as in the previous case.

An analysis like the previous one was made to verify the behavior of the algorithm to arrive at the following solution.

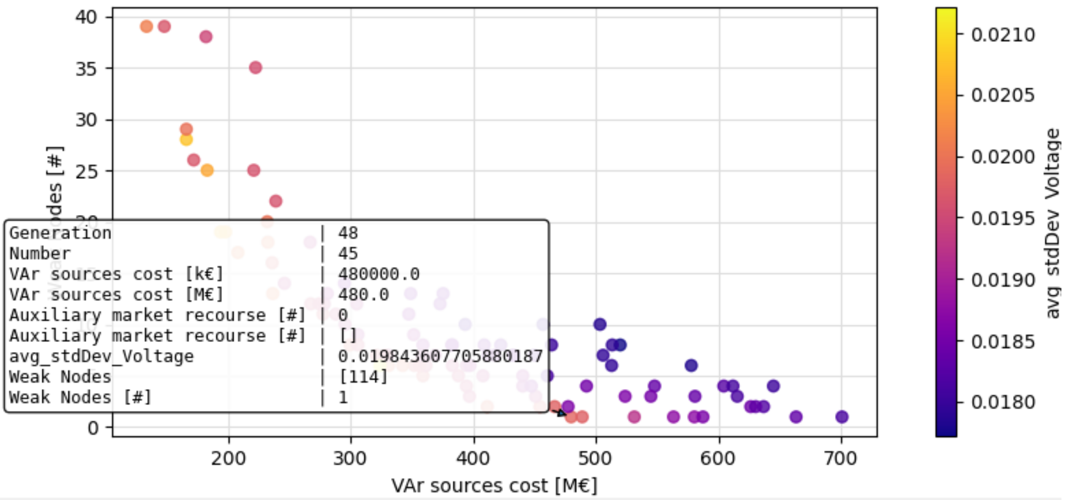

Figure 9.27 – Solutions with no auxiliary market recourse, only Pareto optimal with candidate selection (103/5000)

The solution is as follows:

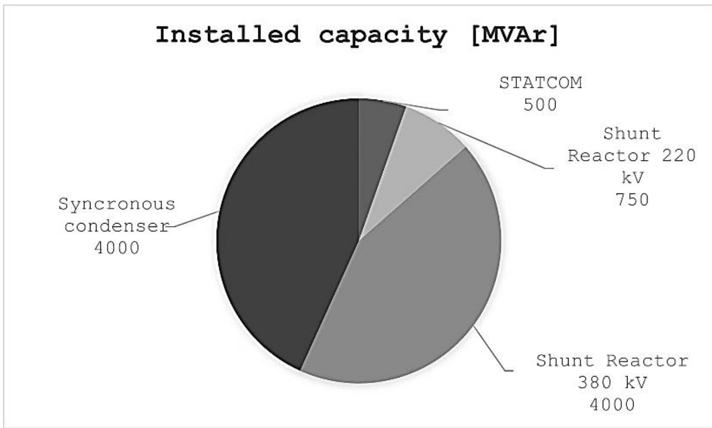

Figure 9.28 – Power distribution among VAR sources

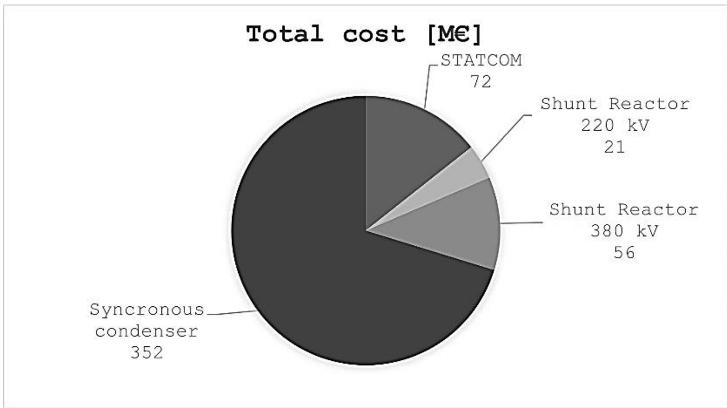

Figure 9.29 – Cost distribution among VAR sources

The cost without the reactors for the 220 kV portion is 480 M€, while considering them is 491 M€. This slight reduction in costs (the second optimization had a total of 565 M€) may be either due to the lower weight of the 220 kV network on the reactive balance or a variation due to the intrinsic randomness of the meta-heuristic optimisation process, which does not guarantee to find the absolute optimum, however close it may be.

This configuration also led to the full convergence of the 8760 hours simulated, hence to a zero reliance on the ancillary service market for voltage regulation.

Solution Response to Changes in Network Structure and Dispatching

A further analysis was conducted on how these means of compensation would react to a grid expansion and a major dispatch change. The grid under consideration was used in a parallel study for a possible expansion plan involving the connection of several offshore wind farms. The study was conducted as a TEP (Transmission Expansion Planning) problem with a DC-OPF. Due to the relatively small distance from the coast, it was possible to connect the new power plants via AC connections. The integration procedure of the wind power plants yielded the following results regarding the grid structure:

- The new power plants are represented by 8 new offshore nodes.
- A new onshore node is required.
- 34 new cable lines are built, these lines are both connecting the hubs to the mainland between the hubs to ensure a more robust system in n-1 to failures. The total extension of the new lines is more than 1900 km.

As for the installed power in the new wind hubs, this amounts to about 11,000 MW and results in an annual production of 30 TWh of energy that must be evacuated in addition to the energy already produced in the grid under consideration as seen above. The total energy produced in the portion of the grid under consideration is therefore 122 TWh.

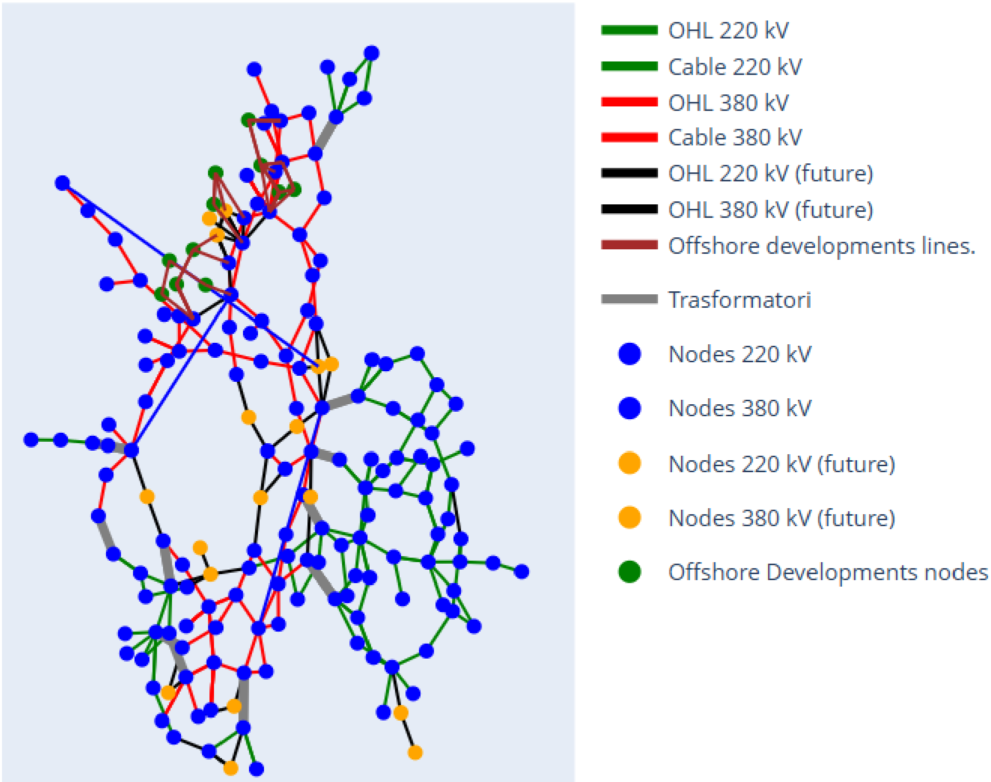

Figure 9.30 – Network structure with offshore additions (blue lines are the HVDC links)

To verify the new AC dispatch, the solution identified by the third optimisation (with the compensated 220 kV urban areas) was used. Given the length of the individual cable lines planned for the wind hubs, these were individually compensated to 95% as is the technical practice for the operation of long cable lines.

The new dispatch was then verified by means of a series of reactive-OPFs considering the reactive resources proposed by the chosen solution. Out of the 8760 hours simulated, only 27 gave rise to problems. When analysing them in detail, it turned out that this was an overload rather than a voltage regulation problem. In particular, one of the new cable lines reached a maximum load of 116%. Two strategies were proposed:

- The first one consists in a simple curtailment action to bring the transiting power back below the nominal value resulting in an energy loss of only 127 MWh.
- The second one (which does not seem justifiable in terms of cost) is to use cables with a larger cross-section for the line under consideration.

Turning to the verification of short-circuit power, this was ensured at all nodes added by TEP's procedure. The addition of the synchronous compensators calculated by the procedure to the existing ones was also sufficient for the new nodes.

As a final analysis, we wanted to check the trend in voltages and reactive power flows precisely at the terminals of the synchronous generators in the network. This was done to check how much adjustment margin there was for possible changes in dispatching and/or reactive power demand.

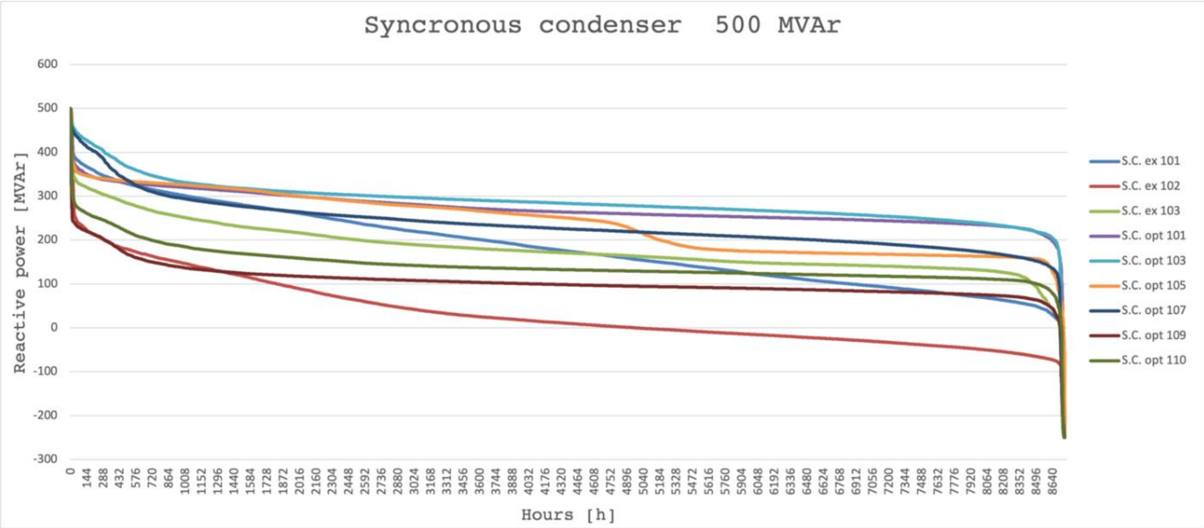

Figure 9.31 - Reactive power synchronous condensers 500 MVAr

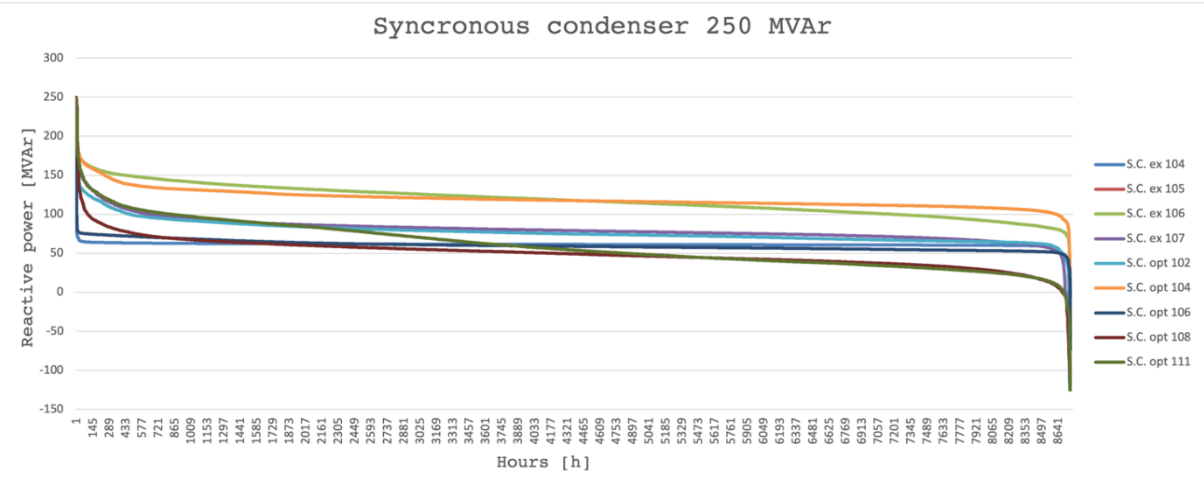

Figure 9.32 - Reactive power synchronous condensers 250 MVAr

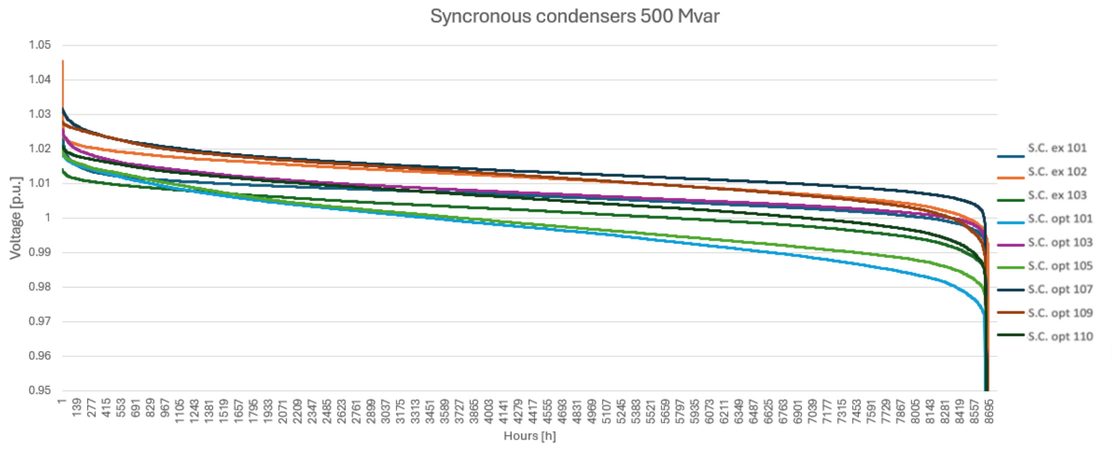

Figure 9.33 - Voltage power synchronous condensers 250 MVAr

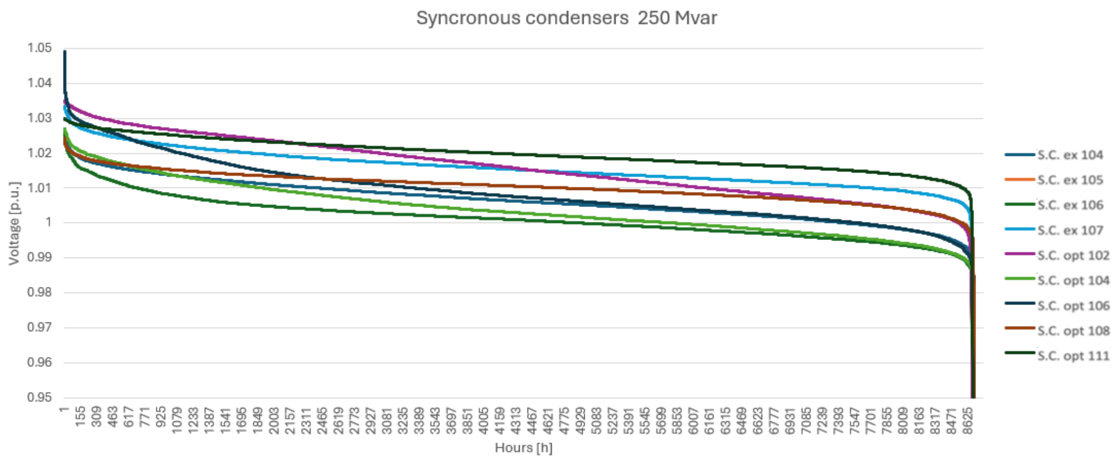

Figure 9.34 - Voltage synchronous condensers 250 MVAr

The results show that in practice the synchronous compensators always operate in overexcitation during the year, which is easily predictable given the disappearance of conventional synchronous generators from the grid; the only exception is the 500 MVAr 'S.C. opt 109' paired unit in Figure 9.32, which operates in underexcitation for 3000 hours per year. The stability in power output shows that there is certain margin in this respect. This does not indicate a waste of resources as the synchronous compensators shown here are in any case necessary for an adequate level of short-circuit power.

As the voltage is concerned, the results also show a strong stability over time, indicating a safety margin.

Chapter 10 –Additional Scientific Contributions

Other topics from both the electrical and more general engineering fields were also addressed during this doctoral program.

Sub-transmission Networks:

A contribution has been given to the modelling of methodologies for reducing reactive power flows going up from the sub-transmission grid to the transmission grid [100]. In this area, new models and methods were designed for the arrangement and sizing of shunt reactors on a grid in a large urban area. This study led to the comparison of the various methodologies by highlighting the strengths and weaknesses of the different approaches. Being in effect a problem of reactive power planning, this study had an important resonance with the main research theme of the doctoral activity. Given the different perspectives and the difference in some constraints, it was decided to adopt different and less general models than those illustrated in the thesis discussed so far [100].

Medium Voltage:

Special attention was paid to the study of overvoltages for single-phase ground faults. A simplified model based on the Clarke transform was developed to estimate the transient overvoltage following single-phase ground fault for isolated neutral networks. The model proved effectiveness for maximum overvoltage estimation in a large parametric study by comparing Clarke transform model data with a full phase coordinate model. Both a test network and a real case study were used, [101].

Regarding the integration of renewable resources, a study was also conducted for the construction of an agri-voltaic plant. The field had to meet both constraints related to agricultural land use and glare constraints given its proximity to an airport. The combination of these constraints led to the development of a methodology that reconciled the various requirements by acting on all fronts, including the exploitation of green barriers. These were instrumental in eliminating glare to the control tower, [102].

A contribution was made to the study of the effect of increasing renewable resources (mainly PV) in distribution networks. In particular, an analysis was conducted on the

Terni distribution grid to evaluate the effect of the increase of these resources in energy communities and assess their self-consumption, [103].

Railways electrification:

The applicability of the optimization algorithms illustrated in this thesis to railway electrification was also evaluated. Substantial contribution was made to the modelling of the components of the railway simulation software illustrated in this study, and the coupling part to the optimization tool was fully taken care of. The simulation software was validated with another extensively tested program to verify the correctness and reliability of the results. A methodology was also developed for evaluating and reducing the impacts of line circuit power substation failures. The complete methodology for optimization algorithm-aided design was tested on both a test rail line and an already electrified line to evaluate its results compared to a line designed without the aid of these tools. The results were encouraging in that the algorithm identified different configurations that without reducing power quality or robustness to faults significantly reduced implementation and operating costs. In particular, the algorithm gave important insights into the effectiveness of parallel points in reducing voltage drops and the effect of faults. Since these longline facilities are currently sparsely used, given the importance of the results we hope for greater use of these facilities [104].

Low voltage:

Starting with low voltage, the topic of utility monitoring and distributed generation was addressed, and a significant contribution was made to the realization of a low cost RaspberryPi-based prototype of a smart meter. This prototype for real-time monitoring was built within the Department's premises and then field-tested to monitor a PV array connected to the low-voltage and an office-use civilian utility, [105,106]

Buildings environmental footprint:

Several studies have been conducted on reducing the energy requirements and environmental impact of residential buildings. These studies have involved both renovations of the currently built stock and the construction of new buildings. Regarding currently constructed buildings, an iconic Roman social housing complex was taken as a case study. The process of identifying the best strategies for reducing consumption and emissions involved the development of a two-stage optimization based on a meta-heuristic optimization algorithm and two energy simulation software. Substantial effectiveness of the implemented method emerged from this case study. The results of the optimizations show an important result from the point of view of CO_2 emission reduction strategies. In particular, the effect of passive strategies (such as improving wall insulation with thermal coats and window replacement) and “active” strategies such as system replacement (switching from gas boilers to heat pumps) and integration of renewable sources (photovoltaic panels) on-site was observed. Among passive strategies, replacement of windows and doors emerged as most effective. Among active strategies, several interventions were considered, including improving the performance of boilers, switching to cogeneration, and total electrification of consumption with heat pumps. Among the active strategies, heat pumps proved to be the most effective strategy from the point of view of emission reduction and the one with the shortest payback time. Finally, comparing active strategies with passive strategies, active strategies showed higher capital efficiency. Indeed, for the same investment, active strategies lead to four times the percentage reduction in emissions, [107,108]. These studies, as unrelated as they seem to the thesis, show that some of the assumptions from which the thesis started are correct: electrification of consumption is an inevitable trend given its effectiveness in reducing CO_2 emissions.

For newly constructed buildings, a study was conducted to evaluate the impact of shape, glazing layout, passive strategies, and active strategies for reducing energy demand and emissions. These various aspects were evaluated by an extensive simulation campaign guided by genetic algorithms. The result led to an energy-optimized building in all aspects, [109]

Finally, the impact of the shape and arrangement of glazed surfaces was evaluated in relation to climate. Nineteen European cities differing in climate and latitude were chosen and the best shape for each climate zone was evaluated using meta-heuristic algorithms. The results show that the “cross” is the most resilient building overall dominating in most sites relegating the other shapes to climates at the extremes of the conditions considered (thus extremely cold or extremely hot), [110].

Chapter 11 – Conclusions and Further Research

This thesis was structured as a monograph on the issue of reactive compensation of transmission networks. Given the unstructured environment of the electricity sector, current de-regulated market rules, and the desire to decarbonize the sector through non-programmable renewables, voltage regulation and Short-Circuit power maintenance are currently facing new paradigms.

These two requirements are increasingly devolved to the transmission system operator who, to contain costs and avoid incurring penalties, must equip itself with its own means for the smooth operation of the grid in these respects.

A careful examination of the state of the art on international journals on this subject made it possible to highlight which methodologies had been used to address these issues. The strengths and limitations of the various network modelling, boundary assumptions and solving algorithms adopted were analysed. This review of the bibliography, allowed for the identification of the set of tools best suited to address the new context in which voltage regulation and Short-Circuit power maintenance must be placed.

It was therefore decided to opt for a representation of the network at the highest accuracy to recreate both the dynamics of the energy market and the operating conditions under which a TSO can operate without resorting to the ancillary service market.

Two optimization algorithms were then developed to address the problem of placing and sizing reactive compensation resources.

Two main case studies were carried out:

- The method was first tested on a standard IEEE network. Several scenarios were generated on which the algorithms were tested. Both algorithms, with slightly different performances, were successful in eliminating the use of the ancillary service market.
- Next, the transmission network of southern Italy was modelled, accompanied by the interventions planned for the coming years by the development plans. The simulated conditions of strong integration of renewable resources and generator behaviours were consistent with the methodologies outlined by Terna in its cost-benefit analysis guidelines.

Several simulations were conducted to verify and refine the results obtained from the methodology. The final result obtained is a set of compensatory means that eliminates the use of the ancillary service market with regard to voltage regulation in the grid under consideration.

The cost of these means of compensation was compared with the current expenses in the ancillary service market. The results show that it is indeed cost-effective for TSOs to use their own means of regulation instead of using the ancillary service market. The solution identified with the proposed methodology proved to be robust even in a situation of dispatch switching and a 30 percent increase in energy produced due to expansion of the generation pool and grid.

Recalling now the very beginning of this study, we realise that when this thesis started in 2020 there was a minor attention to the reactive power flows, and to the costs of the ancillary service market. The two directives of ARERA regarding the reactive compensation of large urban areas and the incentives for the reduction of expenses on the ancillary service market underline the relevance and actuality of this work proposed by the research group of the DIAEE department.

Parts of this thesis has been extracted to be submitted for publication in international journals.

As effective as the methodology has proven to be, some developments are possible including:

- Testing its effectiveness on the issue of counterflows.
- Also, the SPEA2 needs to be tested on bigger grids. Future works can regard a confrontation between more algorithms like DiscretePSO, Crow search or ant colony) and the determination of the best meta-parameters of the algorithm involved.
- Trying a decoupling of the short-circuit power problem with that of voltage regulation. Short-circuit power optimization requires the use of meta-heuristic algorithms, but once the position of synchronous compensators is fixed, the error of some methods such as network linearization and the use of sensitivity matrices and load-flow is reduced by being able to reduce the computational complexity of the problem compared to a sequence of NLPs due to the reactive-OPFs.

I hope that future studies will follow the methodology proposed in this thesis.

References

[1] Energy use per person vs. GDP per capita, 2022, Our World in Data (2023). https://ourworldindata.org/grapher/energy-use-per-person-vs-gdp-per-capita (accessed August 20, 2024).

[2] Climate Change 2021 Working Group I contribution to the Sixth Assessment Report of the Intergovernmental Panel on Climate Change Summary for Policymakers, (n.d.).

[3] Life Cycle Assessment of Electricity Generation Options, 2023. https://unece.org/sites/default/files/2021-11/LCA_final.pdf (accessed August 27, 2024).

[4] R. Turconi, A. Boldrin, T. Astrup, Life cycle assessment (LCA) of electricity generation technologies: Overview, comparability and limitations, Renewable and Sustainable Energy Reviews 28 (2013) 555–565. https://doi.org/10.1016/J.RSER.2013.08.013.

[5] European Commission, The 2030 climate and energy framework - Consilium, n.d. https://www.consilium.europa.eu/en/policies/climate-change/2030-climate-and-energy-framework/ (accessed August 21, 2024).

[6] The European Green Deal - European Commission, (2020). https://commission.europa.eu/strategy-and-policy/priorities-2019-2024/european-green-deal_en (accessed August 21, 2024).

[7] REPowerEU, (2022). https://commission.europa.eu/strategy-and-policy/priorities-2019-2024/european-green-deal/repowereu-affordable-secure-and-sustainable-energy-europe_en (accessed August 21, 2024).

[8] National energy and climate plans, (n.d.). https://commission.europa.eu/energy-climate-change-environment/implementation-eu-countries/energy-and-climate-governance-and-reporting/national-energy-and-climate-plans_en (accessed August 20, 2024).

[9] Share of electricity generation from fossil fuels, renewables and nuclear, Europe, (2023). https://ourworldindata.org/grapher/electricity-fossil-renewables-nuclear-line?time=2000..latest&country=~OWID_EUR (accessed August 22, 2024).

[10] H. Ritchie, P. Rosado, M. Roser, Electricity Mix, Our World in Data (2024). https://ourworldindata.org/electricity-mix (accessed September 6, 2024).

[11] Carbon Neutrality in the UNECE Region: Integrated Life-cycle Assessment of Electricity Sources, 2022. https://unece.org/sites/default/files/2022-04/LCA_3_FINAL%20March%202022.pdf (accessed August 27, 2024).

[12] Energy Institute, Statistical Review of World Energy | 72 nd edition, (2023).

[13] I. Energy Agency, Net Zero Roadmap: A Global Pathway to Keep the 1.5 °C Goal in Reach - 2023 Update, (2023). www.iea.org/t&c/ (accessed September 14, 2024).

[14] European Electricity Review 2024 | Ember, (n.d.). https://ember-climate.org/insights/research/european-electricity-review-2024/ (accessed September 14, 2024).

[15] J. Blazquez, R. Fuentes, B. Manzano, On some economic principles of the energy transition, Energy Policy 147 (2020) 111807. https://doi.org/10.1016/J.ENPOL.2020.111807.

[16] V. Costanzo, F. Nocera, M. Detommaso, G. Evola, Decarbonizing cities through electrification: A strategic study for densely built residential districts in Southern Italy, Sustain Cities Soc 113 (2024) 105651. https://doi.org/10.1016/J.SCS.2024.105651.

[17] Y. Kaya, Keiichi. Yokobori, Environment, economy, energy and sustainable development, (1997) 381.

[18] Kaya identity: drivers of CO_2 emissions, European Union (27), (2023). https://ourworldindata.org/grapher/kaya-identity-co2?time=2010..latest&country=~OWID_EU27 (accessed August 23, 2024).

[19] Statistics | Eurostat, (n.d.). https://ec.europa.eu/eurostat/databrowser/view/sdg_08_10/default/table (accessed August 22, 2024).

[20] D.P. Schlachtberger, T. Brown, S. Schramm, M. Greiner, The benefits of cooperation in a highly renewable European electricity network, Energy 134 (2017) 469–481. https://doi.org/10.1016/J.ENERGY.2017.06.004.

[21] K. Schaber, F. Steinke, P. Mühlich, T. Hamacher, Parametric study of variable renewable energy integration in Europe: Advantages and costs of transmission grid extensions, Energy Policy 42 (2012) 498–508. https://doi.org/10.1016/J.ENPOL.2011.12.016.

[22] R.A. Rodríguez, S. Becker, G.B. Andresen, D. Heide, M. Greiner, Transmission needs across a fully renewable European power system, Renew Energy 63 (2014) 467–476. https://doi.org/10.1016/J.RENENE.2013.10.005.

[23] R. Golombek, A. Lind, H.K. Ringkjøb, P. Seljom, The role of transmission and energy storage in European decarbonization towards 2050, Energy 239 (2022) 122159. https://doi.org/10.1016/J.ENERGY.2021.122159.

[24] HVDC projects by EMEA country 2022-2025 | Statista, (2020). https://www.statista.com/statistics/1360821/high-voltage-direct-current-hvdc-projects-by-country-forecast/ (accessed October 8, 2024).

[25] TERNA, Il progetto hypergrid e necessità di sviluppo infrastrutturale, 2023. https://download.terna.it/terna/Terna_Piano_Sviluppo_2023_Progetto_Hypergrid_necessit%C3%A0_Sviluppo_infrastrutturale_8db2549ed056bf0.pdf (accessed September 7, 2024).

[26] Renewable Energy Progress Tracker – Data Tools - IEA, (n.d.). https://www.iea.org/data-and-statistics/data-tools/renewable-energy-progress-tracker (accessed October 8, 2024).

[27] Direttiva - 96/92 - EN - EUR-Lex, (92AD). https://eur-lex.europa.eu/legal-content/IT/TXT/?uri=CELEX%3A31996L0092 (accessed October 3, 2024).

[28] Gazzetta ufficiale delle Comunità europee, (1996).

[29] About ENTSO-E, (2024). https://www.entsoe.eu/about/ (accessed October 11, 2024).

[30] Member Companies, (2024). https://www.entsoe.eu/about/inside-entsoe/members/ (accessed October 11, 2024).

[31] ARERA, Definizione di un sistema di incentivazione ai fini della riduzione dei costi di dispacciamento - Arera, 2022. https://www.arera.it/atti-e-provvedimenti/dettaglio/21/597-21 (accessed October 8, 2024).

[32] Terna, RELAZIONE 2022 INCENTIVO PER LA RIDUZIONE DEI COSTI DI DISPACCIAMENTO, (2022).

[33] Terna, Piano di Sviluppo 2023 della rete elettrica nazionale, (2023). https://www.terna.it/it/media/comunicati-stampa/dettaglio/piano-sviluppo-2023 (accessed October 4, 2024).

[34] Ministero per l'ambiente e lo sviluppo economico, ELMED: Il MASE autorizza il collegamento Italia-Tunisia, (2024).

[35] F. Gatta, Impianti Elettrici 1, (2022). https://books.google.com/books?hl=it&lr=&id=FYqJEAAAQBAJ&oi=fnd&pg=PA35&dq=related:g_HjkufNUnoJ:scholar.google.com/&ots=1iSq7FZJMF&sig=4DOYScQH6V-CypD-ROxfhRWeaBo (accessed October 11, 2024).

[36] F. Iliceto, Impianti Elettrici, Patron Editore, 1981.

[37] P. Charles, F. Mehazzem, T. Soubdhan, A review on optimal power flow problems: Conventional and metaheuristic solutions, 2020 2nd International Conference on Smart Power and Internet Energy Systems, SPIES 2020 (2020) 577–582. https://doi.org/10.1109/SPIES48661.2020.9242994.

[38] IEC 60909-0:2016 | IEC, (2016). https://webstore.iec.ch/en/publication/24100 (accessed August 30, 2024).

[39] D.P. Kroese, T. Brereton, T. Taimre, Z.I. Botev, Why the Monte Carlo method is so important today, Wiley Interdiscip Rev Comput Stat 6 (2014) 386–392. https://doi.org/10.1002/WICS.1314.

[40] A. Barbu, S.C. Zhu, Monte carlo methods, Monte Carlo Methods (2020) 1–422. https://doi.org/10.1007/978-981-13-2971-5/COVER.

[41] E. Fermi, R. Richtmyer, Note on census-taking in Monte-Carlo calculations, U.S. Department of Energy (1948). https://www.osti.gov/servlets/purl/4423221 (accessed October 12, 2024).

[42] J.A.P. Lopes, N. Hatziargyriou, J. Mutale, P. Djapic, N. Jenkins, Integrating distributed generation into electric power systems: A review of drivers, challenges and opportunities, Electric Power Systems Research 77 (2007) 1189–1203. https://doi.org/10.1016/j.epsr.2006.08.016.

[43] A. Alabdulwahab, A. Abusorrah, X. Zhang, M. Shahidehpour, Coordination of Interdependent Natural Gas and Electricity Infrastructures for Firming the Variability of Wind Energy in Stochastic Day-Ahead Scheduling, IEEE Trans Sustain Energy 6 (n.d.) 606–615. https://doi.org/10.1109/TSTE.2015.2399855.

[44] M. Panteli, C. Pickering, S. Wilkinson, R. Dawson, P. Mancarella, Power System Resilience to Extreme Weather: Fragility Modeling, Probabilistic Impact Assessment, and Adaptation Measures, Volume 32, Issue 5, Pages 3747 - 3757 32 (n.d.) 3747–3757. https://doi.org/10.1109/TPWRS.2016.2641463.

[45] L. Wu, M. Shahidehpour, T. Li, Stochastic security-constrained unit commitment, Volume 22, Issue 2, Pages 800 - 811 22 (2007) 800–811. https://doi.org/10.1109/TPWRS.2007.894843.

[46] Z. Liu, F. Wen, G. Ledwich, Optimal siting and sizing of distributed generators in distribution systems considering uncertainties, Volume 26, Issue 4, Pages 2541 - 2551 26 (n.d.) 2541–2551. https://doi.org/10.1109/TPWRD.2011.2165972.

[47] WG 38-01, TB 030 - Reactive power compensation analyses and planning procedure, 1989.

[48] R. Nadira, W.M. Lebow, P.B. Usoro, DECOMPOSITION APPROACH TO PREVENTIVE PLANNING OF REACTIVE VOLT AMPERE (VAR) SOURCE EXPANSION., IEEE Transactions on Power Systems PWRS-2 (1987) 72–77. https://doi.org/10.1109/TPWRS.1987.4335076.

[49] J.F. Benders, Partitioning procedures for solving mixed-variables programming problems*, Numer Math (Heidelb) 4 (1962) 238–252.

[50] A.M. Geoffrmn, V. Balakrishnan, Generalized Benders Decomposition 1 Communicated by A, J Optim Theory Appl 10 (1972).

[51] W. Tinney, C.H.-I.T. on P. Apparatus, undefined 1967, Power flow solution by Newton's method, Ieeexplore.Ieee.OrgWF Tinney, CE HartIEEE Transactions on Power Apparatus and Systems, 1967•ieeexplore.Ieee.Org (n.d.). https://ieeexplore.ieee.org/abstract/document/4073219/?casa_token=457tp4wkPcYAAAAA:073nWcTtFqolYotEfIeketRSB9UPtx2iSCjxNt-jCzl-l_3i3JS8GCIw-63cgYUNOmm5Ut0 (accessed October 8, 2024).

[52] K. Iba, H. Suzuki, K. ichi Suzuki, K. Suzuki, Practical reactive power allocation/operation planning using successive linear programming, IEEE Transactions on Power Systems 3 (1988) 558–566. https://doi.org/10.1109/59.192907.

[53] L.L. Lai, J.T. Ma, Application of evolutionary programming to reactive power planning-comparison with nonlinear programming approach, IEEE Transactions on Power Systems 12 (1997) 198–206. https://doi.org/10.1109/59.574940.

[54] Z. Michalewicz, M. Schoenauer, Evolutionary Algorithms, Encyclopedia of Information Systems (2003) 259–267. https://doi.org/10.1016/B0-12-227240-4/00065-4.

[55] C.G. Broyden, A class of methods for solving nonlinear simultaneous equations, Math Comput 19 (1965) 577–593. https://doi.org/10.1090/S0025-5718-1965-0198670-6.

[56] B. Cova, N. Losignore, P. Marannino, M. Montagna, Contingency constrained optimal reactive power flow procedures for voltage control in planning and operation, IEEE Transactions on Power Systems 10 (1995) 602–608. https://doi.org/10.1109/59.387894.

[57] A.J. Urdaneta, A Hybrid genetic algorithm for optimal reactive power planning based upon successive linear programming, IEEE Transactions on Power Systems 14 (1999) 1292–1298. https://doi.org/10.1109/59.801887.

[58] V. Gopalakrishnan, P. Thirunavukkarasu, R. Prasanna, Reactive power planning using hybrid evolutionary programming method, 2004 IEEE PES Power Systems Conference and Exposition 3 (2004) 1319–1323. https://doi.org/10.1109/PSCE.2004.1397618.

[59] W. Zhang, F. Li, L.M. Tolbert, Review of reactive power planning: Objectives, constraints, and algorithms, IEEE Transactions on Power Systems 22 (2007) 2177–2186. https://doi.org/10.1109/TPWRS.2007.907452.

[60] M. Alonso, H. Amaris, C. Alvarez-Ortega, A multiobjective approach for reactive power planning in networks with wind power generation, Renew Energy 37 (2012) 180–191. https://doi.org/10.1016/j.renene.2011.06.021.

[61] R. Hemmati, R. Hooshmand, A. Khodabakhshian, State-of-the-art of transmission expansion planning : Comprehensive review, Renewable and Sustainable Energy Reviews 23 (2013) 312–319. https://doi.org/10.1016/j.rser.2013.03.015.

[62] J. Preetha Roselyn, D. Devaraj, S.S. Dash, Multi Objective Differential Evolution approach for voltage stability constrained reactive power planning problem, International Journal of Electrical Power and Energy Systems 59 (2014) 155–165. https://doi.org/10.1016/j.ijepes.2014.02.013.

[63] X. Fang, F. Li, Y. Wei, R. Azim, Y. Xu, Reactive power planning under high penetration of wind energy using Benders decomposition, IET Generation, Transmission & Distribution 9 (2015) 1835–1844. https://doi.org/10.1049/IET-GTD.2014.1117.

[64] S. Wogrin, D. Tejada-Arango, S. Delikaraoglou, A. Botterud, Assessing the impact of inertia and reactive power constraints in generation expansion planning, Appl Energy 280 (2020) 115925. https://doi.org/10.1016/j.apenergy.2020.115925.

[65] N. Karmakar, B. Bhattacharyya, Sustainable Energy , Grids and Networks Optimal reactive power planning in power transmission network using sensitivity based bi-level strategy, Sustainable Energy, Grids and Networks 23 (2020) 100383. https://doi.org/10.1016/j.segan.2020.100383.

[66] A.H. Shojaei, A.A. Ghadimi, M.R. Miveh, F. Mohammadi, applied sciences Multi-Objective Optimal Reactive Power Planning under Load Demand and Wind Power Generation Uncertainties Using ε -Constraint Method, (n.d.).

[67] R. Syah, P.K. Mianaei, M. Elveny, N. Ahmadian, D. Ramdan, R. Habibifar, A. Davarpanah, A new hybrid algorithm for multi-objective reactive power planning via facts devices and renewable wind resources, Sensors 21 (2021). https://doi.org/10.3390/s21155246.

[68] N. Karmakar, B. Bhattacharyya, Hybrid intelligence approach for multi-load level reactive power planning using VAR compensator in power transmission network, Protection and Control of Modern Power Systems 6 (2021) 1–17. https://doi.org/10.1186/s41601-021-00202-1.

[69] S. Shekarappa G, S. Mahapatra, S. Raj, Voltage Constrained Reactive Power Planning Problem for Reactive Loading Variation Using Hybrid Harris Hawk Particle Swarm Optimizer, Electric Power Components and Systems 49 (2021) 421–435. https://doi.org/10.1080/15325008.2021.1970060.

[70] H. Abdi, M. Moradi, R. Rashidi, Hybrid transmission expansion planning and reactive power planning considering the real network uncertainties, International Journal of Numerical Modelling: Electronic Networks, Devices and Fields 35 (2022) 1–25. https://doi.org/10.1002/jnm.2937.

[71] S.S. Gudadappanavar, S. Mahapatra, Metaheuristic nature-based algorithm for optimal reactive power planning, International Journal of System Assurance Engineering and Management 13 (2022) 1453–1466. https://doi.org/10.1007/s13198-021-01489-x.

[72] N. Karmakar, B. Bhattacharyya, Optimal reactive power planning in power transmission system considering facts devices and implementing hybrid optimisation approach, IET Generation, Transmission and Distribution 14 (2020) 6294–6305. https://doi.org/10.1049/iet-gtd.2020.1356.

[73] V.K. Gupta, R. Babu, Reactive power planning problem considering multiple type of FACTS in power systems, International Journal of System Assurance Engineering and Management 13 (2022) 1885–1894. https://doi.org/10.1007/s13198-021-01588-9.

[74] Y. Wu, J. Fang, X. Ai, X. Xue, S. Cui, X. Chen, J. Wen, Robust co-planning of AC/DC transmission network and energy storage considering uncertainty of renewable energy, Appl Energy 339 (2023) 120933. https://doi.org/10.1016/j.apenergy.2023.120933.

[75] E.G. Morquecho, S.P. Torres, F. Astudillo-Salinas, C.A. Castro, H. Ergun, D. Van Hertem, Security constrained AC dynamic transmission expansion planning considering reactive power requirements, Electric Power Systems Research 221 (2023) 109419. https://doi.org/10.1016/j.epsr.2023.109419.

[76] R. Elazab, M. Ser-Alkhatm, M.A. Abu Adma, K.M. Abdel-Latif, Allocation and sizing of reactive power compensators considering PV power and load demand uncertainty using beetle-antenna grey wolf optimization, Clean Energy 7 (2023) 350–362. https://doi.org/10.1093/ce/zkac078.

[77] Codice di Rete Capitolo 4-Regole per il dispacciamento, DOCUMENTO PER LA CONSULTAZIONE, (n.d.).

[78] Welcome to Python.org, (n.d.). https://www.python.org/ (accessed August 30, 2024).

[79] General Python FAQ — Python 3.12.5 documentation, (n.d.). https://docs.python.org/3/faq/general.html#what-is-python (accessed August 30, 2024).

[80] A.L.S. Saabith, T. Vinothraj, M. Fareez, POPULAR PYTHON LIBRARIES AND THEIR APPLICATION DOMAINS, International Journal of Advance Engineering and Research Development 7 (2020). https://www.researchgate.net/publication/349828209 (accessed August 30, 2024).

[81] L. Thurner, A. Scheidler, F. Schafer, J.H. Menke, J. Dollichon, F. Meier, S. Meinecke, M. Braun, Pandapower - An Open-Source Python Tool for Convenient Modeling, Analysis, and Optimization of Electric Power Systems, IEEE Transactions on Power Systems 33 (2018) 6510–6521. https://doi.org/10.1109/TPWRS.2018.2829021.

[82] CIGRE > Home, (n.d.). https://www.cigre.org/ (accessed August 30, 2024).

[83] IEEE - The world's largest technical professional organization dedicated to advancing technology for the benefit of humanity., (n.d.). https://www.ieee.org/ (accessed August 30, 2024).

[84] CIGRE Networks — pandapower 3.0.0 documentation, (n.d.). https://pandapower.readthedocs.io/en/latest/networks/cigre.html (accessed August 30, 2024).

[85] Power System Test Cases — pandapower 3.0.0 documentation, (n.d.). https://pandapower.readthedocs.io/en/latest/networks/power_system_test_cases.html (accessed August 30, 2024).

[86] R. Bolgaryn, G. Banerjee, D. Cronbach, S. Drauz, Z. Liu, M. Majidi, H. Maschke, Z. Wang, L. Thurner, Recent Developments in Open Source Simulation Software pandapower and pandapipes, 1st International Workshop on Open Source Modelling and Simulation of Energy Systems, OSMSES 2022 - Proceedings (2022). https://doi.org/10.1109/OSMSES54027.2022.9769084.

[87] R. Bolgaryn, G. Banerjee, S. Meinecke, H. Maschke, F. Marten, M. Richter, Z. Liu, P. Lytaev, B. Alfakhouri, J. Kisse, D. Lohmeier, Open Source Simulation Software pandapower and pandapipes: Recent Developments, 2023 2nd International Workshop on Open Source Modelling and Simulation of Energy Systems, OSMSES 2023 - Proceedings (2023). https://doi.org/10.1109/OSMSES58477.2023.10089685.

[88] Short-Circuit — pandapower 3.0.0 documentation, (n.d.). https://pandapower.readthedocs.io/en/latest/shortcircuit.html (accessed August 30, 2024).

[89] K. Deb, A. Pratap, S. Agarwal, T. Meyarivan, A fast and elitist multiobjective genetic algorithm: NSGA-II, IEEE Transactions on Evolutionary Computation 6 (2002) 182–197. https://doi.org/10.1109/4235.996017.

[90] K. Deb, S. Agrawal, A. Pratap, T. Meyarivan, A fast elitist non-dominated sorting genetic algorithm for multi-objective optimization: NSGA-II, Lecture Notes in Computer Science (Including Subseries Lecture Notes in Artificial Intelligence and Lecture Notes in Bioinformatics) 1917 (2000) 849–858. https://doi.org/10.1007/3-540-45356-3_83/COVER.

[91] E. Zitzler, L. Thiele, Multiobjective evolutionary algorithms: A comparative case study and the strength Pareto approach, IEEE Transactions on Evolutionary Computation 3 (1999) 257–271. https://doi.org/10.1109/4235.797969.

[92] D.H. Wolpert, W.G. Macready, No free lunch theorems for optimization, IEEE Transactions on Evolutionary Computation 1 (1997) 67–82. https://doi.org/10.1109/4235.585893.

[93] IEEE reliability test system: A report prepared by the Reliability Test System Task Force of the Application of Probability Methods Subcommittee, IEEE Transactions on Power Apparatus and Systems PAS-98 (1979) 2047–2054. https://doi.org/10.1109/TPAS.1979.319398.

[94] Renewables.ninja, (n.d.). https://www.renewables.ninja/ (accessed May 19, 2023).

[95] PVGIS Online Tool, (n.d.). https://joint-research-centre.ec.europa.eu/pvgis-online-tool_en (accessed May 19, 2023).

[96] Terna, Documento metodologico per l'applicazione dell'analisi costi benefici applicata al Piano di Sviluppo 2023, (2023).

[97] F.M. Gatta, A. Geri, S. Lauria, M. MacCioni, L. Nati, A global DC branch model incorporating power system flexibility, 2022 (n.d.) 2022. https://doi.org/10.1109/ENERGYCON53164.2022.9830461.

[98] F. Carere, F.M. Gatta, A. Geri, S. Lauria, M. Maccioni, L. Nati, Technical/economic feasibility of the adequacy of a fully renewable power system: The case study of the Sardinia island, Volume 31 31 (100726). https://doi.org/10.1016/j.segan.2022.100726.

[99] Terna, Workshop utenti di dispacciamento, (2023). https://download.terna.it/terna/Workshop%20incentivi%20febbraio23_8db1f2f63848dac.pdf (accessed October 22, 2024).

[100] T. Bragatto, J. Dell'olmo, F.M. Gatta, A. Geri, M. Graziani, S. Lauria, M. MacCioni, L. Nati, Reactive Power Flows and Voltage Issues in Urban Distribution and Subtransmission Networks, 2023 (n.d.) 2023. https://doi.org/10.23919/AEIT60520.2023.10330363.

[101] J. Dell'Olmo, F.M. Gatta, A. Geri, M. Graziani, S. Lauria, M. Maccioni, Clarke Transform Based Fast Assessment of Switching Overvoltages in an MV Distribution Network, Volume 212 212 (108255). https://doi.org/10.1016/j.epsr.2022.108255.

[102] F. Salata, J. Dell'Olmo, V. Ciancio, Agri-voltaics near airport facilities. Reconciling the risk of solar glare with power generation, Volume 275 275 (112653). https://doi.org/10.1016/j.solener.2024.112653.

[103] M.A. Bucarelli, A. Curci, A. Geri, T. Bragatto, M. MacCioni, M. Paulucci, J. Dell'olmo, Technical-economic Impact of the Deployment of Renewable Energy Communities: An Italian Case Study, 2023 (n.d.) 2023. https://doi.org/10.23919/AEIT60520.2023.10330415.

[104] A. Ruvio, M.C. Falvo, R. Lamedica, J. Dell'olmo, M. Scanzano, A Novel Railway Power Systems Design Methodology Using Genetic Algorithms: Models and Application, Volume 12, Pages 128468 - 128481 (2024). https://doi.org/10.1109/ACCESS.2024.3455945.

[105] A. Geri, F.M. Gatta, M. MacCioni, J. Dell'olmo, F. Carere, M.A. Bucarelli, P. Poursoltan, N. Hadifar, M. Paulucci, Distributed generation monitoring: a cost-effective Raspberry Pi-based device, 2022 (n.d.) 2022. https://doi.org/10.1109/IRASET52964.2022.9737768.

[106] A. Geri, F.M. Gatta, M. Maccioni, J. Dell'Olmo, F. Carere, M.A. Bucarelli, P. Poursoltan, N. Hadifar, M. Paulucci, A Low-Cost Smart Monitoring Device for Demand-Side Response Campaigns, Volume 448, Pages 593 - 603 448 (n.d.) Online. https://doi.org/10.1007/978-981-19-1610-6_52.

[107] A. Ciardiello, J. Dell'Olmo, F. Rosso, L.M. Pastore, M. Ferrero, F. Salata, An Innovative Multi-objective Optimization Digital Workflow for Social Housing Deep Energy Renovation Design Process, Volume Part F813, Pages 111 - 121 Part F813 (2023) 111–121. https://doi.org/10.1007/978-3-031-29515-7_11.

[108] A. Ciardiello, J. Dell'Olmo, M. Ferrero, L.M. Pastore, F. Rosso, F. Salata, Energy Retrofit Optimization by Means of Genetic Algorithms as an Answer to Fuel Poverty Mitigation in Social Housing Buildings, Volume 14, Issue 1 14 (2001). https://doi.org/10.3390/atmos14010001.

[109] A. Ciardiello, F. Rosso, J. Dell'Olmo, V. Ciancio, M. Ferrero, F. Salata, Multi-objective approach to the optimization of shape and envelope in building energy design, Volume 280 280 (115984). https://doi.org/10.1016/j.apenergy.2020.115984.

[110] F. Salata, A. Ciardiello, J. Dell'Olmo, V. Ciancio, M. Ferrero, F. Rosso, Geometry optimization in the schematic design phase of low-energy buildings for all European climates through genetic algorithms, Volume 112 112 (105639). https://doi.org/10.1016/j.scs.2024.105639.